2013

Optimizing peak gust and maximum sustained wind speed estimates from mid-latitude wave cyclones

Timothy Andrew Joyner
Louisiana State University and Agricultural and Mechanical College, tjoyne1@tigers.lsu.edu

OPTIMIZING PEAK GUST AND MAXIMUM SUSTAINED WIND SPEED ESTIMATES FROM MID-LATITUDE WAVE CYCLONES

A Dissertation
Submitted to the Graduate Faculty of the
Louisiana State University and
Agricultural and Mechanical College
in partial fulfillment of the
requirements for the degree of
Doctor of Philosophy

in

The Department of Geography and Anthropology

by
Timothy Andrew Joyner
B.S., Louisiana State University, 2008
M.S., University of Florida, 2010
May 2013

To my wife, Jessica – I could not have completed this dissertation without your love and support. I love you!

ACKNOWLEDGMENTS

Oh, where do I begin? First and foremost, I thank my wife, Jessica, for her love and encouragement throughout the entire graduate school process. Through the courses, the papers, the deadlines, the late nights, and long weekends, she has always been supportive and I could not have completed my doctorate without her. I also thank my parents, grandparents, brother, and sister-in-law in North Carolina for always being just a phone call or short plane trip away. They have provided the foundation for everything I have done and will do in life, and I am forever grateful. I also thank my wife's family here in Louisiana who has welcomed me into their family with open arms, lots of food, and plenty of dog-sitting. Thank you!

I cannot say enough about my dissertation advisor, Robert "Bob" Rohli. He has been incredibly supportive of every endeavor and idea I have had throughout the nearly 9 years I have known him. He provided constant mentoring throughout my undergraduate, masters, and doctoral degrees, without which I would not have made it this far. It has been a true pleasure to work with him on projects here at LSU and I look forward to many more collaborative projects, papers, and grants in the future. Most importantly, Bob is a friend that I can count on for the rest of my life.

Additionally, I thank my committee members: Carol Friedland, Melanie Gall, and Barry Keim. Without Carol, this dissertation would not have even happened. I am forever indebted to her for the opportunity she gave me to work on a "4 week project" involving wind storm wind speeds – I'm glad it took longer! Without Melanie, I never would have started my PhD. She provided an assistantship through the LSU Hazard Mitigation Plan and jumpstarted my interest in hazards geography and disaster science. Along the way, she has provided numerous other opportunities and I could never begin

to repay her. Without Barry, I would not have rediscovered my love for basketball AND my final semester at LSU would have been much more difficult financially. I cannot thank him enough for his support and friendship over the past several years and for looking out for me in tough times.

I am also very thankful for a fun and supportive group of friends that I have enjoyed working (and playing!) with over the past several years. Ryan Orgera, Kyle Brehe, Anna Treviño, and Hal Needham, for multiple trips to the Chimes and Zippy's, ping pong, coffee breaks, lunch breaks, hours of talking, YouTube videos, Atlanta Braves bashing, and everything in-between, thank you.

TABLE OF CONTENTS

LIST OF TABLES

LIST OF FIGURES

LIST OF ABBREVIATIONS

ANN	Artificial Neural Networks
CGIAR-CSI	Consultative Group on International Agricultural Research – Consortium for Spatial Information
EBK	Empirical Bayesian Kriging
ESA	European Space Agency
ESDA	Exploratory Spatial Data Analysis
ESRI	Environmental Systems Research Institute
FMAFEWM	Federal Ministry of Agriculture, Forestry, Environment, and Water Management
GIS	Geographic Information Systems
H*WIND	Real-time Hurricane Wind Analysis System
HRD	Hurricane Research Division
IDW	Inverse Distance Weighting
LC	Land Cover
MATLAB	MATrix LABoratory
MAUP	Modifiable Areal Unit Problem
ME	Mean Error
NAO	North Atlantic Oscillation
NASA	National Aeronautics and Space Administration
NN	Nearest Neighbor
PCA	Principal Components Analysis
PNW	Pacific Northwest
PR	Polynomial Regression

RMSE	Root Mean Square Error
RMSPE	Root Mean Square Prediction Error
SA	Simulated Annealing
SBL	Surface Boundary Layer
SE	Standard Error
SRTM	Shuttle Radar Topographic Mission
TIN	Triangular Irregular Network
WMO	World Meteorological Organization
ZAMG	Zentralanstalt fur Meteorologie und Geodynamik

ABSTRACT

Wind storms cause significant damage and economic loss and are a major recurring threat in many countries. Maximum sustained and peak gust weather station data from multiple historic wind storms occurring over more than three decades across Europe were analyzed to identify storm tracks, intensities, and areas of frequent high wind speeds. Wind surfaces for maximum sustained and peak gust winds were estimated based on an anisotropic (directionally-dependent) kriging interpolation methodology. Overall, wind speed magnitudes and high intensity locations were identified accurately for each storm. Directional trends and wind swaths were also consistently located in appropriate locations based on known storm tracks. Anisotropic kriging proved to be superior to isotropic (non-directional) kriging when modeling continental-scale wind storms because of the identification of strong directional correlations across space. Results suggest that coastal areas and mountainous areas experience the highest wind intensities during wind storms. These same areas also experience high variability over short distances and thus the highest error measurements associated with concurrent interpolated surfaces. For this reason, various covariates were utilized in conjunction with the cokriging interpolation technique and improved the interpolated wind surfaces for five wind storms that impacted both the mountainous and topographically-varied Alps region and the coastal regions of Europe. Land cover alone reduced station-measured standard error most significantly in a majority of the models, while aspect and elevation (singularly and collectively) also reduced station standard error in most models as compared to the original kriging models.

Additional comparisons between different areal scales of kriging/cokriging models revealed that some surface wind variability is muted at the continental scale, but identifiable at the local scale. However, major patterns and trends are more difficult to ascertain for local-scale surfaces when compared to continental-scale surfaces. Large station error can be reduced through local kriging/cokriging, but additional research is needed to merge local-scale semivariograms with continental-scale models. Results showed substantial improvements in wind speed surface estimates over previous estimates and have major implications for catastrophe modeling companies, insurance needs, and construction standards. Implications of this research may be transferrable to other geographies and create an impetus for database and covariate improvement.

Keywords: European wind storms, sustained winds, peak gust, anisotropic, kriging interpolation, semivariogram, cokriging, local-scale, continental-scale

CHAPTER 1. INTRODUCTION

Destructive mid-latitude cyclones, specifically wind storms, in Europe occur predominantly during the late fall and winter months and are responsible for most of the natural hazard-related insured losses in the region (Pinto et al. 2010). Much of the infrastructure-related destruction is attributable to extreme winds that often impact multiple countries (Leckebusch et al. 2007, Pinto et al. 2010). In central Europe alone, 56 percent of economic and 64 percent of insurance losses caused by natural hazards are due to these storms (Hofherr and Kunz 2010). The Lothar storm (25-27 December 1999) is considered one of the most expensive storms in European history for insurance companies (Wernli et al. 2002, Leckebusch et al. 2007). Other similarly dangerous recent storms include Jeanette (26-28 October 2002), Kyrill (16-19 January 2007), Paula (24-26 January 2008), and Emma (29 February – 2 March 2008) (Heneka and Hofherr 2011).

Improved modeling of wind storm-induced surface winds is critical to the advancement of wind engineering, while also propelling geospatial analytical techniques forward. Catastrophe modeling and insurance companies currently use inaccurate wind speed surface maps for major wind storms. These maps use simplistic interpolation techniques that poorly illustrate wind patterns and variability on the surface. Inaccurate maps lead to incorrect predictions of high-low wind speed locations and potentially a misunderstanding of the manner in which wind storm-induced winds move across Europe. Currently, upper-level winds are commonly used to estimate wind surfaces in wind storms (e.g., Della-Marta et al. 2009), but interpolations of wind speeds at higher levels in the atmosphere do not reflect the complexity of winds at the surface. The use of modeled wind data based on upper-level geopotential height gradients is less

accurate than meteorological station readings as they are not based on observed surface wind measurements. In addition, the length of the record is usually shorter than station data, preventing long-term studies. Station data can depict fluctuations of wind at the local scale better than other data types, and are therefore most appropriate for this project. We hypothesize that because aspect, elevation, and land cover affect surface-level wind speeds, it is important to consider their influence since human populations and the built environment are impacted the most by surface-level winds.

1.1 European Wind Storms

Similar to hurricanes in the United States, European wind storms are named, but the names sometimes differ from country to country. Major storms normally follow the same nomenclature. While similarities between wind storms and hurricanes exist, it is also important to understand a few major differences between each of the storms. Hurricane cyclogenesis occurs in tropical regions and hurricanes consequently have a warm, moist core and no attached frontal boundary, while wind storm cyclogenesis occurs in mid-latitude regions, resulting in a cold, drier core with an attached frontal system (Mass and Dotson 2010). Additionally, the highest wind speeds of a hurricane occur predominantly in the right front quadrant (northeast quadrant), while the highest winds of a wind storm typically occur on the cold side of the attached front (e.g., for wind storms in Europe taking a west-east track, this area is to the south of the storm track's low pressure center) (Steenburgh and Mass 1996).

Another difference between the meteorological setting of a mid-latitude wind storm and a tropical cyclone is in the upper-level flow configuration. Tropical cyclones require little upper-level shearing (particularly west-to-east shear that would remove the developing cloud tops as the storm migrates westward. By contrast, mid-latitude wind

storm development is enhanced by the overhead presence of strong west-to-east flow, particularly on the trough-to-ridge side of the Rossby wave, where uplift and upper-level divergence is favored (e.g., Newtonu and Palmén 1963). Additionally, the pressure differences are more drastic between adjacent air masses with more dissimilar characteristics; these are the types that are associated with wind storms. High winds can be enhanced by flow perpendicular to the storm movement along mountain valleys in advance of a storm to equalize the pressure differences (Steenburgh and Mass 1996).

1.2 Modeling Wind Fields Using Station Data

Wind station data must be analyzed accurately and appropriately to determine wind speed-damage relationships associated with these storms. Some limitations complicate use of station data to represent a wind field across a single storm. Klawa and Ulbrich (2003) noted that a single station can represent a local climate that is very different from the regional climate, highlighting the uncertainty that microclimatology may present when examining macro-climatological patterns. Hofherr and Kunz (2010) emphasized the importance of high spatial resolution of station data to estimate wind-storm climatology accurately and to evaluate how local topographic features influence the wind field. At the local scale, orographic influences, land use, friction, and boundary layer processes modify both the strength and direction of the synoptically-generated surface winds. Gusts are highly dependent on the surface roughness, roughness length, and height above surface (Wieringa 1973, 1986, Oke 1987). Roughness lengths can often be estimated around a station based on high resolution land cover data, but the dominant wind azimuth and seasonal variations in land cover must be accounted for if correction factors for roughness are calculated (Gatey 2011). Wind speed correlation

between nearby stations is much higher in fall/winter (October through March; >80%) compared to spring/summer (as low as 45% in May) because of a decrease in foliage and other vegetation (Gatey 2011). Because of these local factors, the wind climatology of a station may depart considerably from those expected from the macroscale climatology (Hofherr and Kunz 2010).

Even though use of station data has some limitations, such data can be preferable to modeled estimates or radiosonde-based observations. Hofherr and Kunz (2010) discussed how wind data from stations are most popularly used in studies that evaluate hazards – both peak gust and mean wind speed values – due to the high level of accuracy on a local scale. Use of modeled wind data based upon upper-level air pressure is less accurate than meteorological station readings as they are not created using observed wind data (Hofherr and Kunz 2010). Furthermore, the length of the record is usually not as long as station data, preventing any long-term studies. Station data can provide a better idea of fluctuations of wind at the local scale than many other data types, and are highly appropriate for this study.

Estimation of peak gust values is necessary when peak gust data are missing. It is important to convert sustained wind speeds to a "probable maximum wind speed" over a shorter period because buildings and other structures are most affected by wind gusts of approximately 3 seconds in duration (Krayer and Marshall 1992). This is usually done by applying a "gust factor," which is the ratio of the mean value of maxima to the mean value of a given effect attributable to wind buffeting (Solari 1993). Krayer and Marshall (1992) reviewed the Durst (1960) and Cook (1986) methods for calculating the gust factor and determined that the Durst method was more accurate in estimating

peak gust wind speeds from mean wind speeds in tropical cyclones. Solari et al. (1993) reviewed various equations that have been used to calculate velocity of peak gusts, and found that the ratio $\frac{V_{1\ s}/V_{600\ s}}{V_{5\ s}/V_{3600\ s}}$ produced by other studies range from 1.07 to 1.68. These values vary largely based on the length of time used to calculate them. For the proposed study, observed wind speeds will be converted and adjusted in accordance with the Durst method.

1.3 Analysis of Peak Gust and Sustained Wind Speeds

WMO standards for wind measurement use a disjunctly-sampled sustained wind speed (sampled 10 minutes prior to each hour) and a continuously-sampled gust speed. Because of the disjunct sampling, 50 minutes of sustained wind data are not collected each hour. Only a handful of studies have addressed the difference in measurement when analyzing extreme wind speeds (e.g., Larsén and Mann 2009, Gatey 2011). Additionally, many stations either do not collect gust wind speeds, or these data were not reported for the storms identified. For these reasons, it is likely that the WMO station data generally misrepresent the true sustained wind speeds at each location and must be adjusted based on which data are collected. This dissertation has developed three different data cases and procedures for adjustment (Figure 1-1): Case I – only gust wind is measured, which is used to estimate a continuously sampled 10-minute sustained wind speed using the Durst method; Case II – only 10-minute, disjunctly sampled sustained wind is measured, which requires calculation of equivalent continuously sampled wind speed using the method developed by Larsen and Mann (2006) as well as application of the Durst method to compute gust wind speeds; and

Case III – both disjunctly sampled sustained wind and continuously sampled gust winds are measured. Case III essentially combines the methodologies of Cases I and II to identify the maximum sustained wind speed.

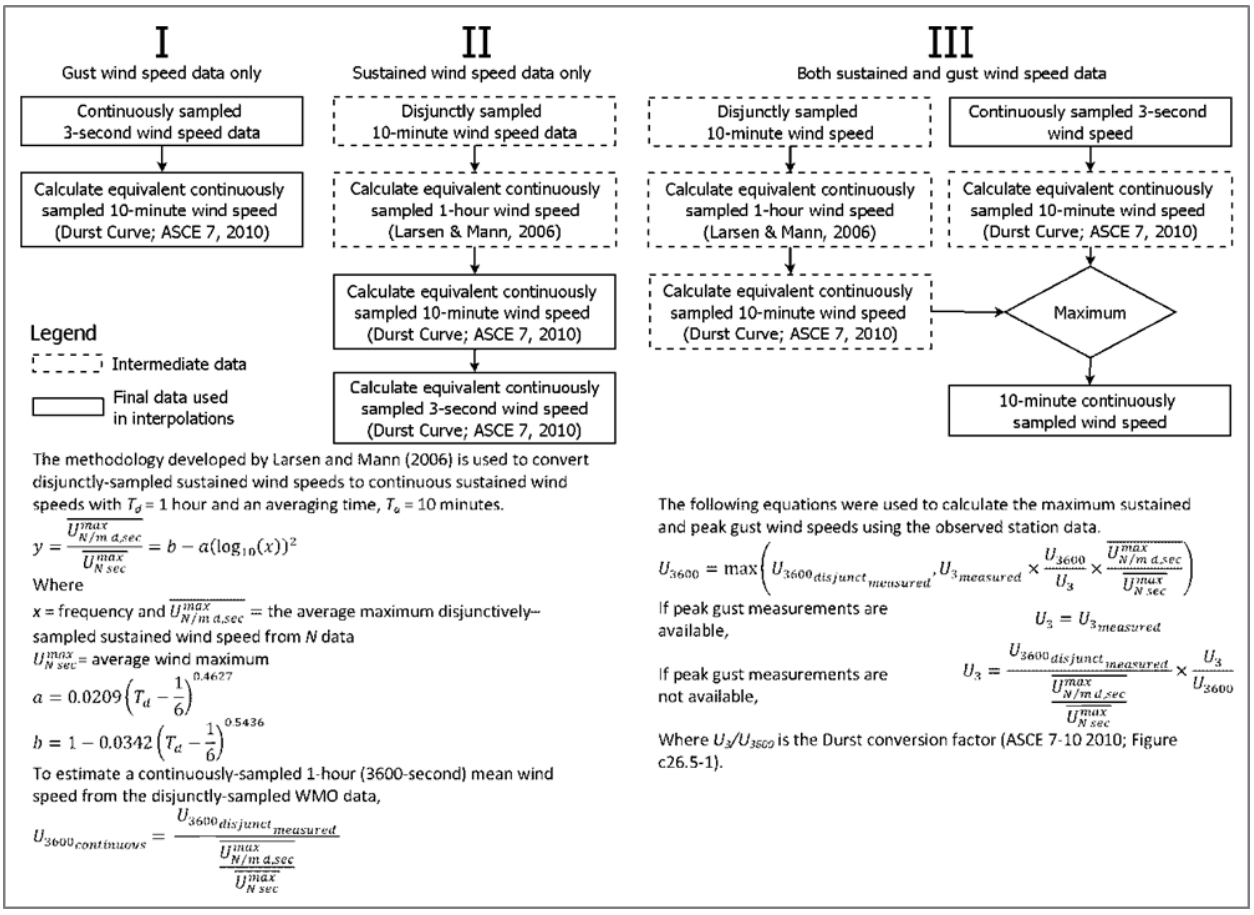

Figure 1-1. Wind conversion methodology.

Implementation of the conversion from a disjunct to continuous sampling basis still revealed inconsistencies in the wind data that could not be explained using the gust factor. A review of the Lothar storm data set found that the actual gust factors (U3/U3600) calculated from the observed data ranged from 0.89 to 10.17 for the 4258 records (out of 214,499 total, 2%) that had both gust and sustained wind speed data available, with an average of 1.83 and a standard deviation of 0.76. Based on the multiple studies discussed earlier in the paper, the expected value is in the range of 1.4.

This initial quality control evaluation indicated that the sustained wind speeds were much lower than expected based on the recorded peak gust wind speeds. This necessitated that both the peak gust and sustained wind speed data be used to calculate the final wind speeds used in the interpolation.

Using the algorithms in Figure 1-1, the Lothar dataset was again evaluated as a test case. Results show that the methodology does not significantly overpredict the gust wind speed data (an average increase of 2%, standard deviation of 5%). Further, the methodology accounted for the underreporting of sustained wind speeds because of the disjunct sampling period. The final gust factors (U3/U3600) for the calculated dataset were reevaluated and were found to range from 1 to 1.4299, with an average of 1.42 and a standard deviation of 0.03 for the 4258 records. Although low gust factors (<1.4) were seen for approximately 5% of the data, this methodology created a dataset that was more consistent. These results demonstrate that the implemented calculation methodology produces wind speeds that are more consistent with standard wind engineering metrics.

Methods are mostly consistent with the methods utilized for wind speed data adjustments in the Hurricane Research Division (HRD) Real-time Hurricane Wind Analysis System (H*WIND) (Powell et al. 1998). Three main adjustments are used for data conformity within the H*WIND system: common observation height, common averaging period, and common exposure (Powell et al. 1996). Surface-level and flight-level winds are used for H*WIND and a major component of H*WIND data adjustment is the conversion of flight-level winds to surface-level winds at the 10 m height (Powell et al. 1996). In this dissertation, flight-level winds were not utilized, but surface-level

observations were at the 10 m height and WMO adjustments produced standard (open terrain) exposure. Common sampling techniques and averaging periods were also identified.

1.4 Research Objectives

The objective of Study One is to quantify the accuracy of an anisotropic semivariogram-derived kriging interpolation methodology for predicting extreme winds for large areas of Europe. Preliminary wind estimates suggested that coastal and mountainous regions often experienced the most extreme wind speeds. Inland Europe, specifically the Black Forest and northern Alps, displayed very high wind speeds relative to the surrounding areas – indicative of a complex topography/wind interaction. Coastal and mountainous weather stations experienced the most intra-storm wind speed variability and also reported some of the highest error measurements.

Because of these high error measurements, the objective of Study Two is to reduce error measurements associated with the original kriging surfaces. Study Two will examine multiple covariates through the cokriging technique to determine whether more accurate surface wind interpolations can be created. Understanding of local wind variability in these environments will be improved if more accurate wind surface interpolations are created through the cokriging methodology. Previous studies that identified cokriging as superior for estimating surface winds only utilized elevation as a singular covariate (e.g., Luo et al. 2008, Sliz-Szkliniarz and Vogt 2011); this study will also utilize aspect and land cover in addition to elevation.

The objective of Study Three is to examine the differences between kriging/cokriging wind surfaces at two different scales: local (e.g., Austria) and continental/regional (e.g., entire storm). This study will also determine the extent that

high wind or other factors (e.g., exposure) influence wind storm-induced damage and provide a means of validation for wind surface estimates.

The specific research questions are as follows:

Study One

1) Which interpolation method creates the most accurate and reasonable wind surface estimates over sections of Europe impacted by wind storms?
2) Which regions consistently experienced the highest wind speeds associated with wind storms?

Study Two

1) To what extent does cokriging improve interpolated wind surfaces in the coastal and mountainous regions of Europe, compared to ordinary kriging methods?
2) Which covariate(s) is/are most influential in improving wind surface interpolations in diverse terrain?

Study Three

1) Are local kriging/cokriging wind surface estimates more accurate than regional estimates?
2) To what extent can tree damage be utilized as a proxy for validating interpolated wind surfaces?

CHAPTER 2. PEAK GUST AND MAXIMUM SUSTAINED WIND SPEED ESTIMATES FOR EUROPEAN STORMS

2.1 Introduction

Wind storms generated by intense mid-latitude cyclones, occur across much of Europe, predominantly during winter, and are responsible for most of the natural hazard-related insured losses in the region (Pinto et al. 2010). Wind storms account for most of the insured losses in Europe (64%) and on average are the cause of approximately $2.5 billion of damage per year (Pinto et al. 2010). Much of the infrastructure-related destruction is attributable to extreme wind speeds that often impact multiple countries (Pinto et al. 2010). Certain atmospheric patterns and modes such as those of the North Atlantic Oscillation (NAO) influence tracks and intensities of mid-latitude cyclones and often provide optimal conditions for cyclogenesis (Raible 2007). These patterns, along with other forcing mechanisms and climatic conditions, are in a constant state of flux with changes potentially attributable to anthropogenic-induced climate change (Handorf and Dethloff 2009), which has led many to suggest that changes in climate are at least partly to blame for recent increases in catastrophes (Schiermeier 2006).

Regardless of climatic changes, the impact from winter storms over the last several decades has been widespread across Europe and recent storms do not suggest a decrease in their frequency and intensity. Reports suggest that storms occurring in early 1990 and late 1999 resulted in large economic and insurance losses (Leckebusch et al. 2007). In central Europe alone, 56 percent of economic and 64 percent of insurance losses caused by natural hazards are attributed to these winter storms (Hofherr and Kunz 2010). The Lothar storm (December 25-27, 1999) is considered one

of the most expensive storms in European history for insurance companies (Wernli et al. 2002, Leckebusch et al. 2007). Lothar was considerably stronger than other storms because of: (1) a stronger than normal upper-level jet, (2) rapid intensification of the storm, resulting in an intensive vortex, and (3) higher than normal Atlantic sea surface temperatures (Wernli et al. 2002). Other similarly dangerous storms during this period included Kyrill (January 16-19, 2007) and Jeanette (October 26-28, 2002) (Heneka and Hofherr 2011).

2.1.1 Simulation of wind surfaces through interpolation of station data

There are many ways to simulate and interpolate wind surfaces. Spatial interpolation can produce both global/local and deterministic/stochastic estimates of unknown variables across a surface. These methods vary widely and it is important to understand the variable(s) in question to select the most appropriate interpolation method (Luo et al. 2008). Deterministic methods do not use probability, meaning that all observed values are considered accurate (Luo et al. 2008). These methods are very common and include polynomial regression (PR), triangular irregular network (TIN), nearest neighbor (NN), splines, and inverse distance weighting (IDW). Stochastic methods, also known as geostatistical methods, use a probabilistic approach for data regularization and include artificial neural networks (ANNs), simulated annealing (SA), and various forms of kriging such as ordinary, universal, cokriging, multi-region, Bayesian, and neural network kriging (Lanza et al. 2001, Cellura et al. 2008, Zlatev et al. 2010).

Within the deterministic family, PR uses a linear regression approach to interpolate values between known or observed variables. PR is well-suited for fairly dense and compact areas, but it predicts poorly outside the range of the observed points (Akkala et

al. 2010). The TIN approach creates triangles across a surface and the balance of mass between points is used to determine the unknown values. TIN produces a linear and coarse output. The NN approach assigns a value based on the value of the closest data point and is one of the simpler interpolation methods, but it is only considered accurate or suitable for a densely sampled surface (Akkala et al. 2010). Splining is a curvature method that still uses the exact observed values; however, the influence of the values decreases over distance, thus producing a two-dimensional curve as opposed to the linear surface produced by many other deterministic methods (Wahba 1981). Splining is considered one of the better deterministic methods of interpolation, but the smooth curves ignore trends and can hide uncertainty when data points are irregularly spaced (Luo et al. 2008, Akkala et al. 2010).

Stochastic interpolation methods are often more time-intensive and require a higher level of user input. ANNs can be applied independently of kriging and are used to reduce the over/under estimation of values through use of a pivot station that “learns” the common correlation between stations. This serves to decrease oversmoothing that other interpolators cause by over-estimating low values and under-estimating high values, but ANNs can over-learn or under-learn a pattern (Akkala et al. 2010). For this reason, ANN's are best used in areas with high input variability over relatively short distances (Öztopal 2006). SA uses a linear regression function similar to the PR deterministic method to produce an interpolated surface, but a probability function is also applied to determine the distance from a point at which the relationship becomes insignificant (Sterk and Stein 1997). SA is best at capturing local variability, but the method is not well-suited to estimate large surface patterns (Sterk and Stein 1997).

Kriging interpolation methods are the most common stochastic techniques and they use probability and spatial correlation to create a surface that is weighted by observed values through a semi-variance function. Distance and direction are both utilized for the semi-variance function so it can account for anisotropic spatial patterns and trends in wind behavior (Luo et al. 2008). Since wind speeds often exhibit a direction in which they are increasing or decreasing across a surface, kriging methods are preferred over deterministic methods and other stochastic methods (Lanza et al. 2001, Luo et al. 2008, Akkala et al. 2010, Zlatev et al. 2010). However, microclimatological effects sometimes produce pockets or patches of high/low wind speed on a surface that can create confusion during kriging surface construction. The anisotropic function selects the dominant surface trend, but this trend may not align with the actual direction of wind speeds relative to a storm track, making it necessary to verify that the anisotropic azimuth direction reflects the direction of storm movement. During surface construction, kriging creates an unbiased surface where a polynomial function has not been forced to fit, thus eliminating edge and circular effects common in other interpolation methods (Akkala et al. 2010).

In a recent study by Luo et al. (2008), various forms of kriging performed better than other interpolation methods based on their root mean square prediction error (RMSPE). Mean error (ME) and RMSPE accuracy metrics indicated that kriging produced an unbiased surface that was found to be ideal when modeling wind speed because values were not manipulated by a polynomial or linear fitting interpolation technique (Luo et al. 2008). ME and RMSPE are commonly used evaluation metrics when determining the quality and reliability of interpolation techniques because they

provide a good means of comparing across various time periods and between various methods. Kriging consistently outperformed deterministic methods such as IDW, which not only received poorer ME and RMSPE scores, but also produced a surface with an illogical “bullseye” effect centered on each weather station (Luo et al. 2008).

When used for wind speeds, kriging is considered an approximate predictor because of the incorporation of a nugget effect – a variation that exists at shorter distances than the distance between sample points. If the nugget size is greater than zero, then there is a nugget effect. The nugget size is used during the kriging process to represent independent error and is calculated as the intersection of the data with the y-axis. For example, the correlation between observed wind speed values is plotted on a 1x1 variable diagram as the first step in creating a semivariogram model. The gap between the origin and where the semivariogram begins is referred to as the nugget size (Figure 2-1 represents a hypothetical example). The plot illustrates the correlation that surrounding values have at varying distances. Once the correlation diminishes to an insignificant amount, then the “sill” is reached, indicating that the values no longer have spatial dependence. The distance between the nugget size and the sill is called the range, and all of these values are used concurrently to create the semivariogram for kriging. Range, sill, and nugget size determine at what distance the interpolated wind speed surface levels off or changes. For example, wind speed may be found to decrease rapidly over land when the wind direction is from the north, but wind speed may be found to decrease less rapidly over land when the wind direction is from the west. This could be caused by a variety of land surface factors (often topography and surface roughness), but anisotropic semivariograms account for wind direction and

distance by examining the sill in each direction when making probabilistic surface estimates.

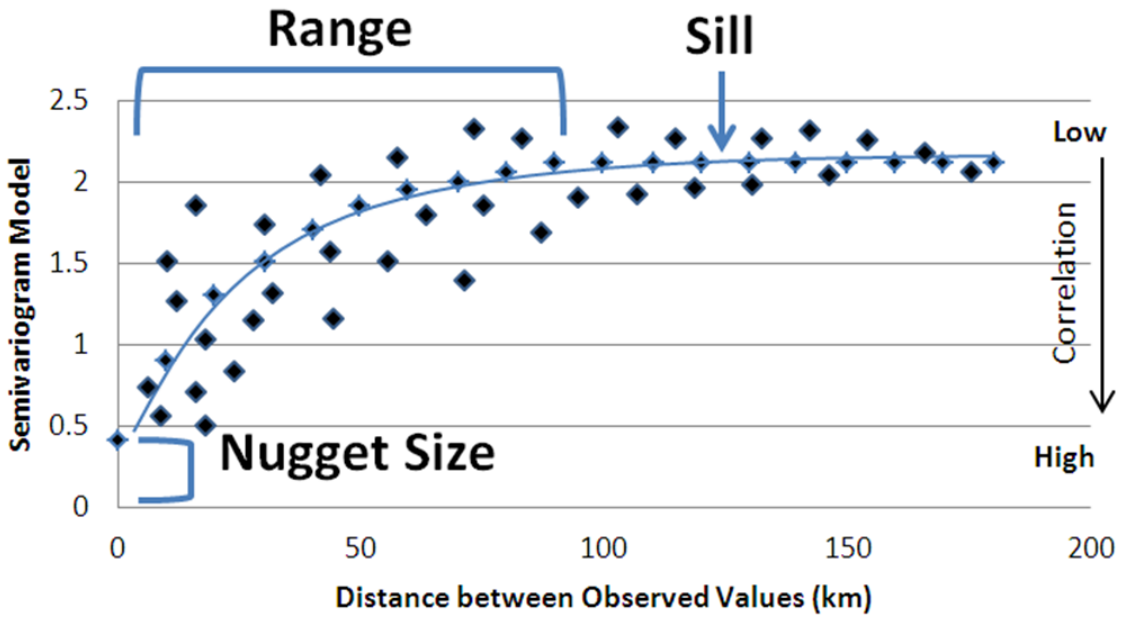

Figure 2-1. Idealized portrayal of semivariogram properties. Nugget size represents where the data and the y-axis intersect. Range is the distance from an observed value at which spatial dependence exists (between the nugget and sill). Sill is the distance where spatial dependence ceases to exist, or where spatial autocorrelation ends.

Ordinary and universal kriging are the two most common forms of kriging. Ordinary kriging assumes an unknown constant trend and utilizes the points within a specified search radius for semivariogram creation, while universal kriging assumes a general linear mean value trend across an entire study area (Cressie 1986, Cressie 1990). Cokriging uses an additional variable or variables sampled from the same location (e.g., elevation) to make an assisted estimation (Helterbrand and Cressie 1994). A spatial correlation is determined between the main variable and covariable(s) and the relationship is modeled. Cokriging is ideal for interpolating wind surfaces when stations are well distributed across a proportionate surface in a study area (e.g., if 10

percent of a study area is mountainous, then 10 percent of the wind stations should be located in the mountainous region) (Luo et al. 2008). However, knowledge-assisted forms of kriging such as cokriging are time-intensive and often require land segmentation and *in situ* verification, making cokriging an illogical choice for large datasets where this information is not available. Bayesian forms of kriging are the most computationally intensive with Monte Carlo or Markov chain techniques used to minimize the impact of uncertainty on model parameters (Lanza et al. 2001). There is currently no precedent for using the Bayesian approach for wind surface interpolation. ANNs have also been coupled with various kriging methods, but similar problems that occur with ANNs used outside of the kriging framework also occur when coupled with kriging (Cellura et al. 2008).

Table 2-1 provides examples of studies investigating the interpolation of wind speeds and other climatic data and highlights the methods that were recommended by each study. The literature does not recommend that deterministic methods be used for wind surface interpolation and the overall trend suggests that kriging (in various forms) continues to be a very good method for interpolating wind surfaces, but other network- and knowledge-based adaptations or improvements to kriging are ongoing. Many kriging adaptations are very promising, but a consensus has yet to be reached on a clear adaptation that will supersede current kriging methodologies. Further, the majority of these advanced studies focused on local- to regional-scale wind surfaces within a single country rather than large-scale surfaces that would include multiple countries. It is very difficult and time-intensive to apply advanced network- and knowledge-assisted kriging adaptations across multiple countries or to an entire continent without more

Table 2-1. Research studies that employed one of more spatial interpolation techniques to examine wind variables.

Source	Study Area(s)	Event Type	Methods Examined	Methods Recommended
(Bentamy et al. 1996)	Tropical Atlantic Ocean	Avg. wind speed (multi-year)	Kriging	Kriging
(Sterk and Stein 1997)	Sahelian zone (Niger)	Wind-blown mass transport from 4 storms (1993)	Linear Interpolation (Simulated Annealing), Ordinary Kriging	Ordinary Kriging was best at predicting unsampled locations; Simulated Annealing was best for local variability
(Phillips et al. 1997)	Southeast US	Ozone exposure (multi-year; used wind direction)	Inverse Distance Weighting, Inverse Distance Squared Weighting, Ordinary Kriging, Cokriging	Cokriging and Ordinary Kriging
(Venäläinen and Heikinheimo 2002)	Finland	Daily wind speed, temperature, humidity, precipitation, radiation	Kriging	Kriging
(Öztopal 2006)	Marmara, Turkey	Daily wind speed over time (potential wind energy)	Artificial Neural Network	Artificial Neural Network
(Cellura et al. 2008)	Sicily, Italy	Avg. wind speed at 50m for wind farm (multi-year)	Neural Network, Radial Basis Functions, Neural Kriging, Ordinary/Universal Kriging, Inverse Distance Weighting	Coupled Neural Network/Kriging Interpolators
(Luo et al. 2008)	England, Wales	Avg. wind speed (Mar. 27, 2001)	Trend Surface Analysis, Inverse Distance Weighting, Local Polynomial, Thin Plate Spline, Kriging, Cokriging	Cokriging and Ordinary Kriging
(Zlatev et al. 2009)	United Kingdom	Avg. wind speed/direction	Ordinary Kriging	Ordinary Kriging
(Zlatev et al. 2010)	United Kingdom	Avg. wind speed (Mar. 27, 2001)	Ordinary Kriging, Universal Kriging, Cokriging, Multi-region Ordinary Kriging	Multi-region Ordinary Kriging (Knowledge-assisted)
(Akkala et al. 2010)	None (Review article)	Multiple meteorological events (including wind storms)	Nearest Neighbor, Triangular Irregular Network, Polynomial Regression, Polynomial Interpolation, Trend Surface Analysis, Inverse Distance Weighting, Splines, Kriging, Radial Basis Functions, Artificial Neural Networks	Knowledge based/assisted techniques

detailed information about stations, microtopography, local environment, and other geographic features. The widely-varying terrain of Europe presents a challenge to these advanced approaches. As new data become available and as these new methods are explored and improved in the coming years, they may prove more useful for large-scale analyses and potentially be included in future software packages (e.g., ArcGIS).

2.1.2 Study area & objectives

This study seeks to develop historical wind speed maps for eighteen (18) wind storms that occurred between 1976 and 2010 over European countries. Storms will be analyzed individually to determine their accuracy and general trends. This study has two main objectives: 1) To identify an interpolation technique that accurately predicts wind speed surfaces over a large heterogeneous region, 2) To identify regions of Europe where high wind speeds have occurred during wind storms.

2.2 Data and Methods

2.2.1 Wind station data

Wind data were obtained from the World Meteorological Organization (WMO) observation stations sourced through a third party provider with support from Guy Carpenter & Company, LLC and ecityrisk (maps showing station locations available in Appendix). The WMO Standard (World Meterological Organization 2008) for measuring sustained wind is an average of values obtained for the 10 minutes previous to the observation time. The WMO Standard for measuring peak gust is a continuous average of values over a 3-second period. Wind instruments according to WMO standards are to be located at a height of 10 m in open terrain, and wind data are adjusted for local topographic effects through the use of a correction factor. For example, a station

located at the top of a hill would have a correction factor applied to the data to account for the changes in wind speed caused by the hill. According to the WMO chapter of wind standards (World Meterological Organization 2008), the wind speed would be more representative of the region rather than the individual hill. For the purpose of this study, all data and instruments were assumed to be in accordance with these WMO standards. A preliminary quality control analysis of the data was conducted by plotting the sustained wind and peak gust values against the mean of each variable. Outliers were examined closely to determine whether the values were reasonable for the given climatological conditions.

Station wind data from 18 major storm events were analyzed over the period 1976-2010 for Europe (Table 2-2). Many more wind storms occurred over this period of record, but storm selection for this study was based on economic impacts, not necessarily the strength of the storm. Each of the 18 storms caused major damage in one or more European countries, resulting in significant insured losses. These storms occurred mainly during cool-season months (October through March). MATLAB® was used to extract sustained wind and peak gust values from the original data files, which contained thousands of rows of observation data. The maximum daily value was extracted at each station for sustained wind and peak gust and the station maxima were identified from the daily maxima. A storm summary showing the statistics of data provided for sustained wind (Table 2-3) and peak gusts (Table 2-4) was produced for each storm. The sustained wind data were consistent between the storms, with only 0.8 percent of the data values missing and an overall mean sustained wind value of 15.0 meters per second ($m\ s^{-1}$). Peak gust measurements were missing for 77.6 percent of

the hourly observations and the overall mean peak gust was 25.5 m s^{-1}. The Durst method was utilized to create gust factors based on known maximum sustained wind speeds at the same location (Durst 1960, Krayer and Marshall 1992).

Table 2-2. European windstorm names and number of stations reporting sustained winds and peak gusts, for European storms analyzed.

Year	Storm	Countries	Sustained	Peak Gust	Sustained & Peak Gust	Total
1976	Capella	UK, Germany	231	56	56	231
1987	87J	France, UK	374	181	181	374
1990	Daria	UK, France, Belgium, Netherlands, Luxembourg, Germany	559	319	319	559
1990	Herta	Belgium, France, Germany, Netherlands, UK	516	276	276	516
1990	Vivian	Germany, UK, Switzerland, Belgium, France, Netherlands	585	337	337	585
1990	Wiebke	Switzerland, Belgium, France, Germany, Netherlands, UK	598	336	336	598
1999	Anatol	Denmark, Sweden, Germany	250	122	122	250
1999	Lothar	France, Switzerland, Germany	321	202	202	322
1999	Martin	France, Switzerland, Germany	324	195	195	325
2002	Jeanette	UK, Denmark, Sweden, Germany, Netherlands, France, Austria, Poland, Czech Republic, Belgium, Ireland	1014	406	406	1016
2004	Dagmar	UK, France, Germany	426	325	325	426
2005	Erwin	Germany, Norway, Sweden	433	125	125	433
2007	Kyrill	France, Netherlands, Germany, UK, Belgium, Austria, Ireland	637	418	418	637
2008	Paula	Poland, Germany, Austria, Denmark, Norway, Sweden	662	130	130	663
2008	Emma	Germany, Austria, Czech Republic, Belgium, Netherlands, Switzerland, Poland	495	216	216	496
2009	Klaus	France, Spain	214	185	185	214
2009	Quinten	France	147	138	138	147
2010	Xynthia	Belgium, Denmark, France, Germany, Poland, Portugal, Spain, Sweden, UK	896	557	557	896

Table 2-3. Summary table of sustained wind speeds (m s^{-1}) for each windstorm analyzed.

Year	Storm	Mean	Median	Minimum	Maximum	Range	Percent Missing
1976	Capella	18.2	18.0	2.5	36.0	33.5	0.0%
1987	87J	15.0	13.4	3.1	42.2	39.1	0.2%
1990	Daria	17.7	17.0	3.1	40.1	37.0	0.6%
1990	Herta	15.0	14.9	1.0	36.5	35.5	0.7%
1990	Vivian	18.6	18.3	2.1	39.6	37.5	0.4%
1990	Wiebke	17.2	17.0	2.1	39.6	37.5	0.4%
1999	Anatol	12.9	11.8	0.5	41.1	40.6	3.5%
1999	Lothar	16.4	15.9	0.0	40.1	40.1	1.4%
1999	Martin	16.1	16.0	0.0	48.0	48.0	1.4%
2002	Jeanette	13.9	13.4	0.0	42.0	42.0	0.5%
2004	Dagmar	13.2	12.0	0.0	39.0	39.0	0.5%
2005	Erwin	12.6	12.0	1.0	35.5	34.5	0.6%
2007	Kyrill	15.8	16.4	1.0	36.8	35.8	0.7%
2008	Paula	10.9	10.0	0.0	42.0	42.0	0.5%
2008	Emma	13.9	14.0	0.0	47.0	47.0	0.1%
2009	Klaus	15.3	14.9	4.6	40.1	35.5	0.9%
2009	Quinten	15.5	15.4	5.1	29.8	24.7	1.1%
2010	Xynthia	11.8	11.8	2.0	37.9	35.9	0.4%
	Average	15.0	14.6	1.6	39.6	38.1	0.8%

Table 2-4. Summary table of peak gust wind speeds (m s^{-1}) for each windstorm analyzed.

Year	Storm	Mean	Median	Minimum	Maximum	Range	Percent Missing
1976	Capella	25.2	25.0	7.2	41.1	33.9	93.7%
1987	87J	24.0	23.0	6.2	46.3	40.1	93.1%
1990	Daria	29.8	30.9	7.2	47.9	40.7	76.6%
1990	Herta	24.7	24.2	9.3	39.1	29.8	79.0%
1990	Vivian	30.3	30.9	12.9	47.8	34.9	69.9%
1990	Wiebke	27.7	27.8	9.3	47.8	38.5	72.5%
1999	Anatol	27.1	25.9	12.9	51.0	38.1	73.4%
1999	Lothar	26.1	24.5	9.3	72.0	62.7	80.0%
1999	Martin	25.4	25.2	8.7	72.0	63.3	90.5%
2002	Jeanette	26.0	27.0	0.0	52.0	52.0	79.3%
2004	Dagmar	20.9	20.1	8.2	45.0	36.8	80.4%
2005	Erwin	23.3	22.0	8.2	46.0	37.8	78.4%
2007	Kyrill	26.2	27.0	0.0	56.0	56.0	69.3%
2008	Paula	21.0	21.0	7.7	48.0	40.3	90.6%
2008	Emma	27.1	26.8	10.3	62.0	51.7	67.1%
2009	Klaus	26.5	25.2	11.3	53.0	41.7	63.0%
2009	Quinten	25.5	26.3	15.4	41.2	25.8	57.3%
2010	Xynthia	22.0	21.1	5.0	50.0	45.0	82.4%
	Average	25.5	25.2	8.3	51.0	42.7	77.6%

2.2.2 Wind Surface Interpolation

Ordinary kriging was chosen to interpolate wind station data based on its superiority over other techniques for representing wind speeds (Table 2-1). Specifically, the spherical method of ordinary kriging was chosen to examine both peak gust and sustained maximum wind speeds for multiple European wind storms because it produces a smooth surface variation with a clear nugget size and range. Anisotropic semivariograms were created during the interpolation procedure to account for directional dependence of wind speeds at varying distances. Dominant directional trends were automatically detected for each storm and wind type. This most often resulted in directional trends that logically corresponded to storm tracks, but occasionally dominant trends were difficult to determine and directionality was adjusted accordingly. Additionally, a variable search radius was determined based on an optimized number of points through cross-validation using the Geostatistical Analysis tool in ArcGIS Version 9.3 (ESRI 2010). A radius of 15 points was determined to adequately reflect spatial covariance, meaning that appropriate range and sill values could be determined by incorporating this number of points to estimate local surface trends similar to a moving window. For semivariogram surface creation, an eight sector elliptical search type with three neighbors per sector was specified to optimize surface variability.

The interpolation parameters were selected to obtain the highest accuracy based on the station data. Multiple measures of accuracy and uncertainty including standardized mean error (ME), standardized root mean square error (RMSE), and minimum/maximum range were used to determine the validity of each kriging-derived surface, but these statistical measures only measure the accuracy as it is related to

observed and estimated variability of wind speed on the surface. The standardized RMSE and ME as well as the minimum/maximum surface estimates were used to evaluate the interpolated surface and compare the accuracy for each storm. Relatively lower values (close to zero) for ME and values closest to one for RMSE are preferred. ME values that are close to zero indicate an unbiased prediction centered on the measurement values. Prediction standard errors were used to assess the uncertainty of the estimated surface; therefore standardized RMSE values estimated the variability of the predictions from the measurement values with values near one indicating lower variability between predicted and measured values. A wider minimum/maximum range estimate infers more variability in wind speeds across the interpolated surface, while a narrower minimum/maximum range estimate infers more conformity in wind speeds across the interpolated surface. Negative ME values infer that variability was underestimated, while positive ME values infer variability was overestimated. RMSE values less than 1 infer that variability was overestimated, while RMSE values greater than 1 infer that variability was underestimated. In addition to measuring the accuracy of the interpolated surfaces variability, storm tracks and other reports were used to validate the actual trends, locations, and magnitudes of estimated wind speeds.

2.3 Results

Spherical kriging was performed for the maximum sustained wind speed and the peak gust wind speed for each of the 18 storms. This resulted in two interpolations for each storm for a total of 36 interpolations. RMSE values close to one and ME values close to zero indicated that each interpolated surface was reasonably accurate (Table 2-5). If ME values were very close to zero (< +/- 0.003), then ME indicated indiscernible variability or no meaningful variability. Likewise, overestimation/underestimation of

Table 2-5. Accuracy metrics for each storm (m s^{-1}) by wind type, including variability and error extent (mean error (ME) and root mean square error (RMSE).

Storm Name	Wind Type	Min Value	Max Value	ME	RMSE
Capella	Max Sustained	10.65	23.00	-0.015	1.053
	Peak Gust	17.07	36.20	-0.008	1.050
87J	Max Sustained	7.89	23.27	0.009	0.945
	Peak Gust	11.56	35.22	0.006	0.982
Daria	Max Sustained	7.85	29.35	0.002	1.087
	Peak Gust	11.61	43.34	0.002	1.101
Herta	Max Sustained	6.54	23.18	0.005	1.035
	Peak Gust	9.45	34.98	-0.001	1.055
Vivian	Max Sustained	9.76	26.73	0.005	1.066
	Peak Gust	16.46	42.22	0.006	1.091
Wiebke	Max Sustained	10.67	25.15	-0.006	1.044
	Peak Gust	16.53	40.01	-0.009	1.069
Anatol	Max Sustained	1.74	26.66	-0.007	0.860
	Peak Gust	2.57	39.60	-0.011	0.872
Lothar	Max Sustained	9.44	28.65	0.009	0.952
	Peak Gust	14.69	45.01	0.009	0.979
Martin	Max Sustained	7.27	26.35	-0.003	0.998
	Peak Gust	11.15	40.31	-0.002	1.009
Jeanette	Max Sustained	4.20	23.58	0.001	1.021
	Peak Gust	6.27	34.43	0.003	1.015
Dagmar	Max Sustained	9.39	20.72	0.002	0.989
	Peak Gust	14.07	30.01	0.004	0.943
Erwin	Max Sustained	2.08	25.53	0.002	1.014
	Peak Gust	2.97	38.17	0.000	1.023
Kyrill	Max Sustained	5.09	23.29	0.008	1.125
	Peak Gust	7.37	35.54	0.000	1.110
Paula	Max Sustained	3.47	21.48	0.004	1.054
	Peak Gust	4.98	37.05	0.009	0.919
Emma	Max Sustained	6.74	22.15	-0.012	0.925
	Peak Gust	10.09	29.83	0.004	0.951
Klaus	Max Sustained	10.56	24.58	-0.022	0.948
	Peak Gust	15.58	36.96	-0.018	0.956
Quinten	Max Sustained	13.06	22.13	0.006	1.210
	Peak Gust	19.92	32.69	0.013	1.178
Xynthia	Max Sustained	4.23	21.08	0.000	1.043
	Peak Gust	5.96	32.52	0.002	1.049

variability was also indiscernible if RMSE was very close to one (within 0.02). If the two metrics conflict (e.g., ME is negative indicating underestimation and RMSE is < 1.0

indicating overestimation), this indicates that some parts of the surface underestimate the variability and other parts of the surface overestimate the variability. This often, but not always, represents a well-fit surface considering the dataset and smoothing parameters. Additionally, standardized error was also examined at the station-level and the locations of those stations that had a high standardized error of +/- 2.0 were identified. To quality-control the interpolation output with known storm tracks and magnitudes, additional reports of some wind storms were obtained. Storm tracks were compared with general trends, locations of highest/lowest winds and maximum wind speed values seen in the interpolation (Aon Benfield , Guy Carpenter & Company Ltd 2005, Risk Management Solutions 2006). Data about maximum wind speed and storm damage were also evaluated for storms where data were available (EQE International , Fink et al. 2009).

Two interpolated surfaces were created for each storm and the corresponding maps represent both the highest maximum sustained wind speeds and the highest peak gust wind speeds for the duration of each storm. The maximum sustained wind speed maps illustrate 10-minute continuously-sampled (adjusted from disjunctly-sampled) sustained wind in open terrain, while the peak gust wind speed maps illustrate continuously sampled 3-second gust in open terrain.

2.3.1 Capella wind storm

A minimum/maximum range estimate (difference between highest and lowest predicted wind speeds on the modeled surface for the storm as a whole) of 12.35 m s^{-1} was produced by the maximum sustained wind speed interpolation (Figure 2-2a). A negative ME value of -0.015 and a RMSE value of 1.053 indicated that maximum sustained wind speed variability was slightly underestimated for the interpolated surface

when compared to observed maximum sustained wind speed variability. A minimum/maximum range estimate of 19.13 m s^{-1} was produced by the peak gust wind speed interpolation (Figure 2-2b). A negative ME value of -0.008 and a RMSE value of 1.050 indicated that peak gust wind speed variability was, similar to the maximum sustained wind speed, slightly underestimated for the interpolated surface when compared to observed peak gust wind speed variability. High wind speeds between 30-36 m s^{-1} occurred through the central United Kingdom and northern Europe around coastal Germany and Denmark. The spatial distribution of high wind speeds is consistent with the actual storm track for Capella which was north of these areas. The highest wind gusts for Capella were reported along the eastern coast of the United Kingdom, which matches areas of high wind speed predicted by the interpolation. The overall west-east trend in wind speeds was also correctly identified by the interpolation.

2.3.2 87J wind storm

A minimum/maximum range estimate of 15.39 m s^{-1} was produced by the maximum sustained wind speed interpolation (Figure 2-2c). A positive ME value of 0.009 and a RMSE value of 0.945 indicated that maximum sustained wind speed variability was slightly overestimated for the interpolated surface when compared to observed maximum sustained wind speed variability. A minimum/maximum range estimate of 23.66 m s^{-1} was produced by the peak gust wind speed interpolation (Figure 2-2d). A positive ME value of 0.006 and a RMSE value of 0.982 indicated that peak gust wind speed variability was, similar to the maximum sustained wind speed, slightly overestimated for the interpolated surface when compared to observed peak gust wind speed variability. The 87J wind storm passed through the southern United Kingdom and proceeded into the North Sea. The interpolation correctly identified the storm track

since it was to the north of the highest wind speeds. Given the southwest to northeast trend in the storm track and wind speeds, the highest wind speeds (30-39 m s^{-1}) occurred south of the track in the coastal areas surrounding the English Channel as expected.

2.3.3 Daria wind storm

A minimum/maximum range estimate of 21.50 m s^{-1} was produced by the maximum sustained wind speed interpolation (Figure 2-2e). A ME value near zero (0.002) and a RMSE value of 1.087 indicated that maximum sustained wind speed variability was slightly underestimated for the interpolated surface when compared to observed maximum sustained wind speed variability. A minimum/maximum range estimate of 31.73 m s^{-1} was produced by the peak gust wind speed interpolation (Figure 2-2f). A ME value near zero (0.002) and a RMSE value of 1.101 indicated that peak gust wind speed variability was, similar to the maximum sustained wind speed, slightly underestimated for the interpolated surface when compared to observed peak gust wind speed variability. The Daria wind storm tracked from the westsouthwest to the eastnortheast and the interpolated wind speeds exhibited a similar pattern with the highest wind speeds occurring in the appropriate location considering the track. The highest wind speeds (36-45 m s^{-1}) were seen in the southern United Kingdom, northern France, and coastal Netherlands, Belgium, and Germany. Wind speeds also maintained or increased speed in the mountainous areas of southeast Germany and the Black Forest area of southwest Germany.

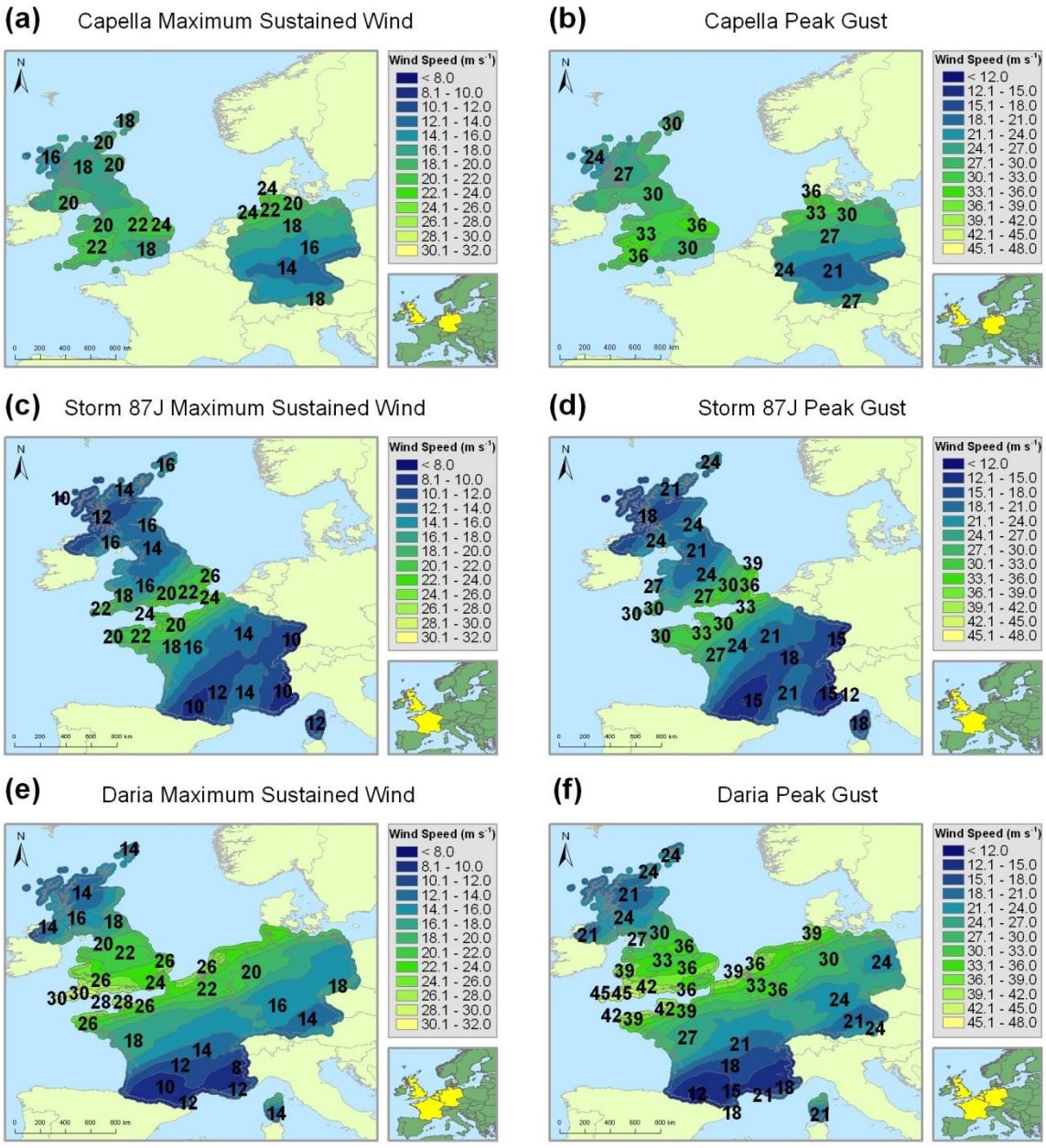

Figure 2-2. Maximum sustained and peak gust wind speed interpolations for the Capella (1976) (a, b), 87J (1987) (c, d), and Daria (1990) (e, f) wind storms.

2.3.4 Herta wind storm

A minimum/maximum range estimate of 16.63 m s^{-1} was produced by the maximum sustained wind speed interpolation (Figure 2-3a). A positive ME value of 0.005 and a RMSE value of 1.035 indicated that maximum sustained wind speed

variability was estimated accurately for the interpolated surface when compared to observed maximum sustained wind speed variability. A minimum/maximum range estimate of 25.53 m s^{-1} was produced by the peak gust wind speed interpolation (Figure 2-3b). A ME value near zero (-0.001) and a RMSE value of 1.055 indicated that peak gust wind speed variability was very slightly underestimated for the interpolated surface when compared to observed peak gust wind speed variability. The storm track generally followed a west-east path through northern France and the interpolation is consistent with previous storm reports. The highest wind speeds (30-36 m s^{-1}) were found south of the storm in northwestern France.

2.3.5 Vivian wind storm

A minimum/maximum range estimate of 16.97 m s^{-1} was produced by the maximum sustained wind speed interpolation (Figure 2-3c). A positive ME value of 0.005 and a RMSE value of 1.066 indicated that maximum sustained wind speed variability was slightly overestimated in some areas and slightly underestimated in other areas when compared to observed maximum sustained wind speed variability. A minimum/maximum range estimate of 25.76 m s^{-1} was produced by the peak gust wind speed interpolation (Figure 2-3d). A positive ME value of 0.006 and a RMSE value of 1.091 indicated that peak gust wind speed variability was also slightly overestimated in some areas and slightly underestimated in other areas when compared to observed peak gust wind speed variability. The regions of highest wind speed shown in the interpolation generally reflect the storm track for Vivian, which was to the north of the highest wind speeds along a general west-east path across the central United Kingdom and into the North Sea. The highest wind speeds (36-42 m s^{-1}) occurred around the English Channel and in northern coastal areas of the Netherlands and Germany as well

as the central United Kingdom. The interpolation coverage would be improved with additional observations from Denmark, Sweden, and Norway. The interpolated wind speed does show an increase in southern Germany near the Black Forest, Alps, and Swiss borders as other reports suggest.

2.3.6 Wiebke wind storm

A minimum/maximum range estimate of 14.48 m s^{-1} was produced by the maximum sustained wind speed interpolation (Figure 2-3e). A negative ME value of -0.006 and a RMSE value of 1.044 indicated that maximum sustained wind speed variability was slightly underestimated for the interpolated surface when compared to observed maximum sustained wind speed variability. A minimum/maximum range estimate of 23.48 m s^{-1} was produced by the peak gust wind speed interpolation (Figure 2-3f). A negative ME value of -0.009 and a RMSE value of 1.069 indicated that peak gust wind speed variability was, similar to the maximum sustained wind speed, slightly underestimated for the interpolated surface when compared to observed peak gust wind speed variability. The highest wind speeds for the Wiebke wind storm were found to the immediate south of the reported track. The winds were highest (30-39 m s^{-1}) in the southwestern United Kingdom, northern France, and at the base of the Alps – consistent with high wind locations identified in previous reports.

2.3.7 Anatol wind storm

A minimum/maximum range estimate of 24.92 m s^{-1} was produced by the maximum sustained wind speed interpolation (Figure 2-4a). A negative ME value of -0.007 and a RMSE value of 0.860 indicated that maximum sustained wind speed variability for the interpolated surface was possibly underestimated in some locations

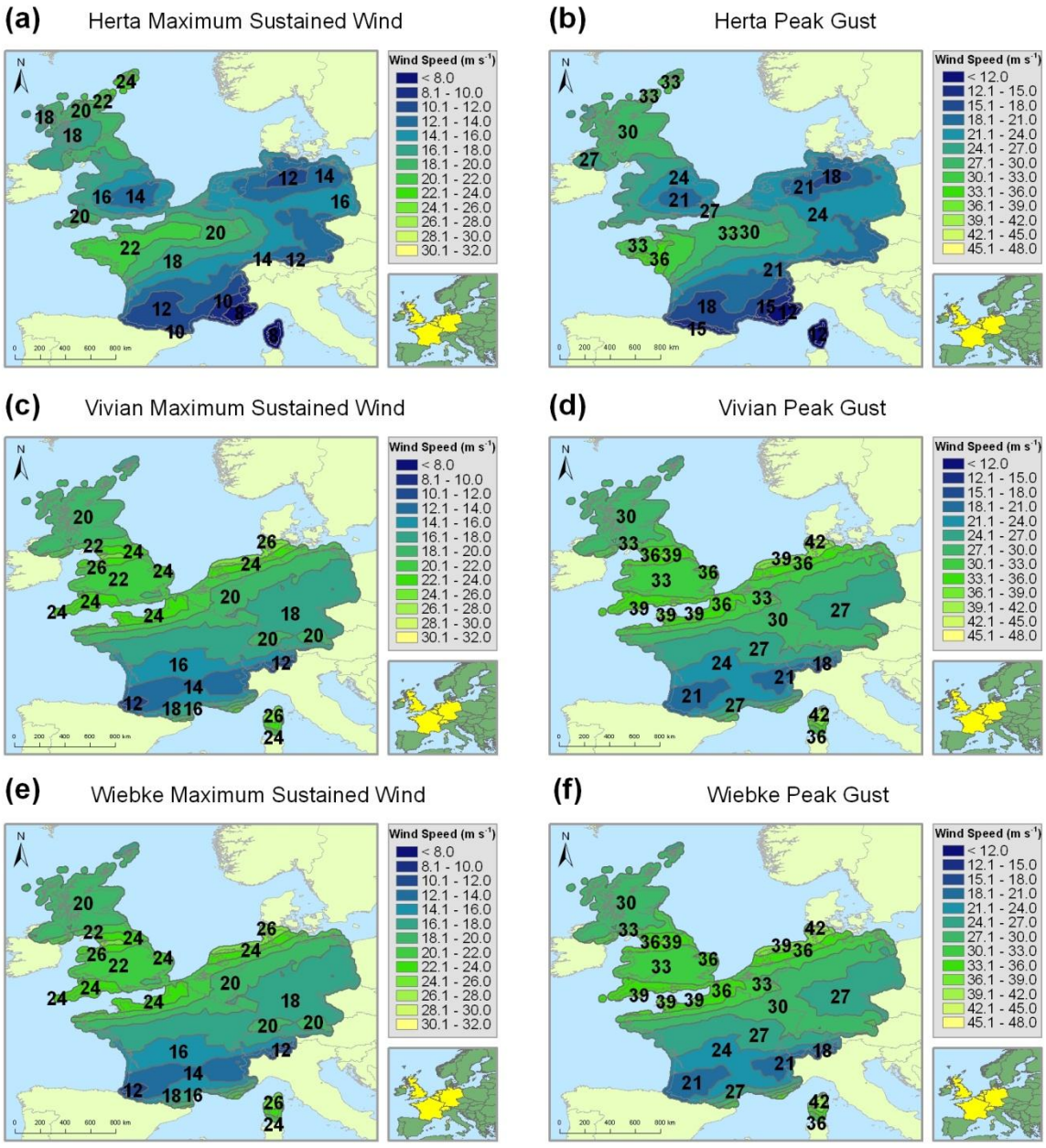

Figure 2-3. Maximum sustained and peak gust wind speed interpolations for the Herta (a, b), Vivian (c, d), and Wiebke (e, f) wind storms; all three storms occurred in 1990.

and overestimated in others when compared to observed maximum sustained wind speed variability, leading to higher conflicting accuracy scores. A minimum/maximum range estimate of 37.03 m s^{-1} was produced by the peak gust wind speed interpolation

(Figure 2-4b). A negative ME value of -0.011 and a RMSE value of 0.872 indicated that peak gust wind speed variability was, similar to the maximum sustained wind speed, underestimated in some locations and overestimated in other locations when compared to observed peak gust wind speed variability. High wind speeds occurred south of the storms' track across northern Europe and Denmark in areas that are consistent with where the storm track was actually located. The interpolation correctly identified this area and the overall west-east trend in wind speeds associated with the Anatol wind storm. Anatol produced some of the higher widespread wind speeds (~42 m s^{-1}) among recent wind storms and this was confirmed by the interpolation.

2.3.8 Lothar wind storm

A minimum/maximum range estimate of 19.22 m s^{-1} was produced by the maximum sustained wind speed interpolation (Figure 2-4c). A positive ME value of 0.009 and a RMSE value of 0.952 indicated that maximum sustained wind speed variability was slightly overestimated for the interpolated surface when compared to observed maximum sustained wind speed variability. A minimum/maximum range estimate of 30.32 m s^{-1} was produced by the peak gust wind speed interpolation (Figure 2-4d). A positive ME value of 0.009 and a RMSE value of 0.979 indicated that peak gust wind speed variability was, similar to the maximum sustained wind speed, slightly overestimated for the interpolated surface when compared to observed peak gust wind speed variability. The Lothar wind storm followed a west-east track through northern France and into central Germany with the highest winds (33-42 m s^{-1}) occurring south of this track in France and southern Germany. Some reports of wind speeds 8-9 m s^{-1} higher than those shown in the interpolation occurred in parts of France. These local extremes were most likely not widespread and thus smoothed by the interpolation.

Similar to other reports, high wind speeds also occurred near the onset of mountainous regions in southeastern Germany bordering Switzerland and Austria.

2.3.9 Martin wind storm

A minimum/maximum range estimate of 19.08 m s^{-1} was produced by the maximum sustained wind speed interpolation (Figure 2-4e). A ME value near zero (-0.003) and a RMSE value of 0.998 indicated that maximum sustained wind speed variability was estimated accurately for the interpolated surface when compared to observed maximum sustained wind speed variability. A minimum/maximum range estimate of 29.16 m s^{-1} was produced by the peak gust wind speed interpolation (Figure 2-4f). A ME value near zero (-0.002) and a RMSE value of 1.009 indicated that peak gust wind speed variability was, similar to the maximum sustained wind speed, estimated accurately for the interpolated surface when compared to observed peak gust wind speed variability. The Martin wind storm followed closely behind Lothar by only one day. The track of this storm was further south than Lothar and the interpolation confirmed this trend. Consistent with other reports, the location of the highest wind speeds (33-42 m s^{-1}) was in western France and the mountainous areas of southern Germany.

2.3.10 Jeanette wind storm

A minimum/maximum range estimate of 19.39 m s^{-1} was produced by the maximum sustained wind speed interpolation (Figure 2-5a). A ME value near zero (0.001) and a RMSE value of 1.021 indicated that maximum sustained wind speed variability was estimated accurately for the interpolated surface when compared to observed maximum sustained wind speed variability. A minimum/maximum range

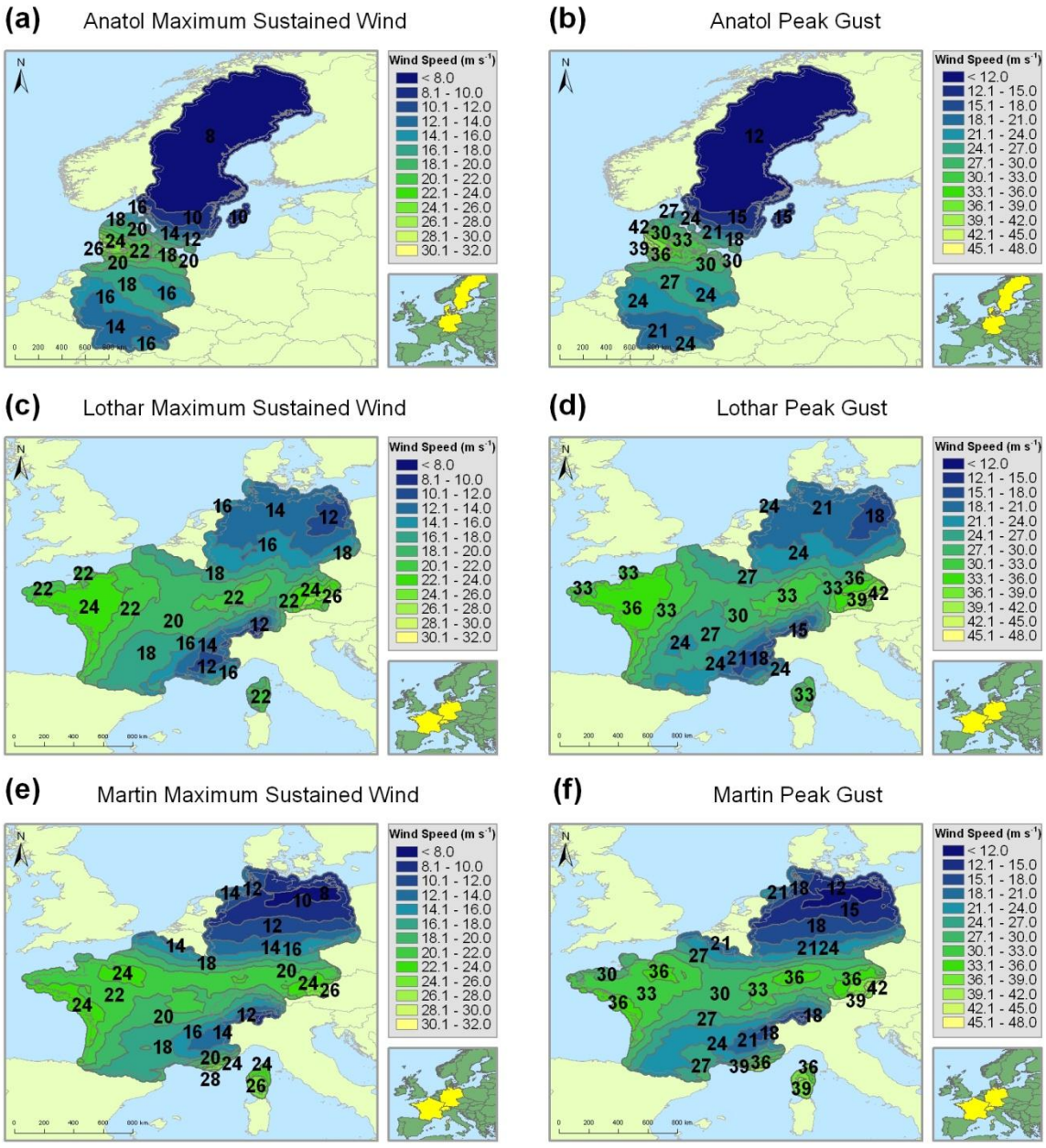

Figure 2-4. Maximum sustained and peak gust wind speed interpolations for the Anatol (a, b), Lothar (c, d), and Martin (e, f) wind storms; all three storms occurred in 1999.

estimate of 28.17 m s^{-1} was produced by the peak gust wind speed interpolation (Figure 2-5b). A ME value near zero (0.003) and a RMSE value of 1.015 indicated that peak gust wind speed variability was, similar to the maximum sustained wind speed,

estimated accurately for the interpolated surface when compared to observed peak gust wind speed variability. Areas of high wind speed (30-36 m s^{-1}) occurred south of the storm track in parts of the central United Kingdom as well as coastal Germany, Netherlands, and Belgium. Some parts of central and eastern Germany also received high winds in the 30-33 m s^{-1} range, similar to those found in other reports.

2.3.11 Dagmar wind storm

A minimum/maximum range estimate of 11.33 m s^{-1} was produced by the maximum sustained wind speed interpolation (Figure 2-5c). A ME value near zero (0.002) and a RMSE value of 0.989 indicated that maximum sustained wind speed variability was estimated accurately for the interpolated surface when compared to observed maximum sustained wind speed variability. A minimum/maximum range estimate of 15.95 m s^{-1} was produced by the peak gust wind speed interpolation (Figure 2-5d). A ME value slightly higher than zero (0.004) and a RMSE value of 0.943 indicated that peak gust wind speed variability was slightly overestimated for the interpolated surface when compared to observed peak gust wind speed variability. According to the interpolation, the highest wind speeds (18-20 m s^{-1}) were in northern France and the southern United Kingdom around the English Channel. The storm followed a west-east path across the southern United Kingdom and into northern Europe.

2.3.12 Erwin wind storm

A minimum/maximum range estimate of 23.45 m s^{-1} was produced by the maximum sustained wind speed interpolation (Figure 2-5e). A ME value near zero (0.002) and a RMSE value of 1.014 indicated that maximum sustained wind speed

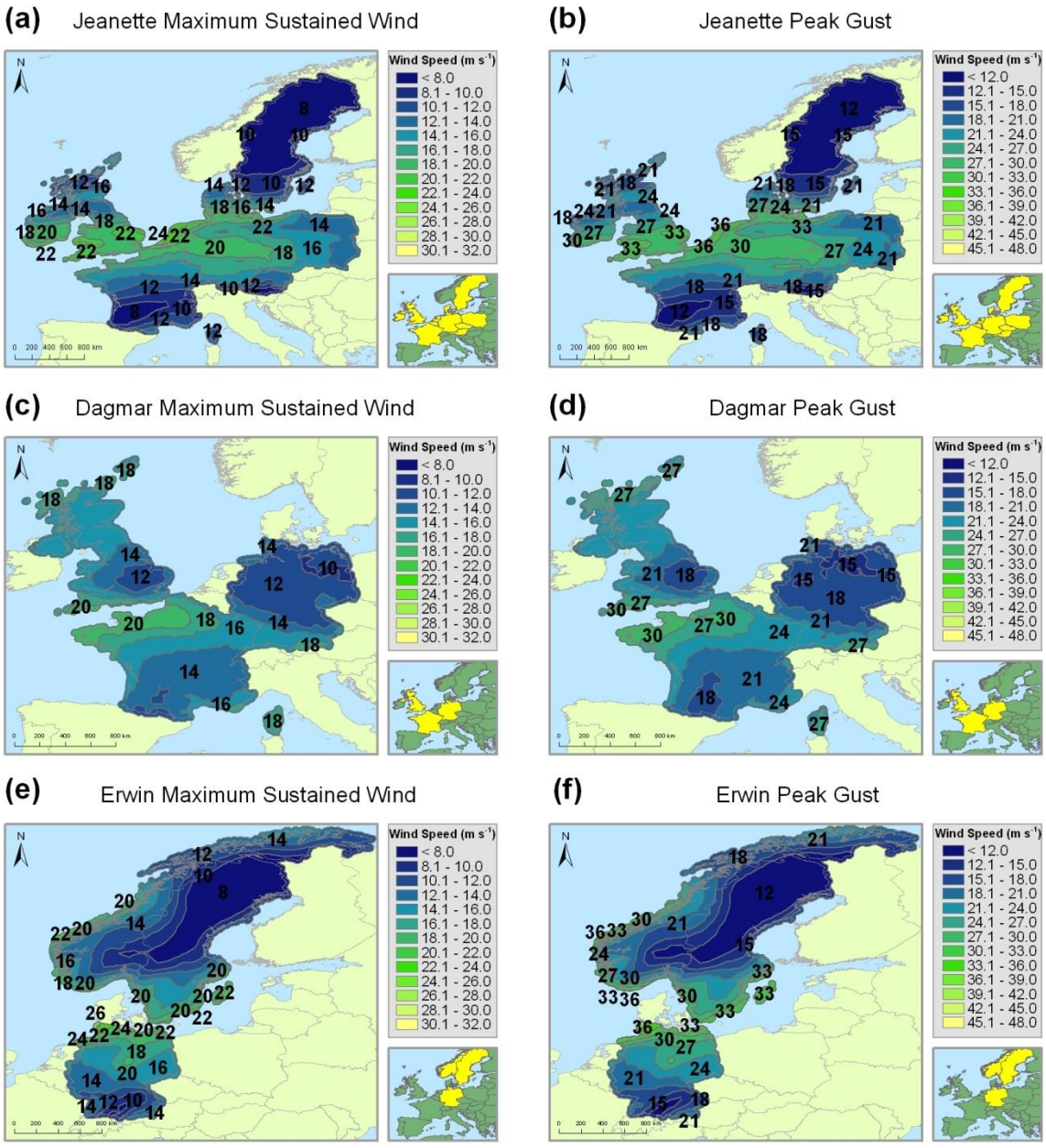

Figure 2-5. Maximum sustained and peak gust wind speed interpolations for the Jeanette (2002) (a, b), Dagmar (2004) (c, d), and Erwin (2005) (e, f) wind storms.

variability was estimated accurately for the interpolated surface when compared to observed maximum sustained wind speed variability. A minimum/maximum range estimate of 35.19 m s^{-1} was produced by the peak gust wind speed interpolation (Figure

2-5f). A ME value near zero (~0.000) and a RMSE value of 1.023 indicated that peak gust wind speed variability was, similar to the maximum sustained wind speed, estimated accurately for the interpolated surface when compared to observed peak gust wind speed variability. The highest wind speeds (33-39 m s^{-1}) were observed in coastal areas of Norway, Sweden, and Germany – consistent with other reports. High wind speeds shifted from being on the western coast of Norway to the southeastern coast of Sweden all within a 24-hour period because of the Erwin storm track. This shift indicates why the interpolations show high wind speeds in both locations even though they are seemingly disconnected since no data were available from Denmark.

2.3.13 Kyrill wind storm

A minimum/maximum range estimate of 18.21 m s^{-1} was produced by the maximum sustained wind speed interpolation (Figure 2-6a). A positive ME value of 0.008 and a RMSE value of 1.125 indicated that maximum sustained wind speed variability was slightly overestimated in some areas and slightly underestimated in other areas when compared to observed maximum sustained wind speed variability. A minimum/maximum range estimate of 28.17 m s^{-1} was produced by the peak gust wind speed interpolation (Figure 2-6b). A ME value near zero (~0.000) and a RMSE value of 1.110 indicated that peak gust wind speed variability was slightly underestimated in some areas when compared to observed peak gust wind speed variability. The southern and central United Kingdom as well as central Germany received the highest widespread winds (30-36 m s^{-1}) associated with the Kyrill wind storm. High winds occurred south of the storm's west-east path.

2.3.14 Paula wind storm

A minimum/maximum range estimate of 18.01 m s^{-1} was produced by the maximum sustained wind speed interpolation (Figure 2-6c). A ME value slightly higher than zero (0.004) and a RMSE value of 1.054 indicated that maximum sustained wind speed variability was slightly overestimated in some areas and slightly underestimated in other areas when compared to observed maximum sustained wind speed variability. A minimum/maximum range estimate of 32.07 m s^{-1} was produced by the peak gust wind speed interpolation (Figure 2-6d). A positive ME value of 0.009 and a RMSE value of 0.919 indicated that peak gust wind speed variability was slightly overestimated for the interpolated surface when compared to observed peak gust wind speed variability. The highest wind speeds (27-36 m s^{-1}) for the Paula wind storm occurred in coastal Norway and Denmark, with a noticeable increase in wind speeds also occurring in the area between mainland Denmark and mainland Sweden. All iterations of the interpolation slightly underestimated expected high wind speeds along the Alps, possibly because of offsetting high and low wind speed observations in the area, but the interpolations were otherwise consistent with other reports.

2.3.15 Emma wind storm

A minimum/maximum range estimate of 15.41 m s^{-1} was produced by the maximum sustained wind speed interpolation (Figure 2-6e). A negative ME value of -0.012 and a RMSE value of 0.925 indicated that maximum sustained wind speed variability was slightly underestimated in some areas and slightly overestimated in other areas when compared to observed maximum sustained wind speed variability. A minimum/maximum range estimate of 19.74 m s^{-1} was produced by the peak gust wind speed interpolation (Figure 2-6f). A slightly positive ME value of 0.004 and a RMSE

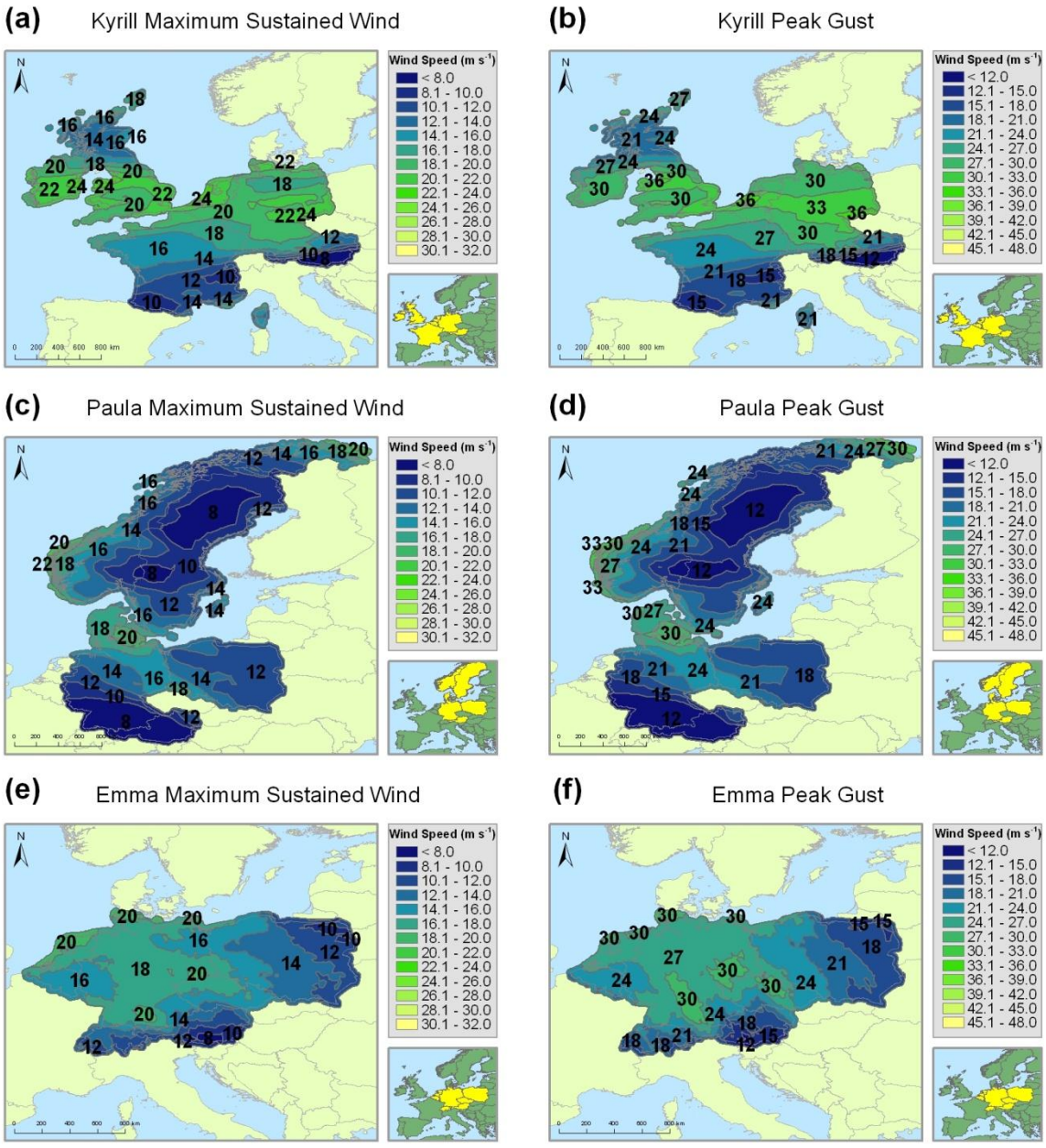

Figure 2-6. Maximum sustained and peak gust wind speed interpolations for the Kyrill (2007) (a, b), Paula (2008) (c, d), and Emma (2008) (e, f) wind storms.

value of 0.951 indicated that peak gust wind speed variability was slightly overestimated for some areas and underestimated for other areas of the interpolated surface when compared to observed peak gust wind speed variability. The wind estimates (27-30 m

s^{-1}) seen in the interpolation were reasonable compared to other reports and the location of high winds in the Netherlands and northern Germany were consistent with the storm's track. Pockets of high wind were also noticeable in southern Germany and the Czech Republic.

2.3.16 Klaus wind storm

A minimum/maximum range estimate of 14.02 m s^{-1} was produced by the maximum sustained wind speed interpolation (Figure 2-7a). A negative ME value of -0.022 and a RMSE value of 0.948 indicated that maximum sustained wind speed variability was underestimated in some areas and overestimated in other areas when compared to observed maximum sustained wind speed variability. A minimum/maximum range estimate of 21.38 m s^{-1} was produced by the peak gust wind speed interpolation (Figure 2-7b). A negative ME value of -0.018 and a RMSE value of 0.956 indicated that peak gust wind speed variability was underestimated for some areas and overestimated for other areas of the interpolated surface when compared to observed peak gust wind speed variability. The highest wind speeds (30-39 m s^{-1}) occurred on the Atlantic coast near the France/Spain border. These high wind speeds occurred south of the storm's path. The interpolated peak gust wind speeds are 2-3 m s^{-1} higher on the Atlantic Ocean side of the France/Spain border and about 7 m s^{-1} higher in the mountainous region between France and Spain than reported elsewhere. This is most likely caused by the relative proximity of high and low wind speed observations in the mountainous region, thus causing a balancing affect.

2.3.17 Quinten wind storm

A minimum/maximum range estimate of 9.07 m s^{-1} was produced by the maximum sustained wind speed interpolation (Figure 2-7c). A slightly positive ME

(0.006) and a RMSE value of 1.210 indicated that maximum sustained wind speed variability was slightly overestimated in some areas and slightly underestimated in other areas when compared to observed maximum sustained wind speed variability. A minimum/maximum range estimate of 12.77 m s^{-1} was produced by the peak gust wind speed interpolation (Figure 2-7d). A positive ME value of 0.013 and a RMSE value of 1.178 indicated that peak gust wind speed variability was slightly overestimated for some areas and slightly underestimated for other areas of the interpolated surface when compared to observed peak gust wind speed variability. The highest wind speeds (30-36 m s^{-1}) for the Quinten wind storm occurred in coastal western France and a small area of northern France along the English Channel – consistent with other reports. The storm moved in a general west-east direction with high wind speeds occurring in concurrent locations south of the reported track.

2.3.18 Xynthia wind storm

A minimum/maximum range estimate of 16.85 m s^{-1} was produced by the maximum sustained wind speed interpolation (Figure 2-7e). A very low ME (~0.000) and a RMSE value of 1.043 indicated that maximum sustained wind speed variability was very slightly underestimated in some areas when compared to observed maximum sustained wind speed variability. A minimum/maximum range estimate of 26.56 m s^{-1} was produced by the peak gust wind speed interpolation (Figure 2-7f). A ME value near zero (0.002) and a RMSE value of 1.049 indicated that peak gust wind speed variability was very slightly underestimated for some areas when compared to observed peak gust wind speed variability. Wind speed magnitudes and locations were similar to other reports for the Xynthia wind storm with the highest wind speeds (27-33 m s^{-1}) occurring

in northern Spain and central France. The storm followed a general southwest to northeast path and the high wind speeds followed a similar directional trend.

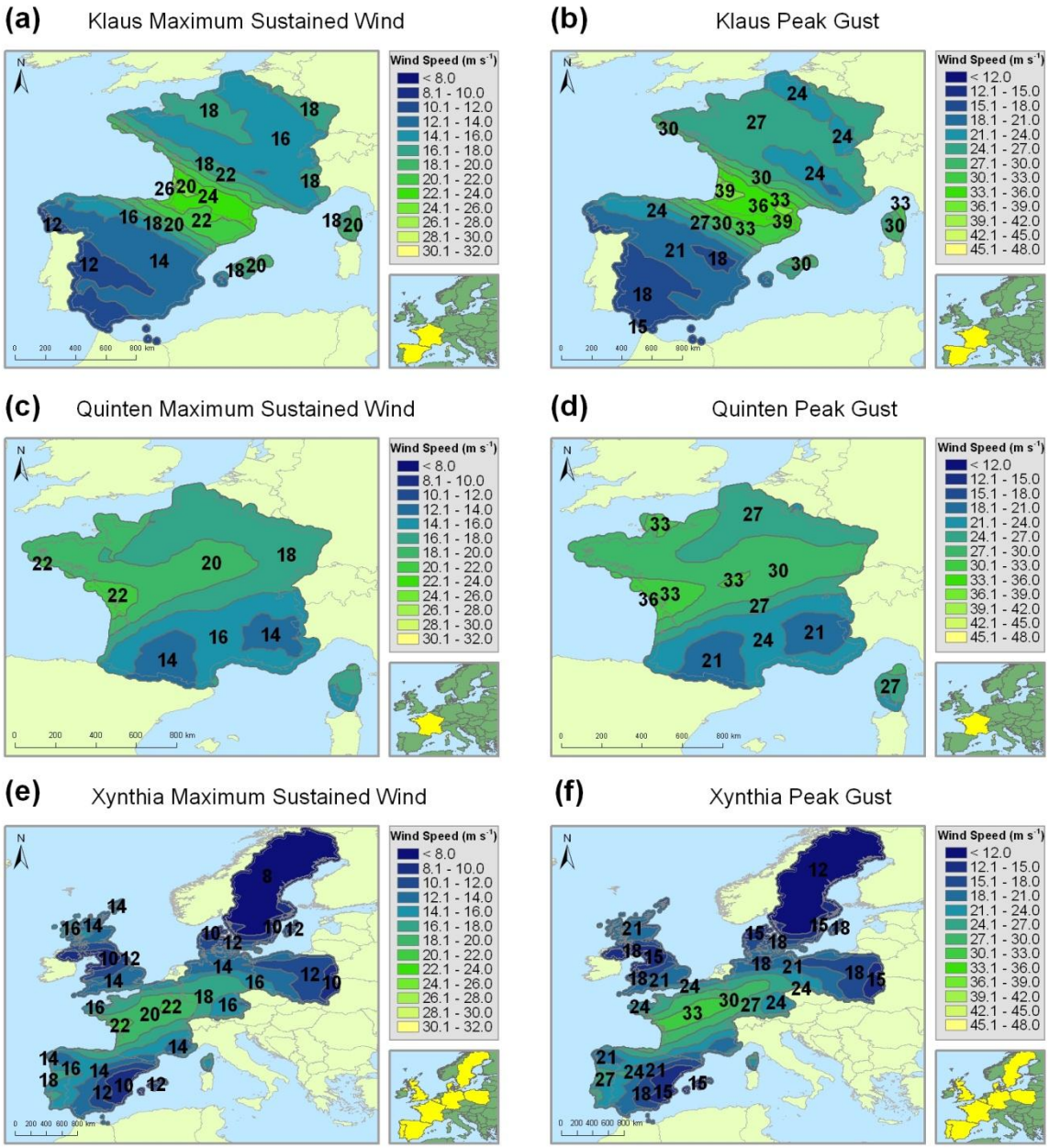

Figure 2-7. Maximum sustained and peak gust wind speed interpolations for the Klaus (2009) (a, b), Quinten (2009) (c, d), and Xynthia (2010) (e, f) wind storms.

2.4 Discussion

The variability of the estimated, or predicted, wind surface, as it relates to the observed surface, is the first statistical means of determining the interpolation's accuracy. Variability accuracy metrics (e.g., standardized ME and RMSE) indicated a reasonable and logical prediction for all storms, but some predicted slightly more accurately than others. The highest ME was reported for the Klaus wind storm interpolation. High negative ME values were found for both maximum sustained wind and peak gust, indicating an underestimation of the surface, but the RMSE was less than one, which indicated an overestimated surface. The conflict was most likely created by high variability in mountainous regions of the Pyrenees along the France/Spain border that has multiple topographic peaks well over 3000 meters. The lowest RMSE was reported for the Anatol wind storm, but the concurrent ME values again conflicted in the opposite direction. The variability between adjacent coastal weather stations may have led to an overestimation of variability in the coastal area, but an underestimation of variability in the interior areas. Also, much of central and northern Sweden were minimally impacted by the Anatol wind storm and including this large area in the interpolation may have impacted the variability of the surface. The highest RMSE values were reported for the Quinten wind storm, inferring that more variability occurred on the surface than was predicted. Some variability along the coast near landfall may have been lost in the interpolation because of the location of weather stations adjacent to coves, peninsulas, or other coastal geographic features.

It is also important to note that standardized error was often highest (+/- 2.0 standard deviations) at stations that were located in mountainous or coastal areas that often experienced the highest wind speeds for each storm. Stations with high positive

standardized error were often adjacent to stations with high negative standardized error, indicating that wind speed can be drastically different across short distances depending on many geographic and atmospheric factors. Stations with high positive/negative standardized error may also need to be examined individually to check their overall accuracy and dependability. It is not expected that kriging, or other interpolation methods, would capture this disparate variability because the method predominantly predicts widespread (macroclimatological) wind speed patterns and not highly local (microclimatological) anomalies. However, kriging, as applied in this study, proved to be an excellent interpolation method for estimating the general wind surface associated with wind storms occurring across the diverse European landscape.

Maximum sustained and peak gust wind speed interpolations consistently underestimated the highest reported winds and overestimated the lowest reported winds. These values were usually in the highest or lowest 3 percent of observed wind speeds and thus would have been considered outliers by the interpolation when creating the distribution of wind speeds across the surface. Extreme local high/low wind speeds are accounted for by kriging because these observations impact the trend and directional covariance of wind speeds, but they are not predicted exactly because they would cause an illogical “eye” effect similar to an IDW-interpolated surface. This, in turn, would have impacted the accuracy of wind speeds surrounding the anomalous stations and increased inaccuracy (Luo et al. 2008).

Use of kriging for this study confirmed its appropriateness for this data type similar to use in previous studies (Luo et al. 2008, Zlatev et al. 2009). The Luo et al. (2008) study, however, did not apply an anisotropic condition to the semivariogram because a

smaller geographic area was examined (only the UK). Luo et al. (2008) indicated that directional covariance related to anisotropy did exist on the surface, but that the sill and maximal area were approximately the same thus eliminating the need to use anisotropy. Because this study modeled wind speeds in a much larger area, the use of anisotropic conditions for semivariogram creation significantly improved our results by capturing the widespread directional distribution of wind speeds in addition to the surface wind speed trends for most storms. The only storm that exhibited large directional wind speed disparities between maximum sustained and peak gust winds was Emma. Peak gust wind speeds exhibited a northwest-to-southeast pattern, while the maximum sustained wind speeds exhibited a west-to-east pattern. This was most likely caused by the presence of a separate storm front immediately preceding wind storm Emma resulting in high winds moving in multiple directions. The weather pattern caused numerous, weak directional trends to occur on the surface and created confusion during the interpolation process since the “dominant” trend was different between peak gust and maximum sustained winds. The peak gust wind speed direction was more accurate relative to the track of the storm, thus the anisotropic azimuth direction for maximum sustained wind speeds was manually changed to a more accurate northwest-to-southeast trend.

Another unique feature found during the modeling process of many wind storms was the location of two separate areas of high wind speeds: coastal areas where the storm made landfall and mountainous areas that were often far away from the actual storm track. These two areas were often separated by a more homogeneous surface where wind speed tended to be lower. One reason for higher winds in mountainous areas located far away from the storm tracks is not only the presence of an exposed

ridgeline, but also the manifestation of pressure gradient differences associated with convergent air masses. Steenburgh and Mass (1996) alluded to the tendency for high winds to flow through mountain gaps/valleys perpendicular to wind storm tracks in North America and it appears that this feature is also present in mountainous regions of Europe. High downgradient flow in gaps and channels occurs because of large north-south pressure gradients so if a storm moves from west to east, then north-south oriented gaps often experience an increase in wind speed (Steenburgh and Mass 1996).

2.5 Future Research

Aspect, or the direction that a mountain slope faces, may be a major contributor to error associated with wind speed interpolations. More research must be conducted to further analyze the legitimacy of this hypothesis, but topographic variation does exert a great influence on wind speeds (Hofherr and Kunz 2010). Elevation has often been used as a covariate during cokriging operations for wind speed interpolation (Luo et al. 2008, Akkala et al. 2010, Zlatev et al. 2010) but aspect has been overlooked. Since correction factors for topographic effects are applied to each WMO weather station, using elevation as a covariate may even be redundant in some cases. Weather stations may share similar elevation, but may be located on opposite sides of a mountain, thus potentially diminishing the covariance between wind speeds and elevation. For example, one weather station may be on the coastal side of a mountain range at an elevation of 1000 meters, while another station may be on the inland side of the same mountain range at the same elevation. The first weather station may report very high wind speeds, but the second weather station may report very low wind speeds because of the blocking and diverting effect of the mountains. To examine aspect within the

cokriging methodology, an involved process of segmenting the land surface may be needed based on defined topographic/geographic areas, similar to Luo et al. (2008). An in-depth examination of topographic variation may also assist in explaining microclimatic impacts that may contribute to conflicting surface trends.

In addition to examining the impact of aspect in future studies, other models and statistical methods should be explored to improve surface wind speed estimates for European wind storms. Through cokriging, additional covariates should also be examined to measure their impact on wind speeds across Europe. Other knowledge-assisted and computational learning methods need to be improved but hold promising capabilities in the field of wind interpolation. Statistical techniques, such as Bayesian-assisted kriging, could also improve interpolation estimates because the technique creates multiple local semivariograms instead of one global semivariogram for an entire dataset.

When considering European wind storms as a whole, further research could help to determine recurrence intervals or return periods of various intensity storms (Della-Marta et al. 2009). In the United States, similar research was conducted to examine hurricane return periods for land-falling Atlantic basin storms (Keim et al. 2007). It may also be useful to examine extreme wind distributions and recurrence intervals across Europe so that not only wind storms are included, but also any other extreme wind events (Simiu and Heckert 1996). Examining each storm individually may allow for the calculation of continuously sampled sustained data based on the storms return period (e.g., is this a common, near-annual storm-type or a 100-year storm-type?). Within the same realm of future research, it may also be useful to include additional data from

countries that were excluded from some storm models. Some countries were included in some models and excluded in others because of the different locations of destructive impacts of each storm. Future studies may examine more consistent spatial extents. These and other potential studies would be useful to help improve our climatic knowledge of European wind storms as well as the potential for repetitive disasters in specific locations.

CHAPTER 3. CROSS-CORRELATION MODELING OF EUROPEAN WIND STORMS: A COKRIGING APPROACH FOR OPTIMIZING SURFACE WIND ESTIMATES

3.1 Introduction

During excessive wind events, wind flows relatively uniformly across mostly flat and smooth terrain, but when terrain changes abruptly (*e.g.*, coastal zones and/or the transition from flat land to hills and mountains), velocity and direction change based on the extent and diversity of terrain roughness (Tieleman 1992). Improved modeling of wind storm-induced surface winds is critical for engineering purposes, while also propelling knowledge of geospatial analytical applications forward. Currently, upper-level winds are commonly used to estimate wind surfaces in wind storms (e.g., Della-Marta et al. 2009), but interpolations of wind speeds at higher levels in the atmosphere do not reflect the complexity of the surface. Use of modeled wind data based on upper-level geopotential height gradients is less accurate than meteorological station readings as the former are not based on observed surface wind measurements. In addition, record length of the former is usually shorter than station data, preventing long-term studies. Station data can depict wind fluctuations at the local scale better than other data types, and are therefore most appropriate for this project. We hypothesize that because aspect, elevation, and land cover affect surface-level wind speeds, it is important to consider their influence.

The proposed project will address research questions that arose in Study One, specifically by developing a deeper understanding of the factors that resulted in high error measurements between the station data and interpolated surfaces in heterogeneous terrain. It is hypothesized that covariates will improve the interpolation model by utilizing elevation, aspect, and land cover as potential predictors of wind

speed. This hypothesis is grounded in the notion that cokriging with one or more covariates improves the accuracy of wind surface estimates previously created by ordinary kriging (Odeh et al. 1995, Luo et al. 2008, Wenxia et al. 2010, Zlatev et al. 2010, Luo et al. 2011, Singh et al. 2011, Wang et al. 2011, Aznar et al. 2012, Li et al. 2012). Section 1.2 identifies literature that informs the current research and forms the basis of this hypothesis.

3.1.1 Cokriging

While ordinary kriging is a common and often-used interpolation method, cokriging is less popular because of the added complexity involved in selecting appropriate covariates. In utilizing various forms of cokriging along with ordinary kriging, universal kriging, multi-linear regression, and regression kriging models to predict soil properties based on landform attributes, Odeh et al. (1995) found that the regression kriging and cokriging models were superior to ordinary kriging models because they accounted for the relationship between the predictor variable (soil properties) and specific terrain attributes (slope angle, aspect, plan curvature, and profile curvature). An earlier study examining soil physics concluded that cokriging reduced the variance and improved estimates of under-sampled variables by accounting for the spatial correlation between available water content, water stored at 1/3 bar, and sand content values. Air pollution surfaces have also been improved through the cokriging process. To produce air pollution maps in Northern Italy, the results of a Chemical Transport Model simulation was used as the covariate, while ozone concentrations and daily mean particulate matter (>10) concentrations were the predictor variables (Singh et al. 2011). Generalized additive models were also used to produce global residuals near nitrogen dioxide and nitrogen oxide sampling locations in

Southern California, with greatly improved predicted oxide surfaces and very high cross-validated R^2 values (~0.9) (Li et al. 2012).

Cokriging has been used to improve interpolated temperature surface estimates. Aznar et al. (2012) applied cokriging to produce a time series of monthly mean temperatures in northeastern Canada between 1961-2000. Temperature recordings from 202 meteorological stations were utilized as the predictor variable and regional climate model-derived temperatures were incorporated as a covariate because of their incorporation of local variance (Aznar et al. 2012). This study resulted in accurate and publicly available monthly mean temperature grids for the region. Mahdian et al. (2009) utilized multiple geostatistical techniques to estimate monthly and annual temperature and found that cokriging with elevation used as a covariate produced a surface with a low mean absolute error compared to most of the other models.

Cokriging has also been proven to be an optimal method for estimating precipitation surfaces through use of various covariates (Wenxia et al. 2010, Luo et al. 2011, Wang et al. 2011). Topography, or elevation, was especially effective for cokriging models that examined the Taihu Lake Basin in China (Luo et al. 2011) and the Chongqing tobacco planting region of China (Wang et al. 2011) in areas where topography varied greatly. Improvements compared with other models were negligible in areas of homogeneous topography. Wenxia et al. (2010) expanded on the traditional covariate of elevation by also including geographic factors (longitude, latitude, terrain, slope, aspect, and shelter degree). Collectively, cokriging models from Wenxia et al. (2010) utilizing both topographic and geographic variables outperformed both the

cokriging technique that incorporated only elevation and the inverse distance weighted method.

On occasion, multiple variables (average daily maximum temperature, wind direction frequencies, nitrous oxide (N_2O) emissions, distance downwind from N_2O emission sources) have been used to estimate a surface ozone exposure. For example, Phillips et al. (1997) revealed the possibility of including wind direction in a spatially anisotropic kriging- and cokriging-based surface ozone estimate. In addition to the inherent ability to account for anisotropy, cokriging of wind speed adds the ability to incorporate many of the covariates (e.g., topography, aspect, terrain, slope, etc.) used in previous studies. In examining seven different methods of spatial interpolation, Luo et al. (2008) concluded that cokriging with elevation as a covariate produced a superior daily mean wind speed surface with better accuracy metrics than the other six surfaces (one of which included ordinary kriging). Similarly, Zlatev et al. (2010) also found cokriging to be superior to other forms of kriging and spatial interpolation based on lower error measurements when estimating daily mean wind speed. In both studies, error reduction occurred over a rugged landscape (United Kingdom), suggesting that use of elevation may have been a key factor in model improvement. By contrast, Sliz-Szkliniarz and Vogt (2011) found that wind surface estimates were changed very little over the ordinary kriging approach by including elevation as a covariate, when applied to the topographically flat terrain of Poland. Results of Luo et al. (2008), Zlatev et al. (2010), and Sliz-Szkliniarz and Vogt (2011) provide substantial evidence that covariates can help improve wind surface estimates in topographically varied regions, while maintaining the previous accuracy of ordinary kriging surface estimates in more

topographically homogeneous regions. Furthermore, the flexibility and robustness of cokriging, and geostatistical methods in general, in accounting for variance in station distribution and density – two very important variables when modeling and mapping data (MacEachren and Davidson 1987) – suggest that they are well-suited for wind observation data.

3.1.2 Study area and objectives

Accurate wind surface estimates that capture regional wind speeds and directions can be created for large areas of Europe using an anisotropic semivariogram-derived kriging methodology (Joyner et al. *in review*). Surface wind estimates suggested that coastal and mountainous regions often experienced the most extreme wind speeds (Joyner et al. *in review*). Inland Europe, specifically the Black Forest and northern Alps, displayed excessive wind speeds relative to the surrounding areas – indicative of a complex topography/wind interaction (Joyner et al. *in review*). Coastal and mountainous weather stations experienced the most intra-storm wind speed variability and also reported some of the highest error measurements – most likely a result of landscape heterogeneity and post-model smoothing (Joyner et al. *in review*). Because of these high error measurements, this study examines multiple covariates through the cokriging technique in an effort to create more accurate surface wind interpolations and to improve understanding of local wind variability in these environments. Previous studies that identified cokriging as superior for estimating surface winds utilized elevation as the singular covariate (e.g., Luo et al. 2008, Sliz-Szkliniarz and Vogt 2011); this study will incorporate aspect and land cover in addition to elevation. The research questions for this study are as follows:

1) To what extent does cokriging improve interpolated wind surfaces in the coastal and mountainous regions of Europe, compared to ordinary kriging methods?
2) Which covariate(s), if any, is(are) most influential in improving wind surface interpolations in heterogeneous terrain?

3.2 Data and Methods

3.2.1 Wind storm and covariate data

Five wind storms occurring between 1999 and 2008 were selected for this study (Table 3-1). These storms were selected based on a combination of factors including extent and degree of impact and intensity as well as the availability of supporting data about each storm. Each of the five storms impacted both coastal and mountainous regions where standard errors were highest, thus increasing the potential to show improvement in predicting surface winds in these areas through utilization of the cokriging methodology.

Table 3-1. European wind storms selected for Study Two and impacted countries.

Year	Date	Popular Name	Countries
1999	25-27 December	Lothar	France, Switzerland, Germany
2002	26-28 October	Jeanette	UK, Denmark, Sweden, Germany, Netherlands, France, Austria, Poland, Czech Republic, Belgium, Ireland
2007	16-19 January	Kyrill	France, Netherlands, Germany, UK, Belgium, Austria, Ireland
2008	24-26 January	Paula	Poland, Germany, Austria, Denmark, Norway, Sweden
2008	29 February-2 March	Emma	Germany, Austria, Czech Republic, Belgium, Netherlands, Switzerland, Poland

When a station that records wind speeds is not located at a 10-m height, the station data are adjusted to a 10-m estimated speed using the logarithmic wind profile

assumption. A preliminary quality control analysis of the European wind storm data was conducted by plotting the sustained and peak gust values against the mean of each variable. Outliers were examined to determine whether the values were reasonable for the given atmospheric conditions. Stations that were modeled most successfully came proportionately from those with 10-m measurements and those at which the 10-m wind was adjusted from measurements at a different height. Based on this analysis, it appears that the model performance is not unduly biased by the vertical adjustment of station-based wind values.

Additionally, covariate data from Europe were obtained for the cokriging process. Elevation data were collected from Version 4 of the NASA Shuttle Radar Topographic Mission (SRTM) 90-m digital elevation dataset through the CGIAR Consortium for Spatial Information (CGIAR-CSI). The land cover covariate was obtained from the European Space Agency (ESA) GlobCover Project Version 2 2008 database at a resolution of 300 m (GlobCover 2008). The elevation and land cover datasets were clipped and resampled to 300 m for use in the present study. Based on the theory behind “ecological fallacy” and the “modifiable areal unit problem (MAUP),” datasets can be aggregated into larger units (e.g., 90 m to 300 m), but cannot be divided into smaller units (e.g., 300 m to 90 m) without jeopardizing the integrity of the data (Robinson 1950, Openshaw 1984, Sayre 2005, Dark and Bram 2007). The GlobCover land cover dataset contains 22 different land cover classification types ranging from various tree types, shrubs, and grasslands to bare land, artificial surfaces, and open water. The covariate of aspect was derived from the 300-m resampled elevation dataset utilizing

tools available in the Spatial Analyst toolbox within ArcMap 10.1, in preparation for further analysis in this research.

3.2.2 Kriging and cokriging methodologies

Kriging and cokriging rely on probability and autocorrelation when creating surface estimates. The use of probability means that there is some variation in output values leading to an approximate, or stochastic, model. Reliance on autocorrelation is based on the tendency for two variables to be related. Within the field of geography, Tobler's first law states that "everything is related to everything else, but near things are more related than distant things" (Tobler 1970). Correlation between objects usually decreases over distance and this is also true of the correlation between wind speeds at different stations. Autocorrelation is a central tenet of geostatistics because observations are not independent of each other and geostatistics includes spatial location and distance during model creation. Kriging and cokriging both rely on the same process for surface estimation, but cokriging incorporates one or more secondary variables to improve predictions in areas where simple autocorrelation may be insufficient. Larger wind speed values may be underestimated in mountainous or coastal areas that lack a dense network of wind observation stations. However, even when considering station location limitations, cokriging has been shown to estimate wind surfaces more accurately and in greater detail, while reducing prediction errors, compared to ordinary kriging (Luo et al. 2008).

While ordinary kriging is described as

$$Z(\mathbf{s}) = \mu + \varepsilon(\mathbf{s})$$

where constant mean μ is a deterministic trend that is associated with errors ε at each location **s** for the variable of interest Z(**s**), ordinary cokriging is described as

$$Z_1(\mathbf{s}) = \mu_1 + \varepsilon_1(\mathbf{s})$$

$$Z_2(\mathbf{s}) = \mu_2 + \varepsilon_2(\mathbf{s})$$

$$Z_n(\mathbf{s}) = \mu_n + \varepsilon_n(\mathbf{s})$$

where constants $\mu_1 \ldots \mu_n$ are unknown and associated with multiple errors ε_n at each location **s** to predict variable of interest $Z_1(\mathbf{s})$, while taking information from covariate(s) $Z_n(s)$ into consideration.

In cokriging, different trends are estimated for each variable and autocorrelation occurs within each variable, while cross-correlation can also occur between the errors for each variable (Journel and Huijbregts 1978, Matheron 1979). Measurement locations do not need to be the same when the level of cross-correlation is calculated between variables – a major advantage of cokriging. Cokriging often utilizes autocorrelation and cross-correlation to make predictions, but the addition of one or more secondary variables (covariates) requires more estimation of unknown autocorrelation parameters and adds more model variability (Matheron 1979). However, the cokriging model is based on the kriging model and if no cross-correlation exists, the original autocorrelation remains the baseline. This infers that cokriging models will not underperform compared to kriging models, but occasionally the added model variability of cokriging can increase standard error on a station-by-station basis (Stein and Corsten 1991). Within kriging, random errors assume second-order stationarity, indicating that errors have a mean of zero and error covariance is not location-dependent, but instead is distance- and direction-dependent (Krige 1951). In addition to ordinary cokriging, other methods of cokriging exist that include universal, simple, indicator, probability, and disjunctive. These methods offer slight variants to the

ordinary cokriging methodology such as the ability to use multiple data thresholds, prediction thresholds, and variable trends (Georgakakos et al. 1990).

Although normally distributed data are not required for kriging, normality is necessary to obtain quantile and probability maps. Additionally, kriging is the optimal unbiased predictor when compared to only techniques produced from weighted averages regardless of data normality, but if the data are normally distributed, then kriging is the optimal predictor compared to all other unbiased predictors. In this study, the data were examined to determine whether a transformation or other corrections was necessary to produce normally distributed data and to ensure that kriging is the "best" prediction compared to other unbiased predictors. Prior to modeling each wind storm, multiple methods of exploratory spatial data analysis (ESDA) were employed using the Geostatistical Analyst within ArcMap 10.1 (ESRI 2010) to examine the univariate distribution (histogram), stationarity and spatial variability (Vornoi map, e.g., Ogniewicz and Ilg 1992), normality (normal QQ plot, e.g., Wilk and Gnanadesikan 1968), global trends (trend analysis), and spatial dependencies (semivariogram/covariance cloud, e.g., Gribov et al. 2000) of the wind observation data as well as the autocorrelation between covariates and between wind observation data and covariates (general QQ plot and crosscovariance cloud, e.g., Wilk and Gnanadesikan 1968, Gribov et al. 2000). The levels of skewness and kurtosis revealed by ESDA indicated that the wind observation data deviates slightly from a normal distribution. Observational data were subsequently tested for normality using the Shapiro-Wilk test (Shapiro and Wilk 1965). The Shapiro-Wilk test examines the null hypothesis that a dataset is distributed normally. Values below a certain alpha level (e.g., $p < 0.05$) indicate that the null

hypothesis of normality should be rejected and values above a certain alpha level indicate the opposite.

3.3 Results

3.3.1 Cokriging assessment and evaluation

Maximum sustained wind speeds and peak gusts were analyzed for each of the five wind storms to determine whether pre-processing data transformations were necessary and to identify the best combinations of covariates that produce optimal wind surface estimates based on multiple criteria. The Shapiro-Wilk test revealed that the null hypothesis of normality for each station could not be rejected since *p*-values were greater than 0.05 for each storm and wind type (Table 3-2).

Table 3-2. Shapiro-Wilk test for normality for each storm and wind type. The null hypothesis (H_0) is non-normality and a *p*-value greater than 0.05 indicates a rejection of this hypothesis and assumed normality of the data.

Storm	Wind Type	Shapiro-Wilk (W)	*p*-value	Reject H_0
Lothar	Max Sustained	0.997	0.79	No
	Peak Gust	0.995	0.38	No
Jeanette	Max Sustained	0.997	0.08	No
	Peak Gust	0.999	0.89	No
Kyrill	Max Sustained	0.999	0.97	No
	Peak Gust	0.998	0.84	No
Paula	Max Sustained	0.998	0.47	No
	Peak Gust	0.998	0.70	No
Emma	Max Sustained	0.998	0.94	No
	Peak Gust	0.996	0.22	No

Based on the results of the Shapiro-Wilk test, no data transformations were necessary for the station observation data. Additionally, regression analysis of covariates revealed extremely low *R*-values ($R < 0.1$) and no values were significant ($p > 0.05$) between covariates and between wind observation data and covariates. This result indicates that correlation between the sets of potential covariates is not a major

issue and that transformation of the covariates was therefore unnecessary. The ESDA tools within Geostatistical Analyst also revealed trends for each wind storm dataset. These trends were generally consistent with expected directional trends based on the track of each wind storm, resulting in west-east or northwest-southeast tendencies.

Daily weather maps and other climatological information from various reports were utilized to characterize the track and synoptic conditions and gather a more holistic view for each wind storm. Ordinary cokriging was employed for each storm and wind type and every possible covariate combination was simulated. The maximum number of combinations resulted in eight interpolated surfaces for each wind type and 16 total interpolated surfaces for each storm. These eight interpolated surfaces included 1) ordinary kriging without covariates, 2) cokriging with elevation, 3) cokriging with aspect, 4) cokriging with land cover, 5) cokriging with elevation and aspect, 6) cokriging with elevation and land cover, 7) cokriging with aspect and land cover, and 8) cokriging with elevation, aspect, and land cover. Corresponding maps were created to represent the maximum sustained wind speeds and peak gusts across the region for the duration of each storm. Accuracy metrics were calculated through a process of cross validation (n - 1) during model simulation and included the root mean square prediction error (RMSPE), mean error (ME), and root mean square error (RMSE). Stations with errors greater than +/- 2.0 standard deviations were identified. Automatic wind direction trends were also recorded by calculating the azimuthal direction (0°=north, 90°=east, etc.) of the major axis of the ellipse derived from the semivariogram. Additional maps were also created for each storm and wind type to identify the locations where high errors from

each cokriging model are found. The optimal model output(s) was (were) determined for each storm and wind type.

3.3.2 Cokriging models

3.3.2.1 Wind storm Lothar

Wind storm Lothar was the first of two major storms to impact northwestern Europe in 1999. A subsequent storm, Martin, followed nearly the same path just one day later. Lothar developed from a depression in the North Atlantic Ocean and collided with a cold air mass on land, resulting in increased surface turbulence along the frontal boundary and the rapid development and geographic expansion of Lothar. The wind storm moved from west to east with major damage occurring in France, Germany, Switzerland, and Austria. Approximately 140 deaths and €10 billion (euros) in damage were attributable to Lothar and Martin collectively (Environmental Quality Engineering - EQE 2000). It is difficult to attribute the damage to Lothar vs. Martin, but Lothar was the stronger storm of the two. During Lothar, several stations reported gusts in excess of 40 m s^{-1} – comparable to Category 2 hurricane wind speeds. Building roofs, communication networks, and fruit trees were particularly hard-hit by winds, while avalanches, mudslides, and flooding also occurred (EQE 2000). A deadly avalanche in Galtuer, Austria, resulted in nine deaths.

Cokriging model estimates of maximum sustained wind speeds (Figure 3-1) and peak gusts (Figure 3-2) provide additional evidence of the general west-east storm track for Lothar. Wind speeds approaching 40 m s^{-1} were estimated by multiple peak gust models in coastal areas of France and mountainous areas of southeastern Germany approaching the Austrian Alps. Some differences in wind speed estimates were observed between most surfaces. For example, Figures 3-1a and 3-1c show higher

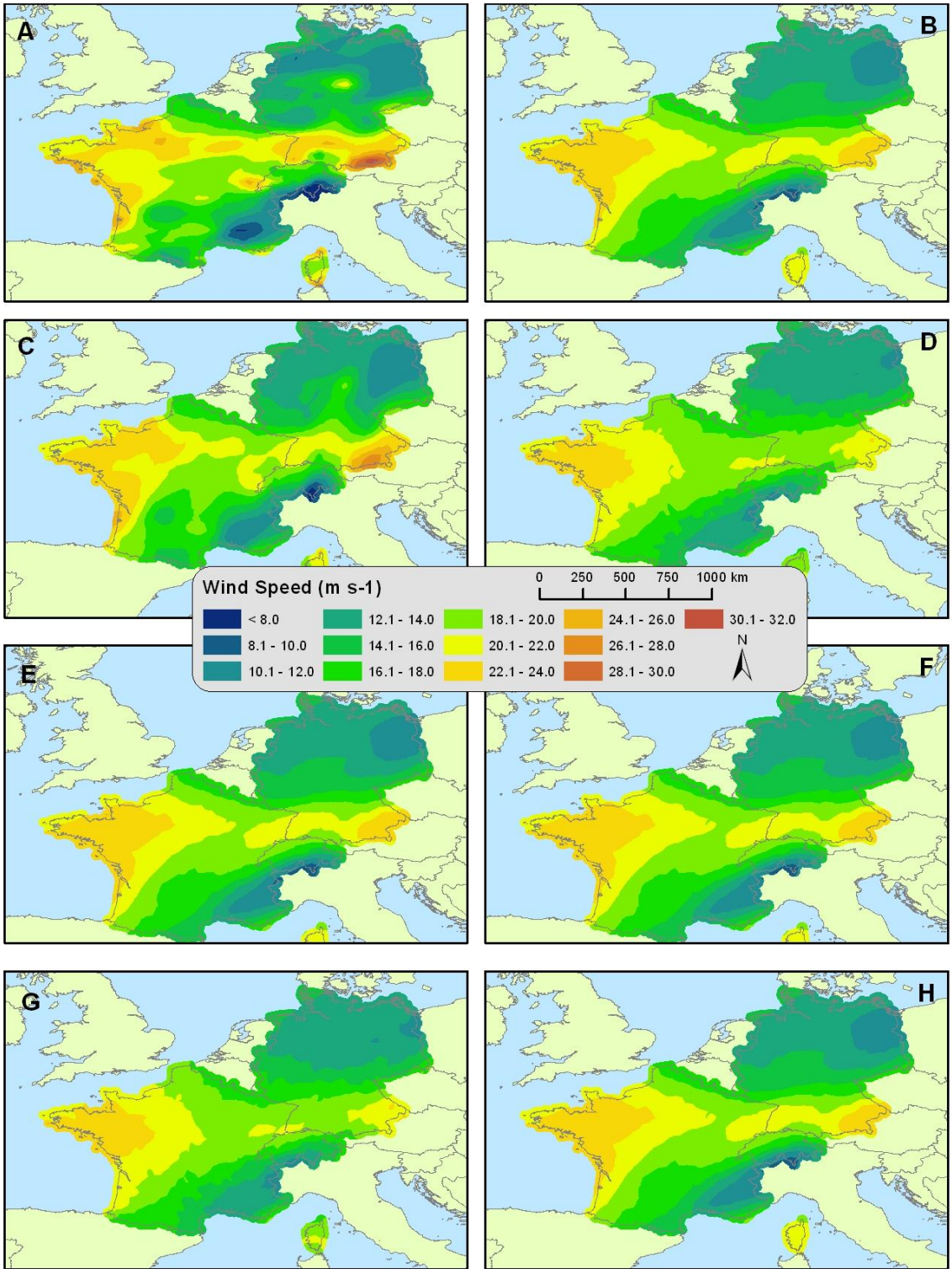

Figure 3-1. Maximum sustained wind surface estimates for wind storm Lothar (1999) produced by the following models: original kriging (A), cokriging with elevation (B), cokriging with aspect (C), cokriging with land cover (D), cokriging with elevation and aspect (E), cokriging with elevation and land cover (F), cokriging with aspect and land cover (G), and cokriging with elevation, aspect, and land cover (H).

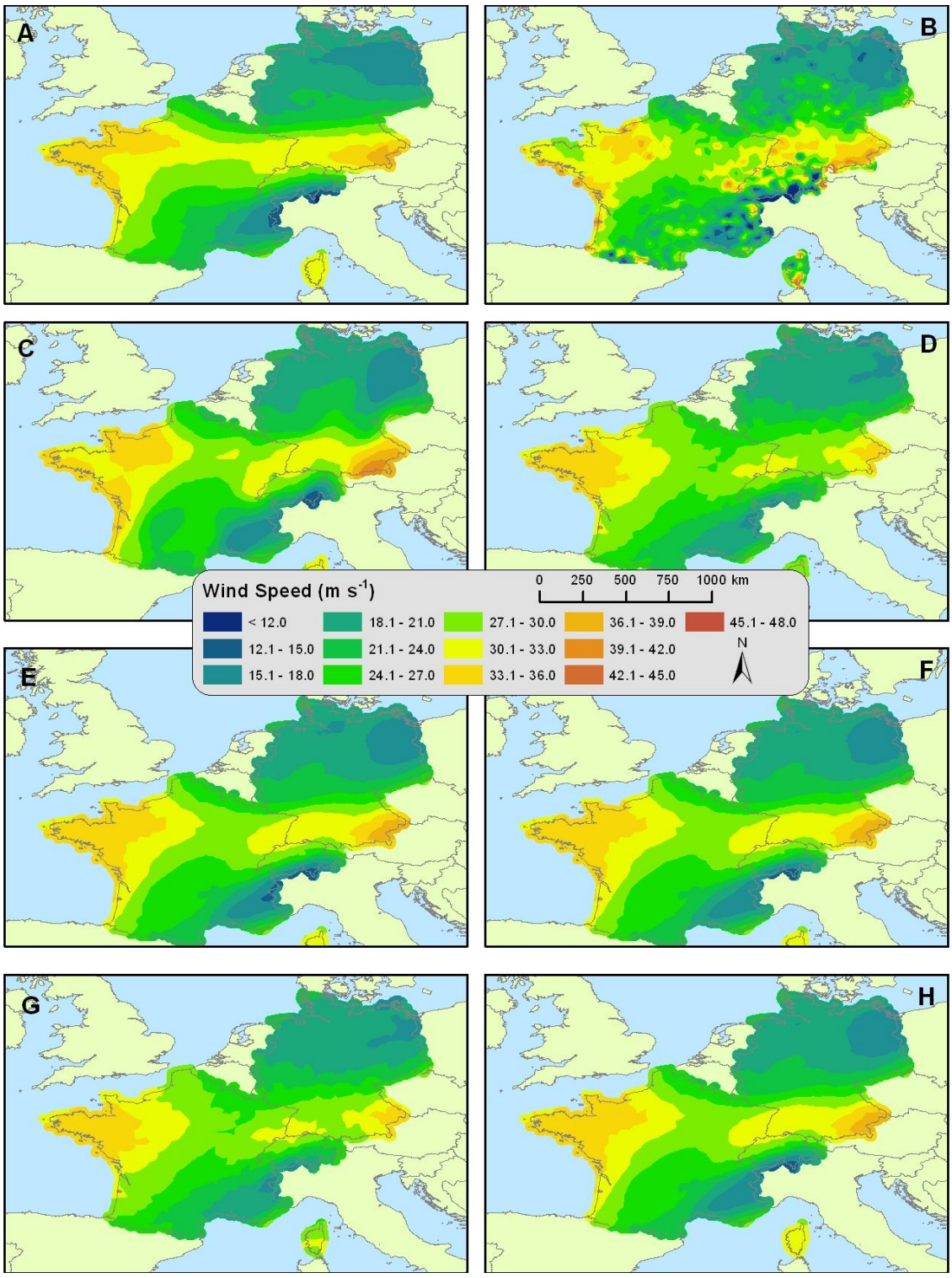

Figure 3-2. Peak gust wind surface estimates for wind storm Lothar produced by the following models: original kriging (A), cokriging with elevation (B), cokriging with aspect (C), cokriging with land cover (D), cokriging with elevation and aspect (E), cokriging with elevation and land cover (F), cokriging with aspect and land cover (G), and cokriging with elevation, aspect, and land cover (H).

maximum sustained wind speed estimates in southeastern Germany, while most models estimated a decline in wind speeds across northeastern France before a reversion to increased wind speeds near Switzerland and southwestern Germany. Figure 3-2c reveals higher peak gust wind speed estimates in southeastern Germany, while Figure 3-2b shows a very spotty surface with smaller, more prominent areas of high and low wind speeds.

To determine the optimal model(s) for each wind speed type for Lothar, multiple accuracy metrics were utilized during model implementation. Accuracy metrics for each model and wind type are listed in Table 3-3. For Lothar's maximum sustained wind, the original kriging methodology produced the automated anisotropic conditions closest to the actual storm track of ~90°, or an approximate west-east track. The model utilizing the covariate aspect produced the RMSE score nearest to 1.0 and the lowest RMSPE score, while the ME nearest to zero was produced by the model utilizing aspect and land cover. All models except two (original kriging and cokriging with aspect) reported only 14 high SE measurements after cross-validation. For the peak gust wind models, the original kriging methodology again produced the automated anisotropic conditions closest to the actual storm track of ~90°. The original kriging model also produced the RMSE score nearest to 1.0 and tied five other models with the fewest stations reporting a SE measurement exceeding +/-2.0. The model utilizing only elevation as a covariate generated the lowest RMSPE score, while the ME nearest to zero was produced by the model incorporating only land cover.

To examine in more detail the locations where high SE measurements occurred, maps were produced for each wind type for Lothar (Figure 3-3a-b). Most stations with

Table 3-3. Wind storm Lothar (1999) accuracy metrics for each model indicating dominant automatic wind speed direction, inter-model error comparison (RMSPE), intra-model error comparison (ME and RMSE), and number of high error stations.

Storm	Method	Anisotropy	RMSPE	ME	RMSE	SE (> +/- 2.0)
Lothar Max Sustained	Original kriging	81.4	6.34	-0.010	1.03	18
	Cokriging w/elev	70.5	6.35	0.004	0.97	14
	Cokriging w/asp	45.4	6.32	0.004	1.00	16
	Cokriging w/LC	63.5	6.55	0.003	0.95	14
	Cokriging w/elev & asp	70.5	6.35	0.004	0.97	14
	Cokriging w/elev & LC	70.3	6.35	0.005	0.97	14
	Cokriging w/asp & LC	63.8	6.55	0.002	0.95	14
	Cokriging w/elev, asp, & LC	70.3	6.35	0.005	0.97	14
Lothar Peak Gust	Original kriging	84.9	10.31	0.002	1.00	16
	Cokriging w/elev	78.4	9.81	-0.030	1.04	20
	Cokriging w/asp	55.2	10.31	0.002	1.02	20
	Cokriging w/LC	63.5	10.58	0.001	0.97	16
	Cokriging w/elev & asp	70.5	10.29	0.002	0.99	16
	Cokriging w/elev & LC	70.3	10.29	0.003	0.99	16
	Cokriging w/asp & LC	63.5	10.59	0.002	0.97	16
	Cokriging w/elev, asp, & LC	70.3	10.29	0.003	0.99	16

high SE measurements received such measurements from multiple models. For the maximum sustained wind speed models, high SE measurements were recorded by stations in mountainous regions of Switzerland and southern Germany approaching Austria, along with one station in the French Pyrenees. Some stations on the island of Corsica also reported high SE measurements. For the peak gust wind speed models, high SE measurements were recorded in near-identical areas in mountainous regions, while the Atlantic and Mediterranean coasts of France also contained stations with high SE measurements. Stations coinciding with the optimal models based on SE measurements were also highlighted in Figure 3-3a-b and occurred in matching

mountainous and coastal areas. In the optimal model, many of the same stations with high SE measurements also showed high SE measurements in other models.

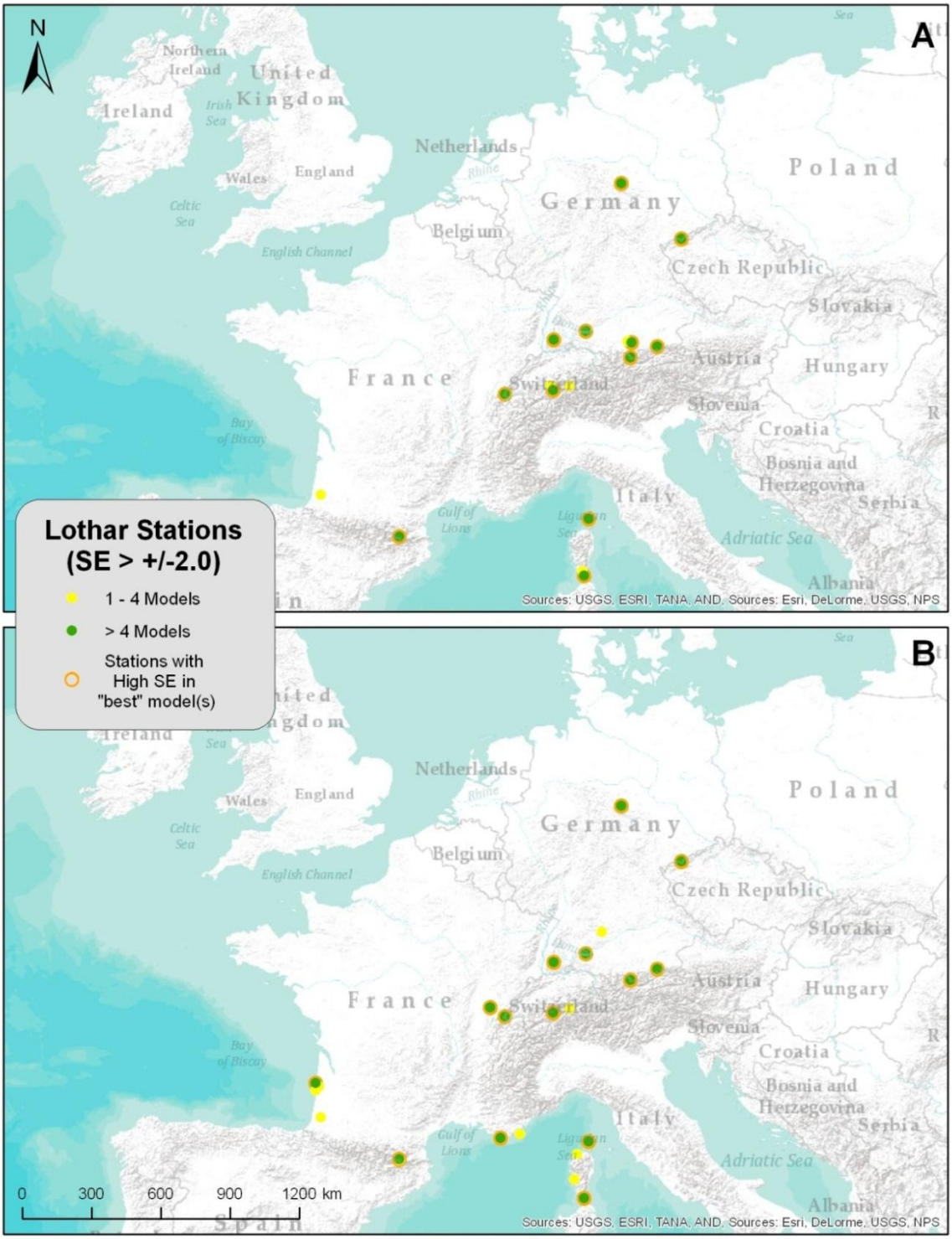

Figure 3-3. Stations reporting high SE measurements for maximum sustained (A) and peak gust (B) winds.

3.3.2.2 Wind storm Jeanette

Jeanette impacted much of northern Europe in late October of 2002 as it tracked across Ireland, the UK, North Sea, Denmark, and Sweden. Jeanette developed from a low pressure system in the North Atlantic Ocean and had a long, attached frontal boundary that extended deep into southern Europe. Because of the size of the storm and extent of the frontal boundary, Jeanette impacted more countries in Europe than most other wind storms with high winds distributed over relatively large areas. The storm moved from west to east with major damage occurring in Ireland, the UK, France, Belgium, the Netherlands, Germany, Denmark, Sweden, Switzerland, Austria, Czech Republic, and Poland. Approximately 30 deaths and €1.5 billion in damage were attributable to Jeanette with insured losses topping €1 billion (EQE Catastrophe - EQECAT 2002, Risk Management Solutions - RMS 2002). The biggest losses occurred in the western and eastern coastal UK, Belgium, the Netherlands, and northern and eastern Germany. Several wind observation stations in France, the Netherlands, Germany, and Poland reported gusts exceeding 40 m s^{-1} – comparable to Category 2 hurricane wind speeds. Buildings, communication and transport networks, power lines, and trees were particularly hard-hit by winds, while flooding was a major concern in Scotland and England (EQECAT 2002).

Results of cokriging models for maximum sustained wind speeds (Figure 3-4) and peak gusts (Figure 3-5) provide additional evidence of the general west-east storm track for Jeanette. Wind speeds approaching 33 m s^{-1} were estimated by multiple peak gust models in coastal areas of the UK, Belgium, and the Netherlands. High wind speeds extended across much of central Germany, with wind speeds increasing in eastern Germany near the Czech Republic border (Figure 3-5c). Some differences in

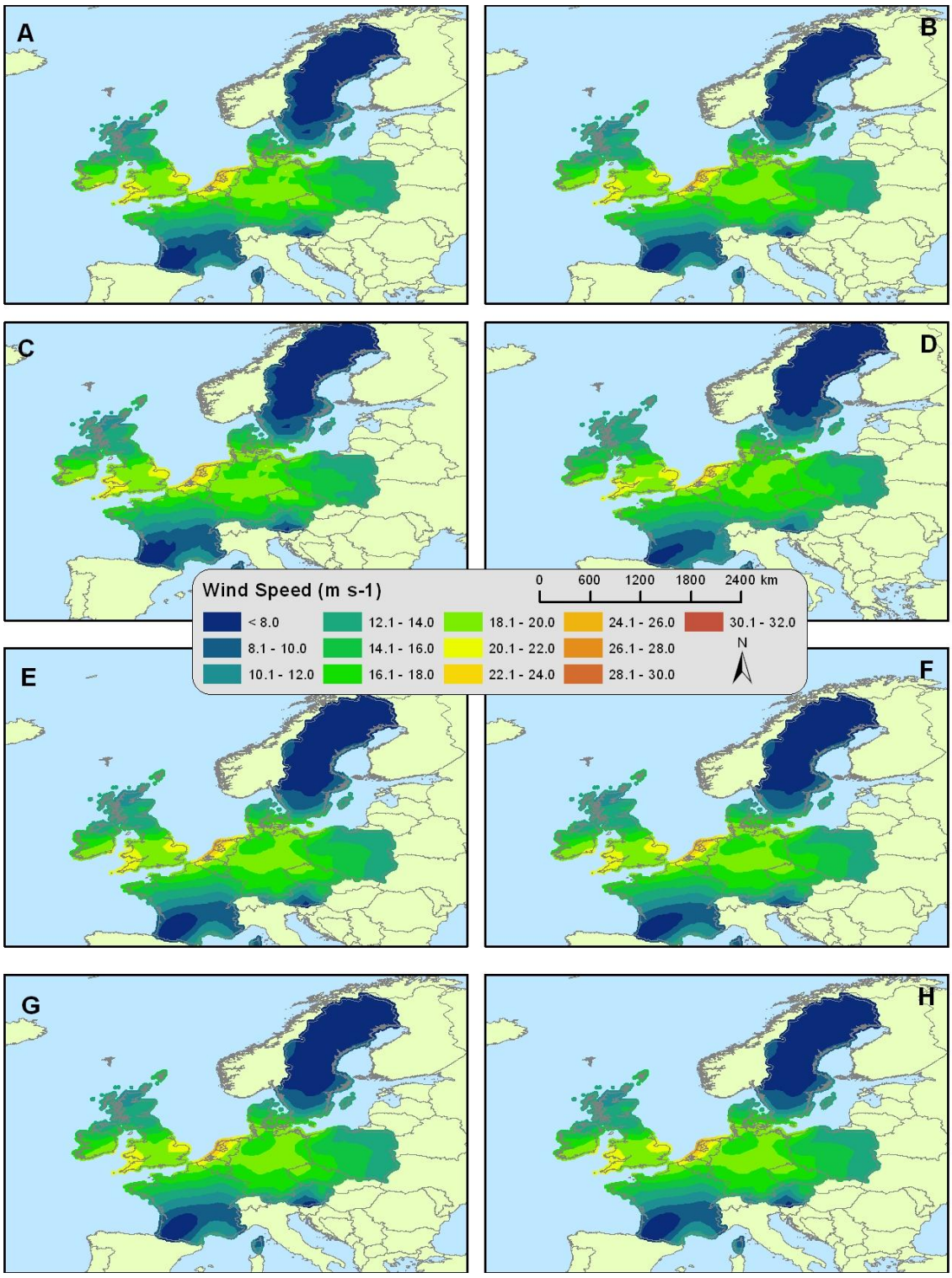

Figure 3-4. Maximum sustained wind surface estimates for wind storm Jeanette (2002) produced by the following models: original kriging (A), cokriging with elevation (B), cokriging with aspect (C), cokriging with land cover (D), cokriging with elevation and aspect (E), cokriging with elevation and land cover (F), cokriging with aspect and land cover (G), and cokriging with elevation, aspect, and land cover (H).

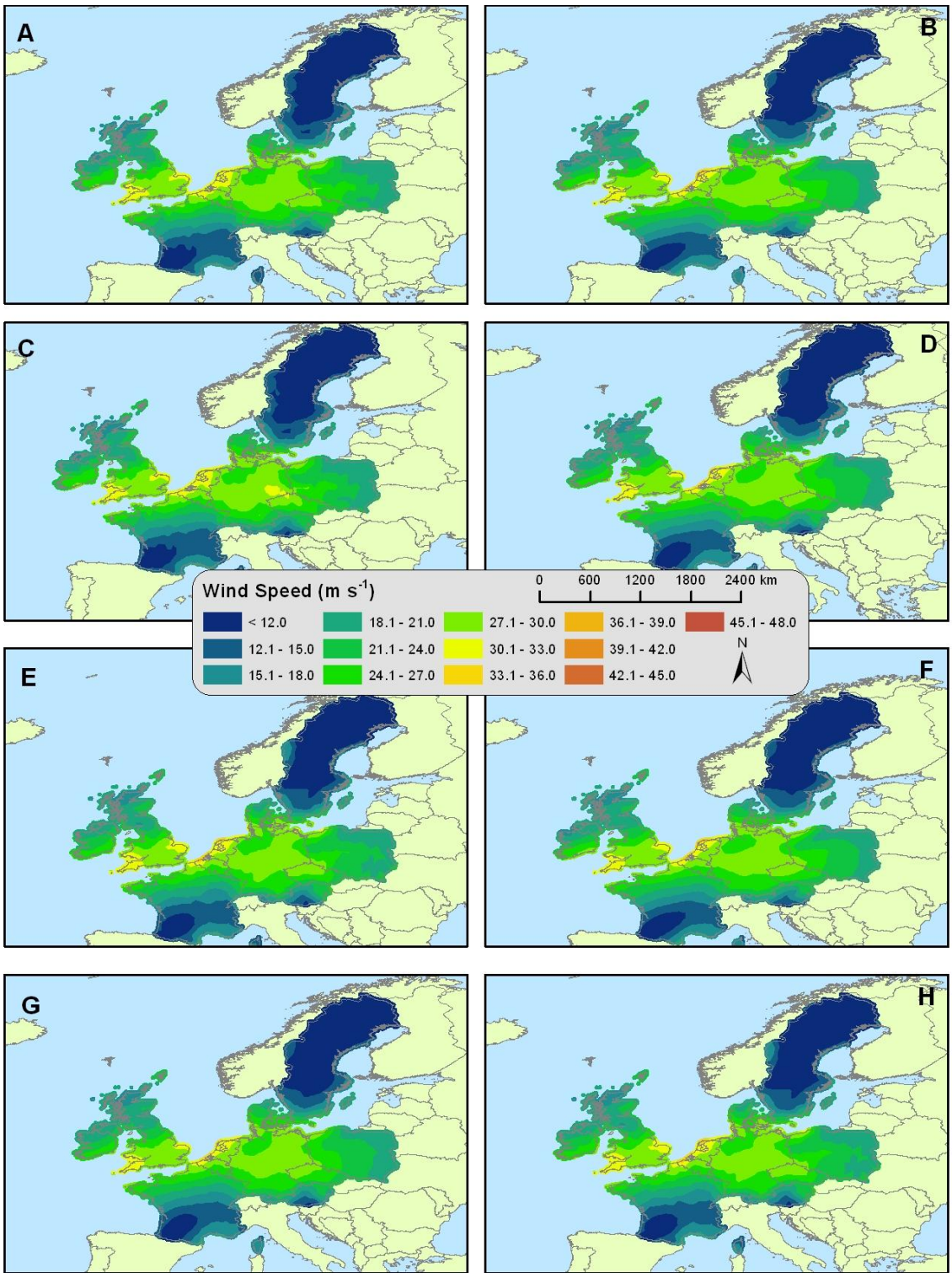

Figure 3-5. Peak gust wind surface estimates for wind storm Jeanette produced by the following models: original kriging (A), cokriging with elevation (B), cokriging with aspect (C), cokriging with land cover (D), cokriging with elevation and aspect (E), cokriging with elevation and land cover (F), cokriging with aspect and land cover (G), and cokriging with elevation, aspect, and land cover (H).

wind speed estimates were observed between most surfaces. For example, Figures 3-4c and 3-4d show variation in inland extent of the maximum wind speeds in eastern Germany, while most models estimated that greater wind speeds were maintained through Germany to the Czech Republic. Figure 3-5c shows higher peak gust wind speed estimates in eastern Germany, while other peak gust models did not identify this area of higher winds.

To determine the optimal model(s) for each wind speed type for Jeanette, multiple accuracy metrics were utilized during model implementation. Accuracy metrics for each model and wind type are listed in Table 3-4. For Jeanette's maximum sustained wind, three models (original kriging, cokriging with aspect, and cokriging with elevation and aspect) produced the automated anisotropic conditions closest to the actual storm track of ~85°. Three models (cokriging with elevation, cokriging with elevation and aspect, cokriging with all three covariates) also produced the lowest RMSPE score, while the ME nearest to zero was produced by five of the eight models. The model that utilized cokriging with elevation and land cover produced the RMSE score nearest to 1.0, while the cokriging model incorporating only land cover reported the fewest stations with high SE measurements (26) after cross-validation. For the peak gust wind models, the original kriging model and the cokriging model utilizing aspect produced the automated anisotropic conditions closest to the actual storm track of ~85°. Four models produced the lowest RMSPE score of 7.80, while three models (cokriging with land cover, cokriging with elevation and land cover, and cokriging with aspect and land cover) generated the ME score nearest to zero. The cokriging model that included elevation and the cokriging model that included elevation and land cover produced the RMSE

score nearest to 1.0. The cokriging model that utilized elevation and aspect resulted in the fewest stations (19) reporting a SE measurement of greater than +/-2.0.

Table 3-4. Wind storm Jeanette (2002) accuracy metrics for each model indicating dominant automatic wind speed direction, inter-model error comparison (RMSPE), intra-model error comparison (ME and RMSE), and number of high error stations.

Storm	Method	Anisotropy	RMSPE	ME	RMSE	SE (> +/- 2.0)
Jeanette Max Sustained	Original kriging	90.0	4.78	0.001	0.87	29
	Cokriging w/elev	71.8	4.77	0.001	0.96	37
	Cokriging w/asp	90.0	4.78	0.008	0.87	29
	Cokriging w/LC	64.3	4.84	-0.001	0.89	26
	Cokriging w/elev & asp	80.0	4.77	0.001	0.96	37
	Cokriging w/elev & LC	69.6	4.78	0.002	0.97	36
	Cokriging w/asp & LC	74.5	4.78	0.001	0.94	35
	Cokriging w/elev, asp, & LC	74.1	4.77	0.011	0.96	37
Jeanette Peak Gust	Original kriging	90.0	7.80	0.007	0.87	33
	Cokriging w/elev	69.6	7.82	0.002	0.96	38
	Cokriging w/asp	90.0	7.80	0.006	0.86	32
	Cokriging w/LC	62.6	7.80	0.001	0.93	38
	Cokriging w/elev & asp	76.9	7.83	0.008	0.72	19
	Cokriging w/elev & LC	69.6	7.82	0.001	0.96	38
	Cokriging w/asp & LC	63.2	7.80	0.001	0.93	38
	Cokriging w/elev, asp, & LC	78.1	7.84	0.009	0.72	20

To examine in more detail the locations where high SE measurements occurred, maps were produced for each wind type for wind storm Jeanette (Figure 3-6a-b). Most stations with high SE measurements received such measurements from multiple models. For the maximum sustained wind speed models, high SE measurements were recorded by stations in mountainous regions of Austria and southern Germany as well as the northern Czech Republic and Scotland. Coastal areas of the UK, France, Germany, and Poland also reported stations with high SE measurements from multiple stations. For the peak gust wind speed models, high SE measurements were recorded

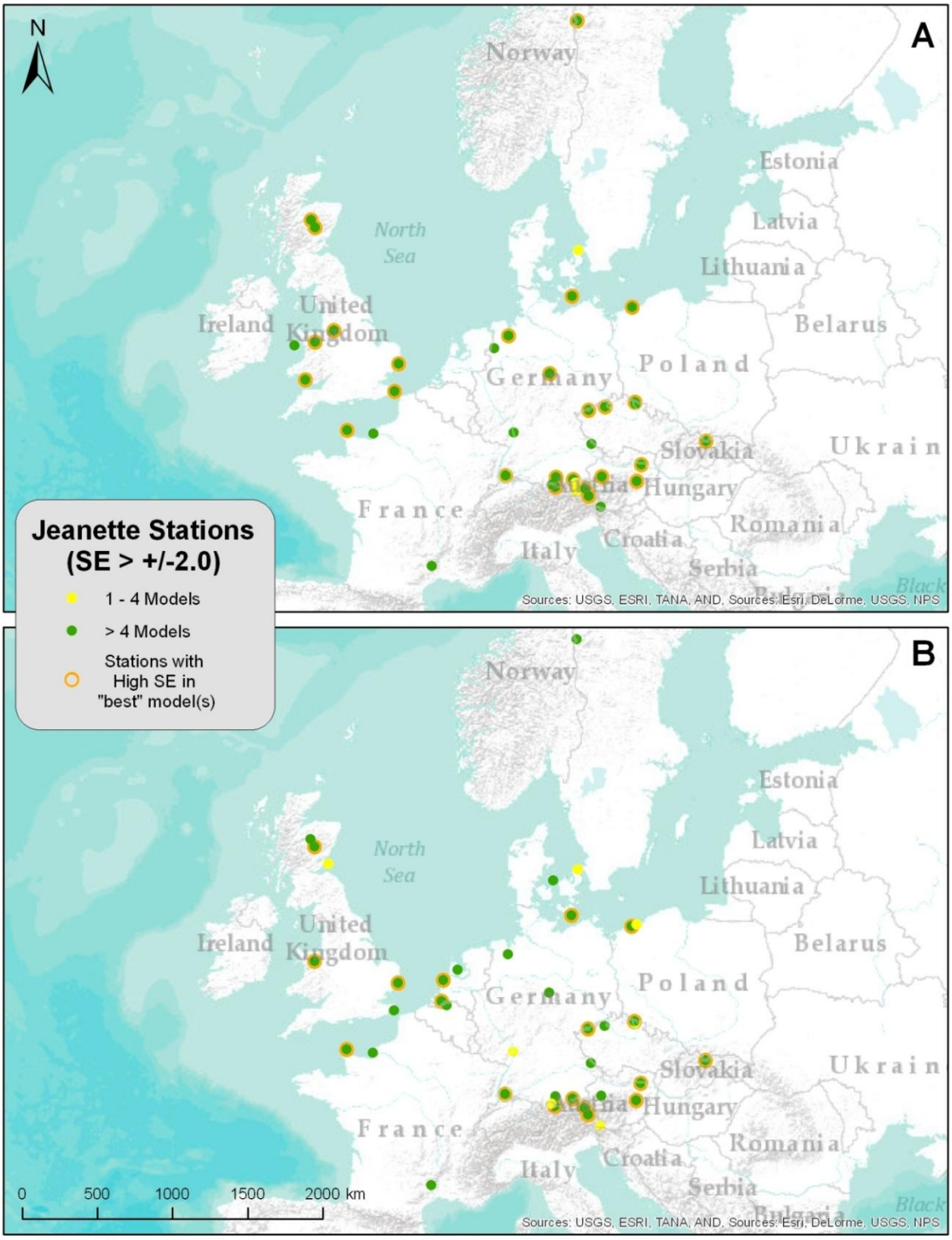

Figure 3-6. Stations reporting high SE measurements for maximum sustained (A) and peak gust (B) winds.

in near-identical areas in mountainous and coastal regions, with the addition of several stations along the coast of the Netherlands. Stations coinciding with the optimal model(s) based on SE measurements were also highlighted and continued to exhibit a mountainous and coastal presence.

3.3.2.3 Wind storm Kyrill

Kyrill impacted large areas of northern Europe in January 2007 as it took a track similar to that of Jeanette across Ireland, the UK, North Sea, Denmark, and Germany. Kyrill developed from a low pressure system near Newfoundland in northeastern Canada on 15 January and moved across the North Atlantic Ocean before making its first landfall in Ireland on 17 January. Hurricane-force winds extended far from the center of the storm and widespread major damage occurred as a result of these extensive high winds. The wind storm moved from west to east with substantial damage reported in the UK, France, Belgium, the Netherlands, Germany, Austria, Czech Republic, and Poland. Approximately 47 deaths and €5 billion in damage were attributable to Kyrill, with insured losses nearing €3.5 billion (EQECAT 2007, Hewston 2007). The biggest losses occurred in the southern UK and throughout most of Germany. During Kyrill, isolated wind observation stations in Germany, Poland, and the Czech Republic reported gusts exceeding 50 m s^{-1} – comparable to Category 3 hurricane wind speeds. Buildings, communication and transport networks, power lines, and trees suffered major wind damage, while flooding was a major concern in Ireland and the Netherlands (EQECAT 2007, Hewston 2007). Additionally, high winds over the Alps produced föhn (foehn) winds -- high, downslope winds that cause rapid adiabatic

warming of air -- across Austria and Italy, resulting in avalanche warnings and road tunnel closures.

The results of cokriging models for maximum sustained wind speeds (Figure 3-7) and peak gusts (Figure 3-8) provide additional evidence of the general west-east storm track for Kyrill. Wind speeds approaching 36 m s^{-1} were estimated by several peak gust models in coastal areas of the UK, the Netherlands, and central/eastern Germany. High wind speeds extended across much of central Germany, with all models indicating an increase in wind speed as the storm tracked eastward towards the Czech Republic. Some differences in wind speed estimates were observed between most surfaces. For example, Figures 3-7d and 3-7g do not show wind speeds over 20 m s^{-1} in eastern Germany, while all other maximum sustained and peak gust models estimated that wind speeds increased across central and eastern Germany. Figures 3-7c and 3-8a show the highest maximum sustained and peak gust wind speed estimates in central and eastern Germany.

To determine the optimal model(s) for each wind speed type for Kyrill, multiple accuracy metrics were utilized during model implementation. The accuracy metrics for each model and wind type are listed in Table 3-5. For Kyrill's maximum sustained wind, the original kriging methodology produced the automated anisotropic conditions closest to the actual storm track of ~82°. The cokriging models utilizing elevation, elevation and aspect, elevation and land cover, and all three covariates the lowest RMSPE score and the RMSE score nearest to 1.0. Three cokriging models (aspect, elevation and aspect, and all three covariates) produced the ME nearest to zero. The cokriging model utilizing only aspect reported the fewest stations (35) with high SE measurements. For the peak

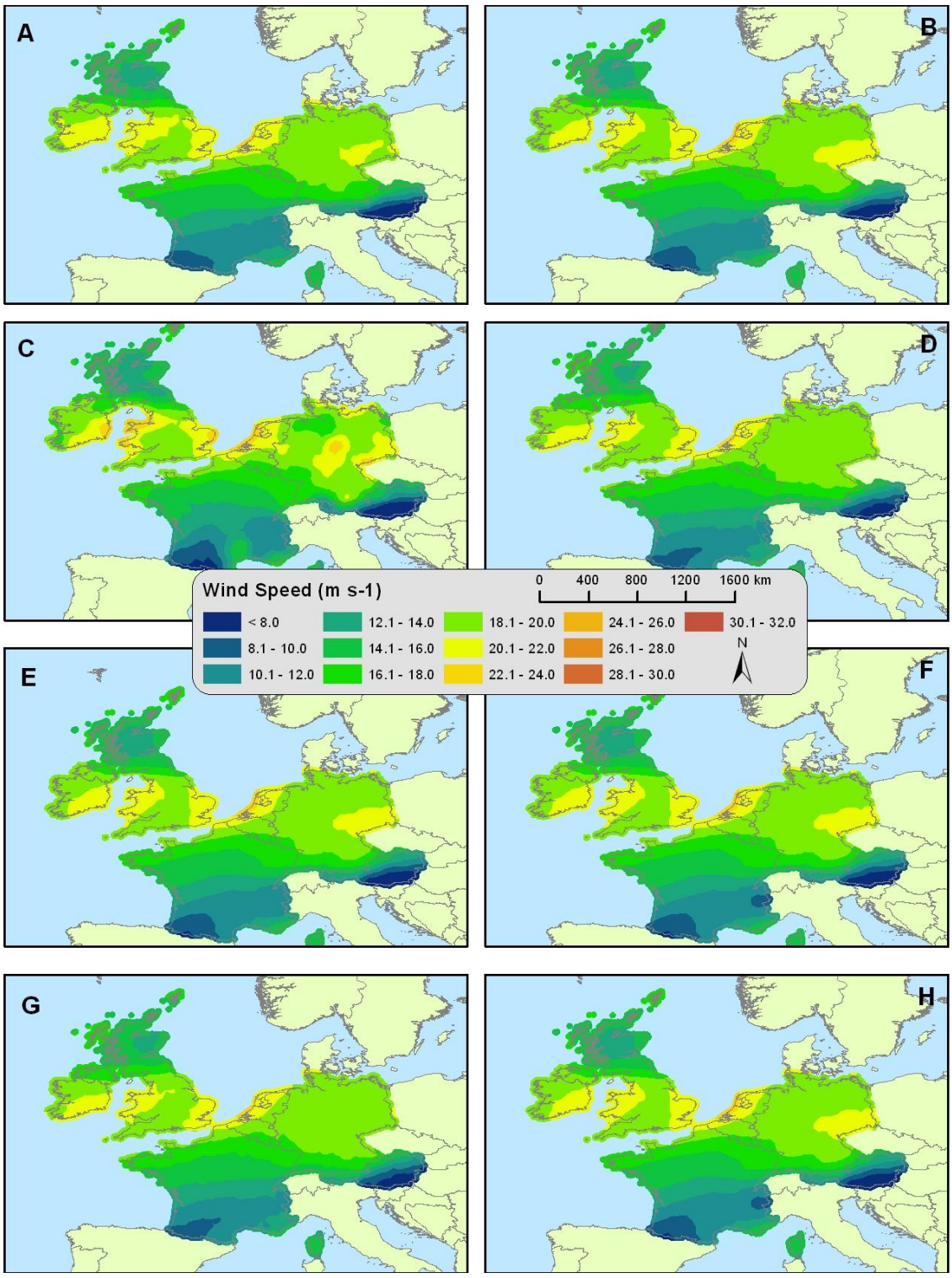

Figure 3-7. Maximum sustained wind surface estimates for wind storm Kyrill (2007) produced by the following models: original kriging (A), cokriging with elevation (B), cokriging with aspect (C), cokriging with land cover (D), cokriging with elevation and aspect (E), cokriging with elevation and land cover (F), cokriging with aspect and land cover (G), and cokriging with elevation, aspect, and land cover (H).

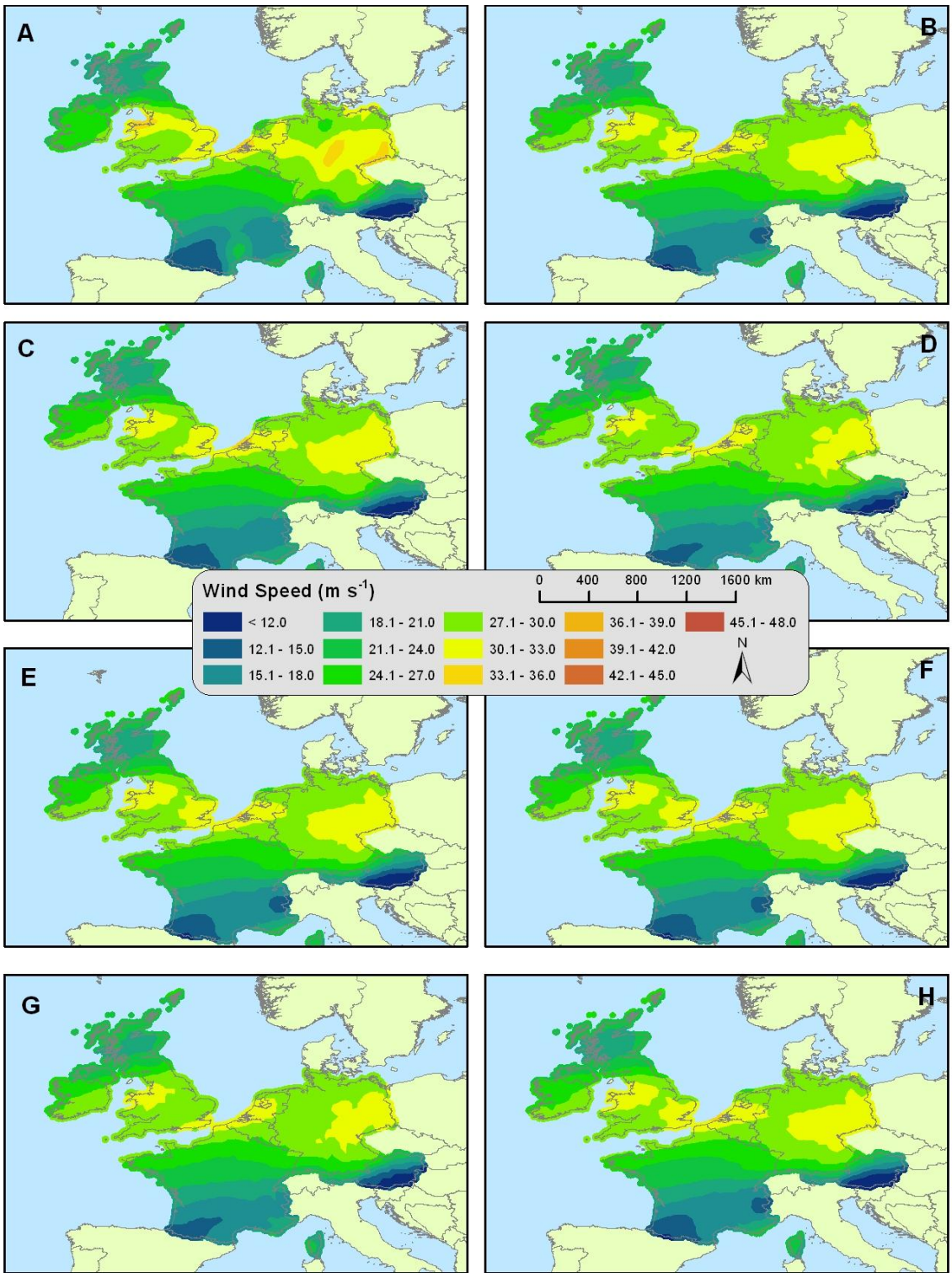

Figure 3-8. Peak gust wind surface estimates for wind storm Kyrill produced by the following models: original kriging (A), cokriging with elevation (B), cokriging with aspect (C), cokriging with land cover (D), cokriging with elevation and aspect (E), cokriging with elevation and land cover (F), cokriging with aspect and land cover (G), and cokriging with elevation, aspect, and land cover (H).

Table 3-5. Wind storm Kyrill (2007) accuracy metrics for each model indicating dominant automatic wind speed direction, inter-model error comparison (RMSPE), intra-model error comparison (ME and RMSE), and number of high error stations.

Storm	Method	Anisotropy	RMSPE	ME	RMSE	SE (> +/- 2.0)
Kyrill	Original kriging	80.3	4.44	0.016	0.98	39
Max	Cokriging w/elev	68.2	4.39	0.009	0.99	41
Sustained	Cokriging w/asp	72.1	4.40	0.008	0.93	35
	Cokriging w/LC	64.0	4.46	0.015	0.97	41
	Cokriging w/elev & asp	68.2	4.39	0.009	0.99	41
	Cokriging w/elev & LC	68.0	4.39	0.008	0.99	41
	Cokriging w/asp & LC	64.2	4.46	0.013	0.97	40
	Cokriging w/elev, asp, & LC	68.0	4.39	0.008	0.99	41
Kyrill	Original kriging	64.8	7.16	0.003	0.94	37
Peak	Cokriging w/elev	68.2	7.19	0.005	0.99	43
Gust	Cokriging w/asp	71.6	7.19	0.005	0.96	38
	Cokriging w/LC	64.2	7.24	0.001	0.96	40
	Cokriging w/elev & asp	68.2	7.19	0.005	0.99	43
	Cokriging w/elev & LC	68.2	7.20	0.005	0.99	42
	Cokriging w/asp & LC	64.5	7.23	0.000	0.96	40
	Cokriging w/elev, asp, & LC	68.2	7.19	0.005	0.99	43

gust wind models, the cokriging model utilizing aspect produced the automated anisotropic conditions closest to the actual storm track of ~82°, while the cokriging model utilizing aspect and land cover generated the ME score nearest to zero. The original kriging model produced the lowest RMSPE score and the fewest stations (37) reporting a SE measurement exceeding +/-2.0. Half of the models produced the RMSE score nearest to 1.0.

To examine in more detail the locations where high SE measurements occurred, maps were produced for each wind type for wind storm Kyrill (Figure 3-9a-b). Most stations with high SE measurements received such measurements from multiple models. For the maximum sustained wind speed models, high SE measurements were

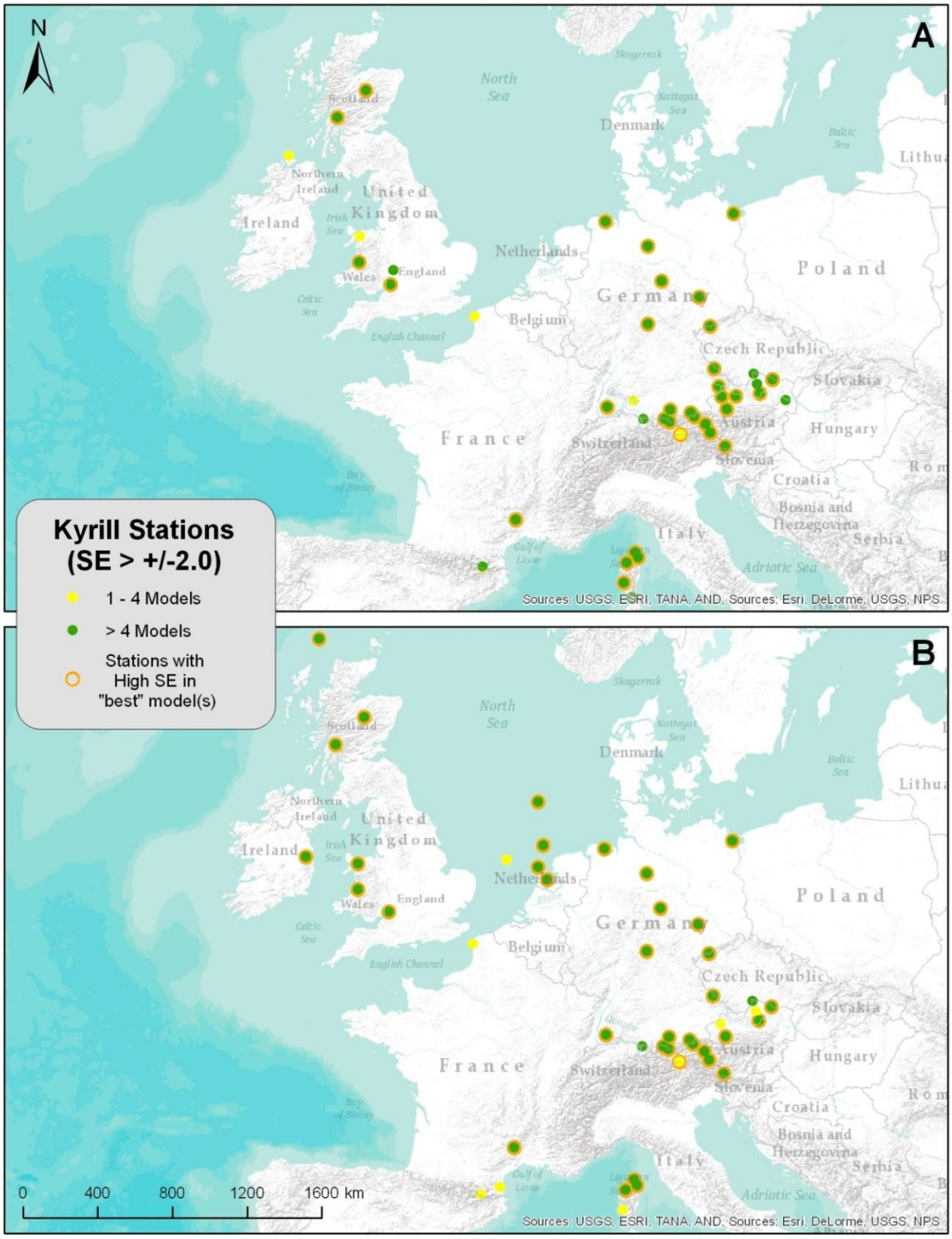

Figure 3-9. Stations reporting high SE measurements for maximum sustained (A) and peak gust (B) winds.

recorded by stations in mountainous regions of Austria and southern Germany as well as coastal and interior areas of central and northern Germany. Coastal areas of the Netherlands, and western and northern UK also contained stations with high SE measurements. Additionally, mountainous areas of southern France and stations on the French island of Corse contained high SE measurements. For the peak gust wind speed models, high SE measurements were recorded in near-identical areas in mountainous and coastal regions with an additional station in Ireland reporting high SE measurements. Stations coinciding with the optimal model(s) based on SE measurements were also highlighted and extended across mountainous and coastal areas.

3.3.2.4 Wind storm Paula

Paula impacted much of northern Europe in January 2008 as it tracked across Norway, Sweden, Finland, and Denmark. Paula developed from a low pressure system in the North Atlantic Ocean and had a long, attached frontal boundary that impacted areas of Europe as far south as Austria. High winds were distributed over relatively large areas with some of the highest winds occurring in the Alps away from the center of circulation. The wind storm moved from west to east with major damage occurring in Scandinavia, Germany, Poland, and Austria. Only one death was reported, but ~€300 million in damage were attributable to Paula in Austria (Lloyds 2008, VRS 2008). During Paula, several wind observation stations in Norway, Germany, Poland, and Austria reported gusts exceeding 40 m s^{-1} – comparable to Category 2 hurricane wind speeds. Building roofs, communication and transport networks, power lines, and trees were damaged by winds (VRS 2008).

While Paula impacted a large area, Austria was particularly hard-hit despite higher winds not being identified in the country by any models. Results of cokriging models for maximum sustained wind speeds (Figure 3-10) and peak gusts (Figure 3-11) provide additional evidence of the general west-east storm track for Paula. Wind speeds approaching 36 m s^{-1} were estimated by multiple peak gust models in coastal western areas of the Norway. Peak gusts exceeding 20 m s^{-1} extended across Denmark, northeastern Germany, and some parts of western Poland. Some differences in wind speed estimates were observed between modeled surfaces. For example, Figures 3-10a, 3-10c, 3-11a, 3-11b, and 3-11c showed a pocket of higher winds around Copenhagen and another pocket in southwestern Poland, while other models estimated a gradual deterioration of wind speeds from west to east. Localized higher winds in Austria may have been smoothed by the global interpolation process but could potentially be identified with regional wind speed models.

To determine the optimal model(s) for each wind speed type for Paula, multiple accuracy metrics were utilized during model implementation. Accuracy metrics for each model and wind type are listed in Table 3-6. For Paula's maximum sustained modeled wind, the original kriging methodology produced the automated anisotropic conditions closest to the actual storm track of ~100°. Four models produced the lowest RMSPE score of 4.49, while the ME score nearest to zero was produced by the original kriging model and the cokriging model utilizing aspect. The RMSE score nearest to 1.0 was produced by four cokriging models utilizing various combinations of all three covariates. Two models (cokriging with land cover and cokriging with aspect and land cover) reported the fewest number of stations (17) with high SE measurements after

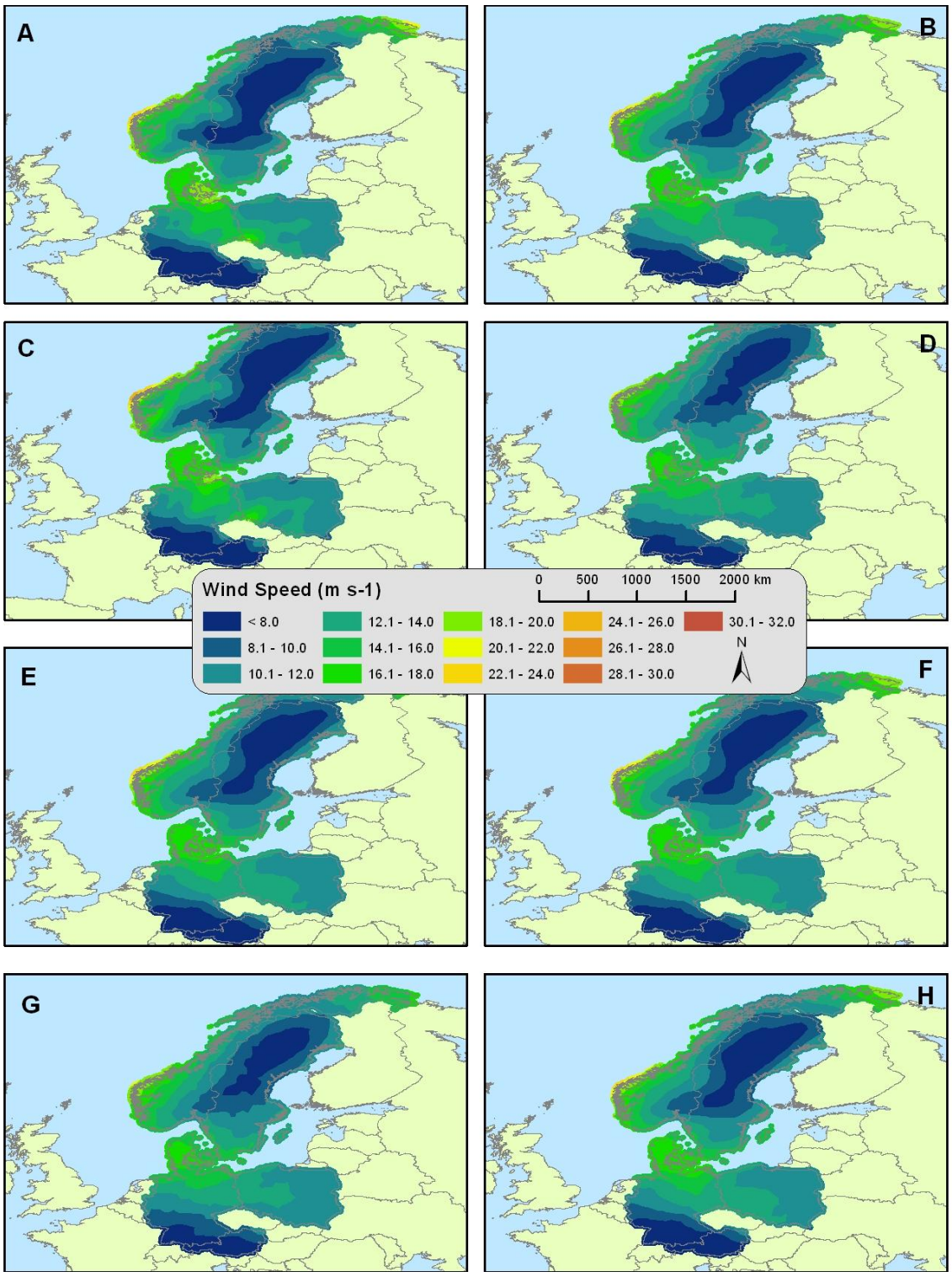

Figure 3-10. Maximum sustained wind surface estimates for wind storm Paula (2008) produced by the following models: original kriging (A), cokriging with elevation (B), cokriging with aspect (C), cokriging with land cover (D), cokriging with elevation and aspect (E), cokriging with elevation and land cover (F), cokriging with aspect and land cover (G), and cokriging with elevation, aspect, and land cover (H).

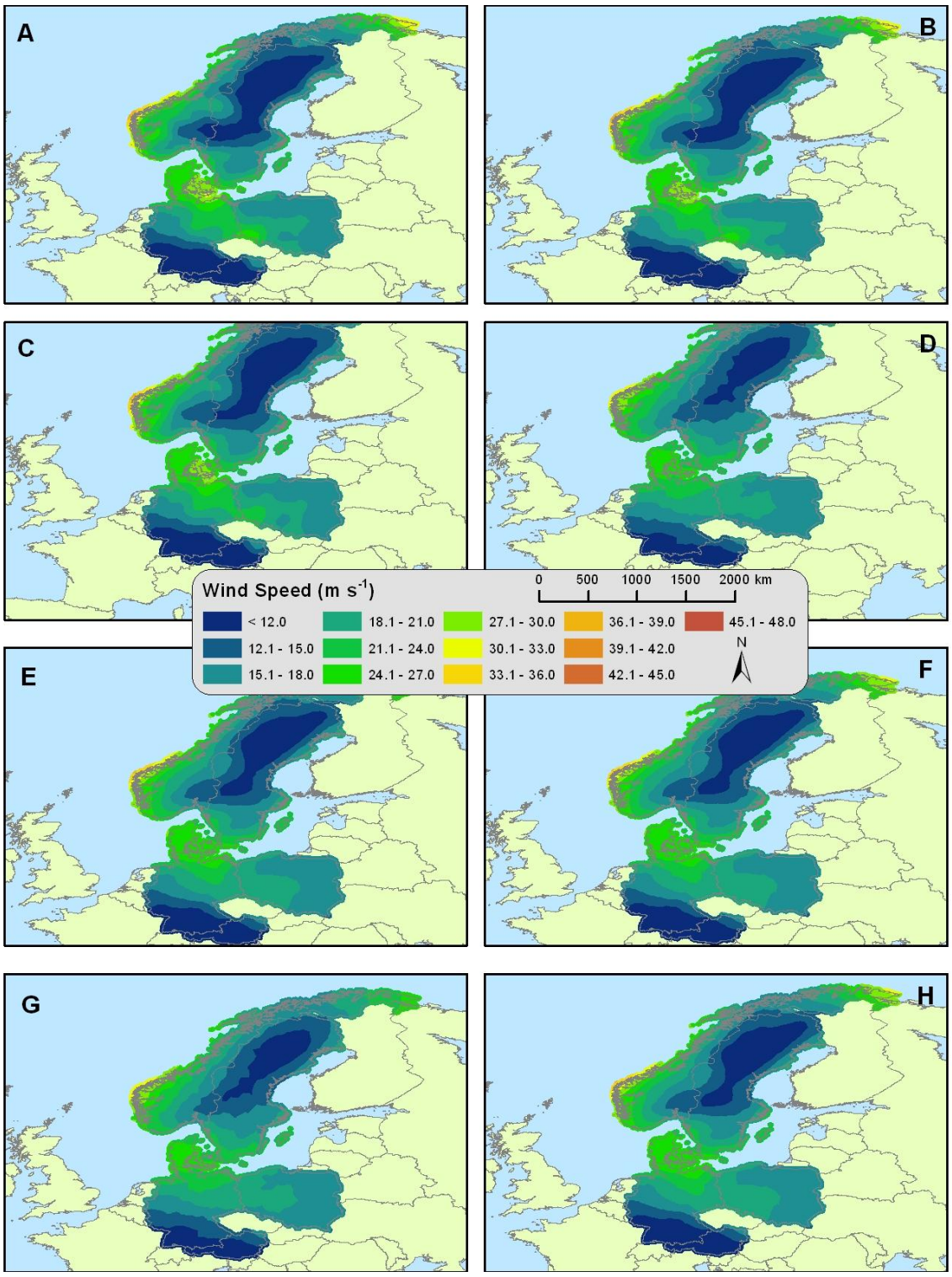

Figure 3-11. Peak gust wind surface estimates for wind storm Paula produced by the following models: original kriging (A), cokriging with elevation (B), cokriging with aspect (C), cokriging with land cover (D), cokriging with elevation and aspect (E), cokriging with elevation and land cover (F), cokriging with aspect and land cover (G), and cokriging with elevation, aspect, and land cover (H).

Table 3-6. Wind storm Paula (2008) accuracy metrics for each model indicating dominant automatic wind speed direction, inter-model error comparison (RMSPE), intra-model error comparison (ME and RMSE), and number of high error stations.

Storm	Method	Anisotropy	RMSPE	ME	RMSE	SE (> +/- 2.0)
Paula Max Sustained	Original kriging	86.3	4.49	0.002	1.06	39
	Cokriging w/elev	68.0	4.49	0.012	1.00	33
	Cokriging w/asp	52.7	4.50	0.002	1.03	33
	Cokriging w/LC	64.0	4.58	0.020	0.89	17
	Cokriging w/elev & asp	68.0	4.49	0.012	1.00	33
	Cokriging w/elev & LC	68.0	4.51	0.014	1.00	33
	Cokriging w/asp & LC	64.0	4.58	0.020	0.89	17
	Cokriging w/elev, asp, & LC	68.0	4.49	0.012	1.00	33
Paula Peak Gust	Original kriging	86.1	7.09	0.002	1.07	38
	Cokriging w/elev	69.1	7.05	0.012	1.00	40
	Cokriging w/asp	44.8	7.15	0.006	1.00	30
	Cokriging w/LC	64.0	7.25	0.019	0.90	18
	Cokriging w/elev & asp	68.0	7.08	0.011	1.01	30
	Cokriging w/elev & LC	68.0	7.12	0.013	1.02	32
	Cokriging w/asp & LC	63.8	7.26	0.019	0.90	18
	Cokriging w/elev, asp, & LC	68.0	7.12	0.013	1.02	32

cross-validation. For the peak gust wind models, the original kriging methodology again produced the automated anisotropic conditions closest to the actual storm track of ~100°. Two models (cokriging with elevation and cokriging with aspect) produced the RMSE score nearest to 1.0, and two different models (cokriging with land cover and cokriging with aspect and land cover) reported the fewest number of stations (18) with SE exceeding +/-2.0. The model utilizing elevation as a covariate generated the lowest RMSPE score, while the ME nearest to zero was produced by the original kriging model.

To examine in more detail the locations where high SE measurements occurred, maps were produced for each wind type for Paula (Figure 3-12a-b). Most stations with

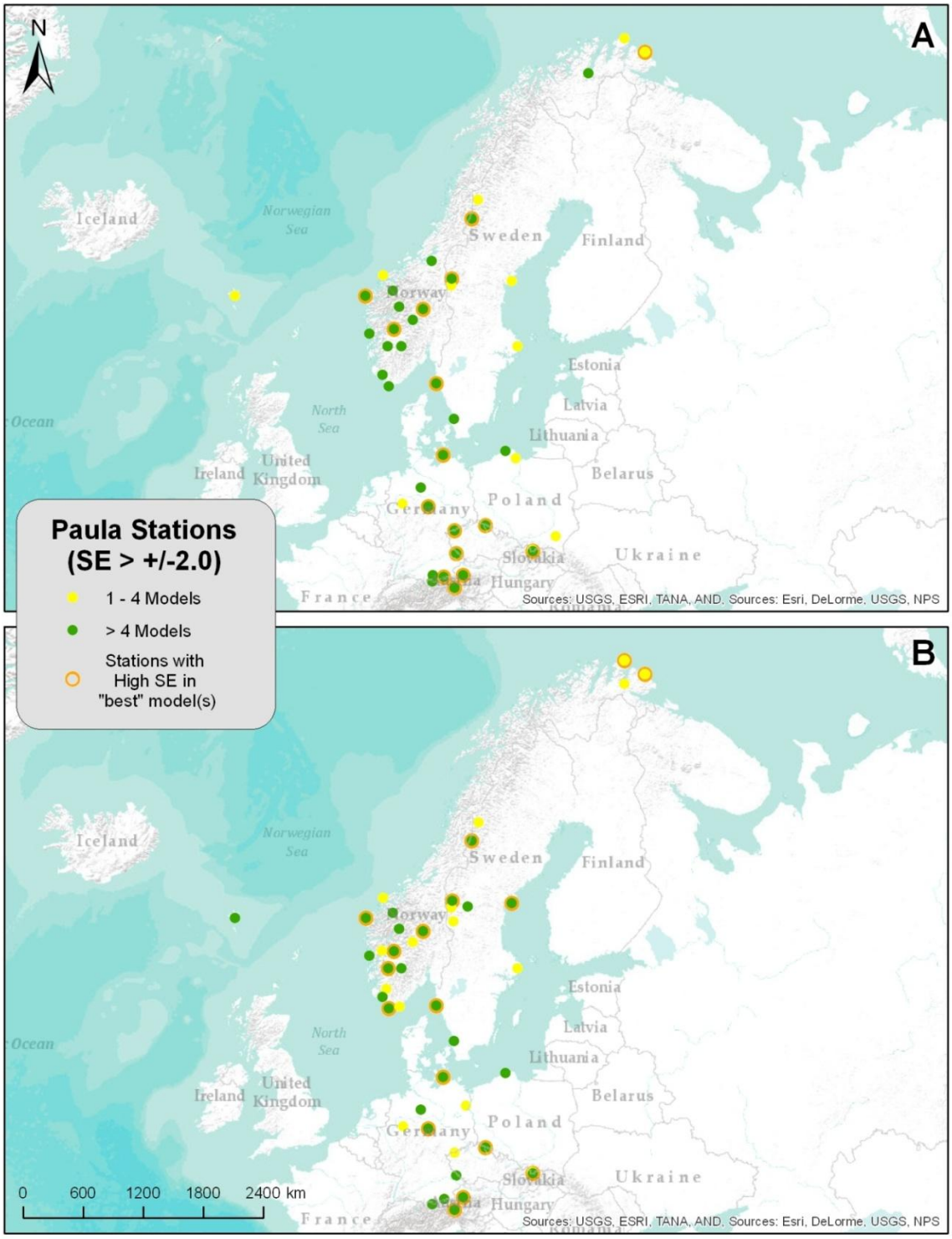

Figure 3-12. Stations reporting high SE measurements for maximum sustained (A) and peak gust (B) winds.

high SE measurements received such measurements from multiple models. For the maximum sustained wind speed models, high SE measurements were recorded by stations in the Alps of Austria and southern Germany, as well as coastal and interior stations in the southern half of Norway. Other stations receiving high SE measurements were scattered in coastal Sweden, Germany, and Poland as well as the rugged border between Germany and the Czech Republic. For the peak gust wind speed models, high SE measurements were recorded in near-identical areas in mountainous and coastal regions with a few exceptions. Stations coinciding with the optimal model(s) based on SE measurements were also highlighted and occurred in concomitant geographical areas.

3.3.2.5 Wind storm Emma

Emma moved across northern and central Europe between 29 February and 1 March 2008, and predominantly impacted the Netherlands, Belgium, Switzerland, Germany, Austria, Czech Republic, and Poland. Emma developed from a low pressure system in the North Atlantic Ocean and joined a separate frontal system as it tracked into northern Europe, making it a very complex storm with disproportionately high sustained wind speeds and widely varying wind directions. Variance in wind directions created confusion during modeling when anisotropy was considered. The wind storm moved from west to east across northern Europe with the frontal boundary extending into southern Europe. Approximately 15 deaths and €1.3 billion in insured losses were attributable to Emma with almost €1 billion of damage in Germany and ~€200 million of damage in Austria alone (Guy Carpenter 2008). The greatest losses occurred in the Bavaria region of southeastern Germany. During Emma, several wind observation

stations in Bavaria and Austria around Salzburg and Vienna reported gusts exceeding 35 m s^{-1} – comparable to Category 1 hurricane wind speeds. Building roofs, communication and transport networks, power lines, automobiles, and trees were particularly hard-hit by winds, while flooding was a major concern in many eastern European countries (Guy Carpenter 2008).

Results of cokriging models for maximum sustained wind speeds (Figure 3-13) and peak gusts (Figure 3-14) provide additional evidence of the general west-east storm track for Emma, while also alluding to the northwest-southeast wind speeds associated with the initial frontal system. Wind speeds approaching 33 m s^{-1} were estimated by several peak gust models near the Germany-Denmark border. Only one peak gust model (Figure 3-14e) indicated similar wind speeds in the Bavaria region of Germany near Austria as well as small areas of the Czech Republic. The highest sustained wind speeds and peak gusts occurred in coastal areas of the Netherlands and Germany as well as interior southern areas of Germany, with a slight decrease in wind speeds evidenced in the northern plains of Germany. Some differences in wind speed estimates were observed between most surfaces. For example, Figures 3-13e, 3-13f, and 3-13g showed very spotty and localized excessive winds that appeared to be influenced by topography since each of those models used elevation and/or aspect as covariates. The other, more smoothed surfaces may be more indicative of wind storm Emma's general wind speeds and patterns based on accuracy analysis – highlighting the complexity of surface winds caused by the unique meteorology associated with Emma.

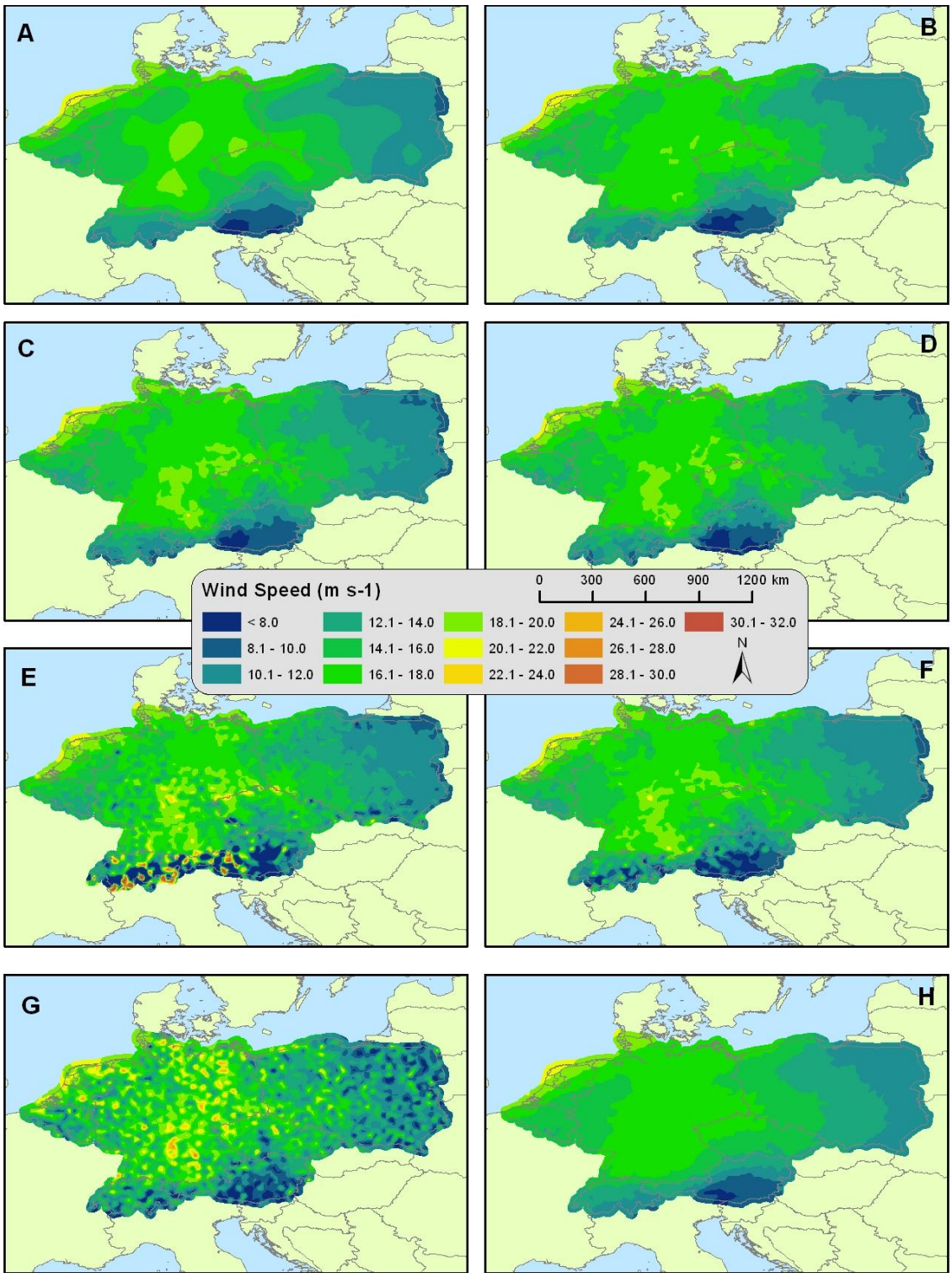

Figure 3-13. Maximum sustained wind surface estimates for wind storm Emma produced by the following models: original kriging (A), cokriging with elevation (B), cokriging with aspect (C), cokriging with land cover (D), cokriging with elevation and aspect (E), cokriging with elevation and land cover (F), cokriging with aspect and land cover (G), and cokriging with elevation, aspect, and land cover (H).

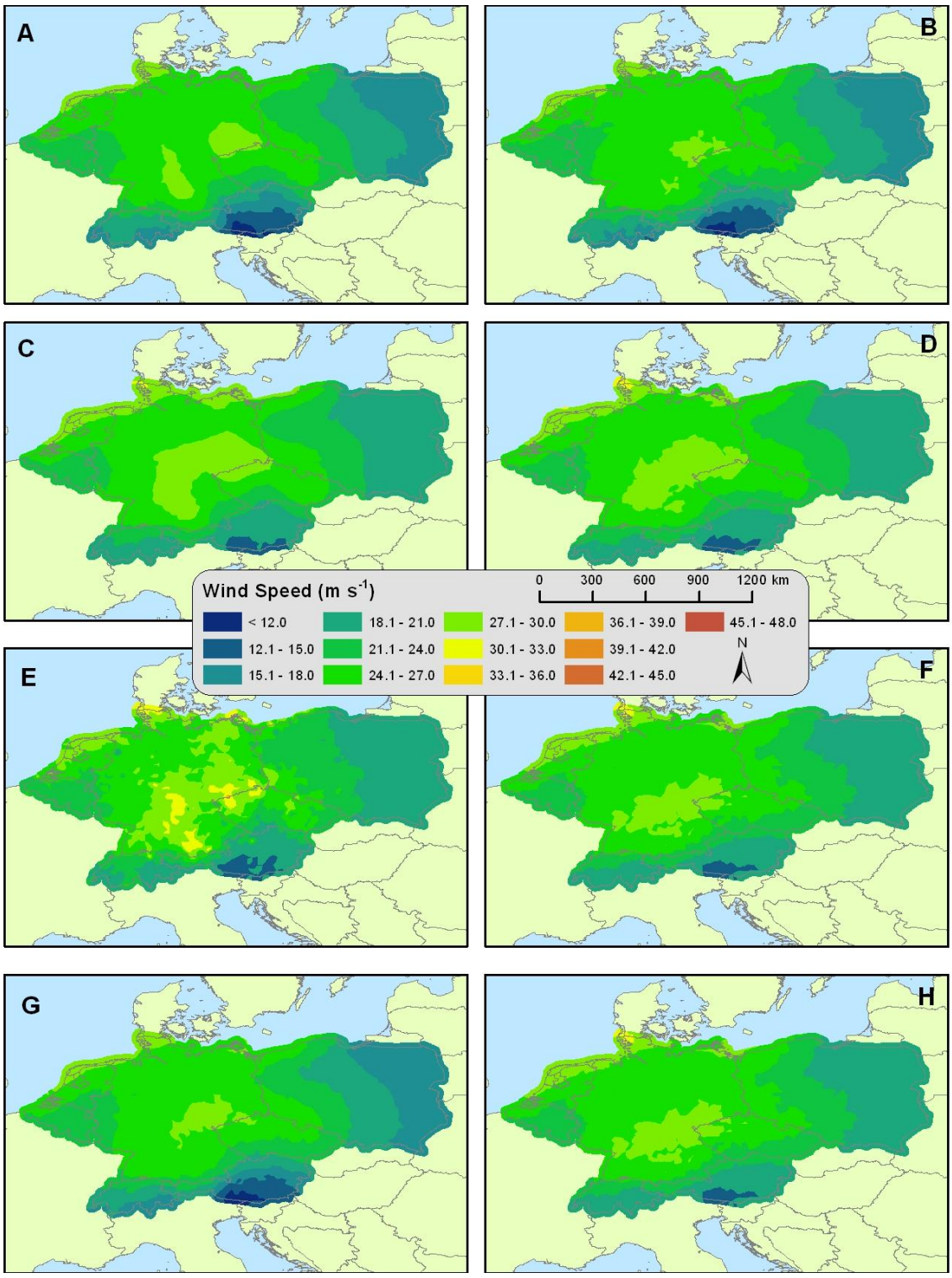

Figure 3-14. Peak gust wind surface estimates for wind storm Emma (2008) produced by the following models: original kriging (A), cokriging with elevation (B), cokriging with aspect (C), cokriging with land cover (D), cokriging with elevation and aspect (E), cokriging with elevation and land cover (F), cokriging with aspect and land cover (G), and cokriging with elevation, aspect, and land cover (H).

Table 3-7. Wind storm Emma (2008) accuracy metrics for each model indicating dominant automatic wind speed direction, inter-model error comparison (RMSPE), intra-model error comparison (ME and RMSE), and number of high error stations.

Storm	Method	Anisotropy	RMSPE	ME	RMSE	SE (> +/- 2.0)
Emma	Original kriging	58.4	5.05	0.002	0.96	20
Max	Cokriging w/elev	159.6	5.02	0.001	0.92	16
Sustained	Cokriging w/asp	1.8	5.16	-0.015	0.82	13
	Cokriging w/LC	71.0	5.16	0.000	0.81	12
	Cokriging w/elev & asp	17.6	10.54	0.130	1.97	91
	Cokriging w/elev & LC	0.0	6.11	0.004	0.94	24
	Cokriging w/asp & LC	3.9	6.26	0.011	1.02	27
	Cokriging w/elev, asp, & LC	68.0	5.02	0.005	0.91	16
Emma	Original kriging	42.7	8.25	0.005	0.96	20
Peak	Cokriging w/elev	159.8	8.21	0.000	0.91	18
Gust	Cokriging w/asp	43.8	8.25	0.006	0.95	20
	Cokriging w/LC	154.3	8.21	0.002	0.94	21
	Cokriging w/elev & asp	16.5	15.99	0.111	1.81	84
	Cokriging w/elev & LC	68.0	8.21	0.003	0.89	16
	Cokriging w/asp & LC	154.3	8.21	0.029	0.94	21
	Cokriging w/elev, asp, & LC	68.0	8.21	0.003	0.89	16

To determine the optimal model(s) for each wind speed type for Emma, multiple accuracy metrics were utilized during model implementation. Accuracy metrics for each model and wind type are listed in Table 3-7. For Emma's maximum sustained wind, the cokriging methodology utilizing only land cover produced the automated anisotropic conditions closest to the actual storm track of ~113°, but automated anisotropy differed greatly between models. The model utilizing the covariate elevation as well as the model utilizing all three covariates produced the lowest RMSPE score, while the ME nearest to zero and fewest stations with high SE measurements (12) was produced by the model utilizing only land cover. The combination of aspect and land cover produced the RMSE score nearest to 1.0. For the peak gust wind models, the model utilizing only

land cover and the model utilizing both aspect and land cover produced the automated anisotropic conditions closest to the actual storm track of ~113°. Multiple models produced the lowest RMSPE score, including the model utilizing only land cover as a covariate. Two models (elevation and land cover, all three covariates) were tied for the fewest stations (16) reporting a SE measurement of greater than +/-2.0. The model utilizing elevation as a covariate generated the ME nearest to zero, while the RMSE nearest to 1.0 was produced by two models: the original kriging model and the model incorporating aspect and land cover.

To examine in more detail the locations where high SE measurements occurred, maps were produced for each wind type for wind storm Emma (Figure 3-15a-b). Most stations with high SE measurements received such measurements from multiple models. The major exceptions were the models that incorporated elevation and aspect collectively as covariates. These models reported a large number of stations with high SE measurements located predominantly in the Alps of Switzerland and Austria. For the maximum sustained wind speed models, most high SE measurements were recorded by stations in mountainous regions of Switzerland, Austria, and southern Germany as well as a rugged area in central Germany and mountainous border between the Czech Republic and Germany. Stations in coastal areas reported very few high SE measurements; only one station on the Baltic Sea coast of Poland reported multiple high SE measurements. For the peak gust wind speed models, high SE measurements were recorded in near-identical areas in mountainous and rugged regions as well as the one coastal station in Poland. Stations coinciding with the optimal model(s) based on SE measurements were also highlighted and, while

improved compared to other models, continued to indicate a complex and difficult-to-model environment in mountainous areas.

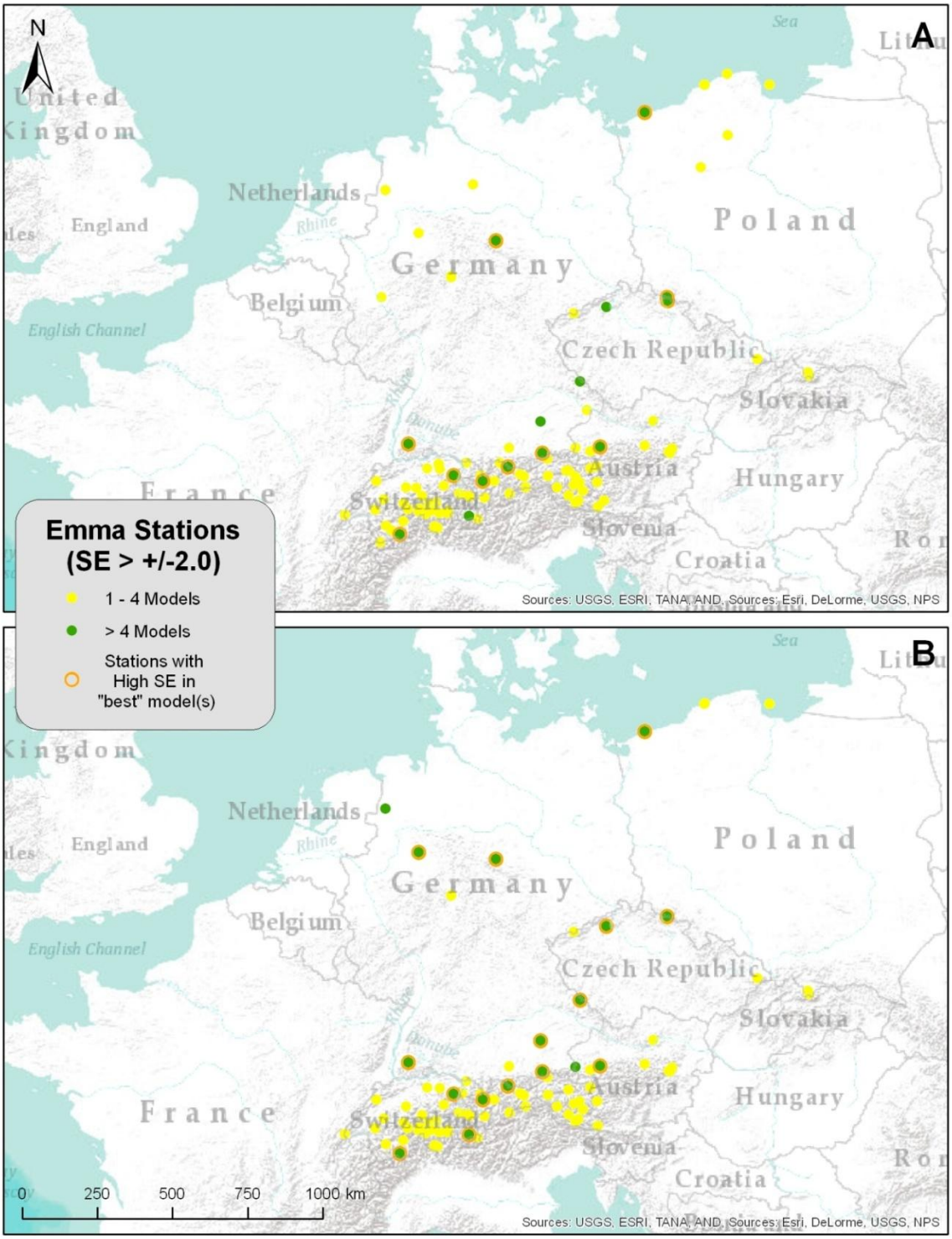

Figure 3-15. Stations reporting high SE measurements for maximum sustained (A) and peak gust (B) winds.

3.4 Discussion

3.4.1 Optimizing surface wind estimates through cokriging

Seven different cokriging models were produced using singular and assimilated combinations of each covariate with varying results of modification compared to results from the original kriging methodology. The original kriging model was also produced for each of the five storms to allow for a side-by-side visual and statistical comparison through the use of multiple accuracy metrics. Overall, 80 different modeled surface estimates were created – 16 for each of the five wind storms – and standard error maps were also created for each wind type. The maps showed that most models produced logical surface estimates based on the known track, wind speed, and wind direction associated with each storm. All wind storms followed a general west-east track across either central or northern Europe with the UK, France, the Netherlands, Belgium, and Germany being impacted the most by winds and infrastructure damage. The strongest winds associated with each storm occurred predominantly in coastal and mountainous areas with a common tendency for winds to subside slightly as they moved inland, then to increase again when approaching the mountainous regions. Higher levels of uncertainty (or error) were associated with both the coastal and mountainous regions. Wind speeds are difficult to model in coastal regions for two reasons: 1) the land-ocean interface creates turbulence and deflection when the surface that wind moves across changes (Wieringa 1973, 1986) and 2) wind observation stations rarely exist over water, thus providing an abrupt departure in station density (MacEachren and Davidson 1987, Wieringa 1997). Wind speeds are difficult to model in mountainous regions for two reasons as well: 1) wind is deflected and funneled in multiple directions by varying topography (Wieringa 1973, 1986) and 2) as winds move upslope and downslope, wind

speed also changes resulting in locally high/low winds (Bowen and Lindley 1977, Hertenstein and Kuettner 2005). These local wind patterns are difficult to estimate using a global model.

Figures 3-13e and 3-13g (wind storm Emma) provide an example of global wind surfaces that were too specific in assigning local wind patterns and created a surface where the general wind patterns were difficult to visualize. These same models also produced higher station error relative to the original kriging surface. Because Emma was a complex storm that coincided with a separate frontal system moving across Europe, some model uncertainly may be expected. Wind direction was also very difficult to model for Emma because of the contrasting atmospheric systems. Excluding the models from Figures 3-13e and 3-13g, the use of covariates most often improves upon the original kriging surface by reducing station error.

Covariates were not significantly spatially autocorrelated, but wind speed was autocorrelated and the use of anisotropy during modeling helped in identifying overall trends in wind direction based on high/low wind speeds. Most modeled surfaces illustrated the general west-east or northwest-southeast movement of each wind storm, but the azimuth directions identified by the automatic anisotropy process sometimes varied widely. For example, azimuth direction varied by as much as ~35° for the models produced for Emma. The greatest disparity was observed between the original kriging surfaces and the model that used only aspect as a covariate. This result may indicate that the addition of aspect resulted in a more nuanced wind surface that possibly contained multiple wind directions at specific locations where one side of a mountain may have deflected the wind in a way that was different from the general wind pattern.

Topography can deflect wind and create changes in turbulence in the area immediately behind a mountain or mountain range (Bowen and Lindley 1977).

Accuracy metrics were highly varied, indicating that one singular covariate does not always improve wind surface estimates for wind storms over large, heterogeneous terrain. However, the major index of standard error (SE) reduction showed improvement over the original kriging surface in eight out of the ten model sets, with only one set (peak gust models for Kyrill) indicating that original kriging was optimal. Several peak gust models for Lothar did not reduce the SE, but also did not increase the SE. The original kriging method also reported the lowest SE measurement in the set of peak gust models for Lothar, but five other models reported the identical stations with high SE (16) as well. The SE for Paula was reduced by more than half (Table 3-6) and provides an example of how a singular covariate (land cover in this case) can improve surface estimates markedly. Additionally, a change detection analysis was performed for Paula to better understand and identify the differences between the original kriging model and the optimal cokriging model that used land cover (Figure 3-16). The change detection map indicates that the border areas of Poland, Germany, and the Czech Republic experienced a large disparity in predicted wind speeds between each model. Predicted wind speeds were also different in areas of central Norway and Sweden as well as the northern coast of Norway. Overall, the model output of the optimal version was greatly improved compared to the original kriging model, as has been found in previous research (Luo et al. 2008, Akkala et al. 2010, Zlatev et al. 2010, Luo et al. 2011).

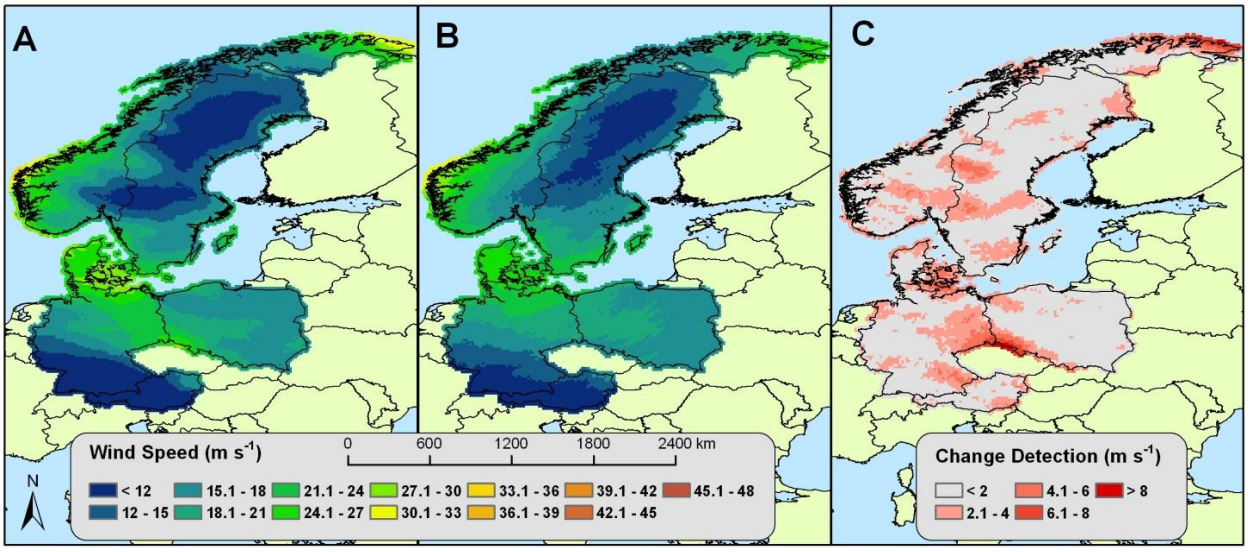

Figure 3-16. Change detection for wind storm Paula, showing original kriging model (A), optimal cokriging model using land cover (B), and the difference between each model (C).

Overall, models utilizing land cover (singularly or in conjunction with elevation and/or aspect) tended to produce optimal wind speed surface estimates, but this was not always true. The optimal maximum sustained wind speed model for Kyrill was produced using only aspect as a covariate, while the optimal peak gust wind speed model for Jeanette was produced using both elevation and aspect collectively. Additionally, models utilizing land cover were much more computational intensive, typically requiring several hours (and occasionally days, e.g., Jeanette), while models utilizing elevation and/or aspect were completed in less than one hour. This was most likely due to the complex nature of actual land cover on the surface as well as the categorical nature of the dataset within the geostatistical modeling environment. Each step of the process was conducted manually, resulting in a more complicated and extended modeling process that would have been improved through automation. Regardless of modeling complexity and intensiveness, the general improvement shown

by models utilizing land cover is promising for future modeling efforts and covariate creation. While land cover proved to be a useful covariate, there is some uncertainty about why it was often a stronger covariate than elevation and aspect since WMO standards indicate that data from all stations are adjusted to reflect wind speed in open terrain. One explanation of this peculiarity may be that even when wind speed is corrected to open terrain, the strong mechanical turbulence produced by the surrounding rugged terrain or land cover features still has an impact on the wind speed, thus resulting in a correlation between land cover types and wind speed. While use of land cover as a covariate provides an opportunity for model improvement, the observed relationship between land cover and wind speed may also suggest that WMO adjustments to open terrain may not fully exclude landscape influences.

3.4.2 Overall impact of improved wind surface estimates

Improved wind surface estimates created through cokriging build on previous research that only utilized one covariate (elevation) to model wind speeds. The addition of aspect and land cover improved surface estimates and may be used for other wind- or even non wind-related research. Use of other covariates within cokriging may help to address other problems, ranging from hazards to energy. Within wind storm research, models and extreme-event climatologies of wind simulation and hazard/risk assessment that are widely used in the insurance/reinsurance industry can be improved through the incorporation of our research results. This study may also help to inform local cost-benefit studies and subsequently save lives and resources for local government, private industry, and consumers. Damage estimates may also be refined based on the resulting wind surface estimates, thus improving construction standards and adapting insurance needs. The known impacts of wind storms on vegetation (e.g., trees; Kirk

and Franklin 1992) and civil infrastructure (Reed 2008) are severe, and improved spatial interpolations for wind storm-induced wind speeds will be fundamental to evaluating damages as well as potential changes needed for forest management and building codes/regulations. Identification of high wind zones will also help to inform local vulnerability assessments that may be included in future hazard mitigation plans. The results may also improve understanding of common wind storm features (*e.g.*, directions, wind movements/patterns, surface interactions, etc.) that have long-term, but not necessarily immediate, impacts on sectors such as transportation, agriculture, and recreation.

3.5 Future Research

Local cokriging surfaces (*e.g.*, country- and state-level) will be the focus of future research and these surfaces will be created to examine more specific wind speeds and directions that are often smoothed when performing regional cokriging (*e.g.*, all of Europe). This smoothing was evident in each of ten model sets because the general wind direction and speed were mapped correctly, but locally-strong winds were more difficult to discern. Damage data (e.g., trees, infrastructure) may also be joined and overlaid spatially with the optimal local wind surface estimates to establish a damage-wind ratio. Proximity analysis and exposure-testing using aspect and slope may further aid in understanding high damage locations associated with wind storms. Excessive wind speeds will likely recur in similar areas, thus there is also a need to identify repetitive windy and susceptible environments. Using the ideal cokriging parameters and covariate combinations identified for Europe in this study, the transferability of the methods may also be tested for various wind storms in the Pacific Northwest region of North America where similar wind storms (called winter storms locally) occur.

Successful transferability of cokriging methods would imply that the techniques are responsive to areas with differing terrains and land covers and that the methods are adaptable.

A major area of future research involves a complete remaking of the covariate dataset. While the cokriging interpolation method improved surface wind estimates, an additional procedure could be tested to reduce the inherent concern of autocorrelation between covariates. Just as principal components analysis (PCA) is used to combine strongly correlated variables into various components, a data reduction technique may be applied to create a “ruggedness” variable. Issues of autocorrelation could potentially be eliminated through the development of one variable that incorporates both elevation and land cover to represent terrain ruggedness. An anisotropic cokriging model will likely improve prediction of the contrasting effects on wind speeds caused by rough-to-smooth *vs*. smooth-to-rough terrain transition areas where ruggedness may change abruptly. Application of only one covariate may also help to reduce the error associated with the use of multiple covariates.

CHAPTER 4. THE INFLUENCE OF SCALE ON KRIGING AND COKRIGING: A CASE STUDY OF AUSTRIA

4.1 Introduction

Issues of scale are integral to geographic research and are constantly debated when exploring various types of spatial data and means of mapping such data (Meentemeyer 1989, Lam and Quattrochi 1992, Atkinson and Tate 2000, Wu 2004, Sayre 2005). When climatic data (e.g., temperature, precipitation, wind speed, snowfall, etc.) are mapped and/or modeled, the choice between small-, medium-, and large-scale visualization is difficult because each scale level has advantages and disadvantages (Meentemeyer 1989, Atkinson and Tate 2000). Within this discussion, scale can be defined as a ratio between the size of mapped objects versus their actual size; small-scale refers to viewing a larger geographic area (e.g., an entire continent), while large-scale refers to viewing a smaller geographic area (e.g., a single country or state). Spatial variation and patterns of spatial dependence and error are not easily identifiable at certain scales (Atkinson and Tate 2000). For example, a small-scale model may identify general trends and patterns across a large area very well, but not be capable of identifying more local disparities and deviations.

These complications lead to what is known as the “scale problem” in geography, in which conclusions are transferred erroneously across scales and hierarchies (Meentemeyer 1989). The related concept of “ecological fallacy” was first acknowledged by Robinson (1950) who identified a common theoretical problem with statistical analysis. Many researchers were treating ecological (or group) correlations the same as individual correlations, thus transferring a relationship between scales without any statistical justification. For example, the assumption that demographic

information at the state level is identical at any particular county in the state is an ecological fallacy (Openshaw 1984). It is acceptable, however, to perform a reverse analysis that aggregates all of the county level data in a state and collectively makes an assumption at the state level (Openshaw 1984).

The modified areal unit problem (MAUP) also describes issues with spatial aggregation (Openshaw and Taylor 1979, Fotheringham and Wong 1991, Dark and Bram 2007). MAUP contains two types of spatial data issues: scale problems and zoning problems (Jelinski and Wu 1996). MAUP scale problems are the same as those discussed earlier, but zoning problems occur when the attribute(s) of two spatial entities is/are considered identical even though the sub-areal attribute(s) is/are distributed differently within the two entities (Jelinski and Wu 1996). Within the context of spatial modeling, two separate models of adjacent areas that overlap in some sections could be combined, but the overlapping areas have slightly different raster cell locations and values resulting in an altered surface (Dark and Bram 2007).

Numerous kriging and cokriging studies (e.g., Gilbert and Simpson 1985, Walter et al. 2001, Cattle et al. 2002, Huang et al. 2006, Tolosana-Delgado and Pawlowsky-Glahn 2007) emphasize the importance of scale when considering how to process and analyze spatial data that may produce widely different results at different scales of analysis. Kriging and cokriging are geostatistical techniques that model stochastically the spatial dependency and correlation across a surface. These techniques can subsequently allow for the re-scaling of data via interpolation (Atkinson and Tate 2000). Scale becomes crucial in two of the stages of kriging/cokriging for identifying the

resulting surface: at the beginning when setting the geographic extent of observation stations and during the semivariogram modeling process.

The validity of kriging and cokriging methods is often evaluated through cross-validation, in which one spatial data point (e.g., weather station) is removed from the model while the variable of interest (e.g., wind speed) at the removed location is predicted based on the wind speed at surrounding stations. The predicted wind speed is compared to the observed wind speed and a standard error measurement is produced. At varying scales, this error measurement can fluctuate greatly because smoothing algorithms are scale-dependent, resulting in “smoother” continent-scale surfaces when compared to country-scale surfaces (Clark 1985). The scale-dependency of kriging/cokriging provides an avenue to explore how local wind surface trends compare and contrast to smaller-scale (i.e., larger-area) trends. Furthermore, areas where wind speeds vary rapidly across space (e.g., mountainous areas) are ideal for local versus global kriging/cokriging model comparison as opposed to more homogenous landscapes (e.g., plains/low hills). Wind speeds in homogenous areas generally remain constant across large expanses and there may be fewer scale-dependent changes in these areas (Sliz-Szkliniarz and Vogt 2011).

4.1.1 Study area and objectives

Maximum sustained and peak wind speeds for four wind storms that impacted the rugged and topographically diverse country of Austria were modeled in this study. The wind storms were Jeanette (2002), Kyrill (2007), Paula (2008), and Emma (2008). Wind speeds from each storm varied, but models from Study One illustrated that the wind speeds of each storm were low and smooth across Austria with a slight north (higher winds) to south (lower winds) gradient (Figure 4-1). Study Two revealed that a plurality

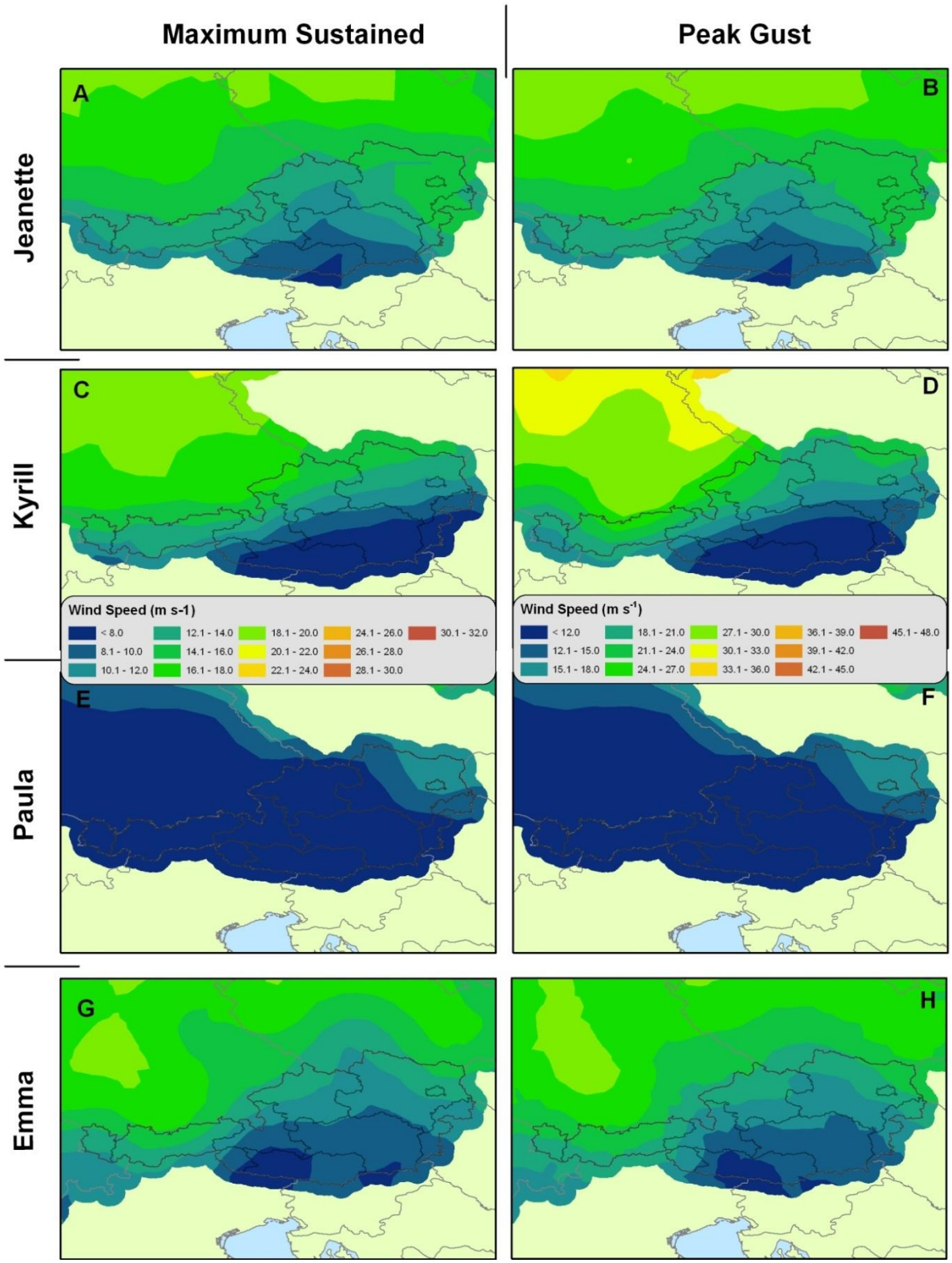

Figure 4-1. A closer examination of maximum sustained and peak gust wind surfaces for each storm impacting Austria derived from optimal methods found in Study Two.

of high error (> +/- 2.0 standard deviations) stations for each storm were located in mountainous areas of Austria, indicating that the wind speed may vary more, particularly in heterogeneous terrain, than the regional-scale models demonstrated. Additionally, wind storm Paula was examined individually because of the excessive tree damage it caused in south-central Austria. The research questions for this study are as follows:

1) Are local kriging/cokriging wind surface estimates more accurate than regional estimates?
2) To what extent can tree damage be utilized as a proxy for validating interpolated wind surfaces?

4.2 Data and Methods

4.2.1 Wind observation and covariate data

Maximum sustained and peak gust data for Austria were extracted from the original, larger datasets for each of the four storms. There were 100 stations reporting data for wind storm Jeanette, 94 stations for Kyrill, and 92 stations for Paula and Emma. Jeanette maximum sustained wind models from Study Two revealed nine high-error (i.e., errors exceeding 2.0 standard deviations) stations in Austria for at least one of the eight models, while the model using peak gust wind identified seven high-error stations for the country. Kyrill maximum sustained wind and peak gust wind models revealed 14 and 10 high-error stations, respectively. Paula maximum sustained and peak gust wind models each revealed two high-error stations. And Emma maximum sustained wind models revealed 34 high-error stations, while peak gust wind models identified 30 high-error stations. Most of the high-error stations for Emma occurred in only one model

(using elevation and aspect as covariates); if this model were excluded, only three stations are characterized as “high-error” for maximum sustained winds and four for peak gust. Increased scrutiny was placed on station locations that consistently received high error measurements from both Study Two and the present study. Specifically, Google Earth® aerial imagery was utilized to examine the physical setting of specific stations and identify commonalities and potential reasons for poor prediction.

Additionally, covariate data were utilized for specific models and included elevation, aspect, and land cover. Similar to Study Two, elevation data were collected from Version 4 of the National Aeronautics and Space Administration (NASA) Shuttle Radar Topographic Mission (NASA-SRTM) 90-m digital elevation dataset through the United Nations Food and Agricultural Organization’s Consultative Group on International Agricultural Research (CGIAR) Consortium for Spatial Information (CGIAR-CSI). The land cover covariate was obtained from the European Space Agency (ESA) GlobCover Project Version 2 2008 database at a resolution of 300 m (GlobCover 2008). The elevation and land cover datasets were clipped to Austria and resampled to 300 m for use in the present study. The GlobCover land cover dataset contains 22 different land cover classification types ranging from various tree types, shrubs, and grasslands to bare land, artificial surfaces, and open water. The covariate of aspect was derived from the 300-m resampled elevation dataset utilizing tools available in the Spatial Analyst toolbox within ArcMap 10 (ESRI 2010), in preparation for further analysis in this research.

4.2.2 Wind storm Paula and damage data

Winds from Paula were particularly damaging in certain areas of Austria and warranted closer examination utilizing local and more specific models as well as

regional damage estimates. Wind storm-induced tree/infrastructure damage data were obtained from the Federal Ministry of Agriculture, Forestry, Environment, and Water Management (FMAFEWM) in Austria (http://www.lebensministerium.at/). These data include maps and imagery showing major forest damage in the Austrian states of Kärnten (i.e., Carinthia) and Steiermark (i.e., Styria) as well as point and polygon shapefiles that contain detailed information about impacted areas in hectares (ha) and in forestry management units (fm). Additional wind speed surfaces were obtained from the Zentralanstalt fur Meteorologie und Geodynamik (ZAMG) (http://www.zamg.ac.at/cms/de/aktuell), which utilized a different spatial weighting method for producing wind storm wind surface estimates.

4.2.3 Wind surface estimates in Austria

Local kriging and cokriging surfaces (i.e., country-level) were created utilizing wind observation data within Austria. Wind observation data were examined using exploratory spatial data analysis methods including histograms, normality (normal QQ plot, e.g., Wilk and Gnanadesikan 1968), trend analysis, stationarity and spatial variability (Vornoi map, e.g., Ogniewicz and Ilg 1992), and spatial dependencies (semivariogram/covariance cloud, e.g., Gribov et al. 2000). Collectively, histograms, normal QQ plots, and trend analysis were used to determine whether data transformation was necessary. Voronoi maps created Thiessen polygons that visually examined spatial variability and stationarity of each station. The polygons identified the wind observation station that was nearest to each location in Austria; this map aided in identifying potentially large data gaps in Austria based on the size of the polygons. Polygon size increases when a station is the nearest station to a large geographical area and decreases when a station is nearest to the collection of points in a smaller

area. Semivariogram clouds were used to examine local characteristics of spatial autocorrelation within a dataset and find local outliers.

During the modeling process, the ordinary kriging/cokriging and prediction output types were selected and no transformations were necessary. Semivariogram modeling was optimized through Geostatistical Analysis in ArcGIS 10.1 and nugget size was enabled with a 100% measurement error. A spherical model type was selected with range and sill calculated based on the lag size with 12 lags. Because winds are not necessarily distributed equally, especially in rugged terrain, anisotropic analysis was selected to account for a directional correlation in wind speeds. To ensure an objective comparison between Studies One, Two, and Three, kriging/cokriging settings were optimized in Study One, then duplicated in the subsequent studies. During the surface creation process, a standard “search neighborhood” type was selected and the “maximum neighbors” was set to 5 and the “minimum neighbors” was set to 2. Neighborhood search numbers establish how many stations to include in a search radius that is centered on each station in a repeated procedure of the surface smoothing process. The inclusion of more neighbors creates a smoother surface, while the opposite is true of the reduction of neighbors. Eight sectors were selected during the neighborhood search process, meaning that there were between 2 and 5 neighbors (stations) included for every 45° section extending outward from each point in an ellipsoid shape based on anisotropic semivariogram angles.

This combination of settings results in a range of between 16 and 40 stations being used for post-model surface smoothing. Prediction errors and individual station errors were produced using a method of *n-1* cross validation, where each station was

removed from the model in an iterative process to examine the differences between measured and predicted values. The variables that were selected for inclusion in the cokriging models varied greatly, with the model for Jeanette incorporating land cover for maximum sustained winds and elevation and aspect for peak gust winds, that for Kyrill including aspect for both wind types, Paula's model incorporating land cover for both wind types, and that for Emma using land cover for maximum sustained winds and land cover and elevation for peak gust winds. Wind surface accuracy was examined through use of the root mean square prediction error (RMSPE), mean error (ME), root mean square error (RMSE), and station standard error (SE) statistics. Lower RMSPE measurements, ME close to zero, RMSE close to one, and station SE less than +/- 2.0 were preferred. Automatic anisotropy was also utilized to test predicted surface trends versus actual surface trends.

4.3 Results

4.3.1 Localized wind surface estimates in Austria for each storm

4.3.1.1 Wind storm Jeanette

Based on results from Study Two, the original kriging algorithm was used to produce a local maximum sustained (4-2A) and peak gust (4-2B) wind surface estimate for Austria, while the cokriging method with land cover as a covariate (maximum sustained) and elevation and aspect as a covariate (peak gust) was utilized to produce the same surface estimates (4-2C and 4-2D) for comparison. The wind surface estimates for Jeanette were very blocky and unlike other local kriging/cokriging models, indicating poor model fit at the local scale. In each of the four models, the strongest winds occurred in the eastern and western states around Wien (i.e.: Vienna) and Innsbruck. Much of the south-central region of Austria consisting of Kärnten and

Steiermark experienced lighter winds. Table 4-1 shows the accuracy metrics for each map. The kriging and cokriging methods produced similar results, with the cokriging peak gust model being a slight outlier. The cokriging peak gust model resulted in fewer high-error stations, but a less optimal RMSE score.

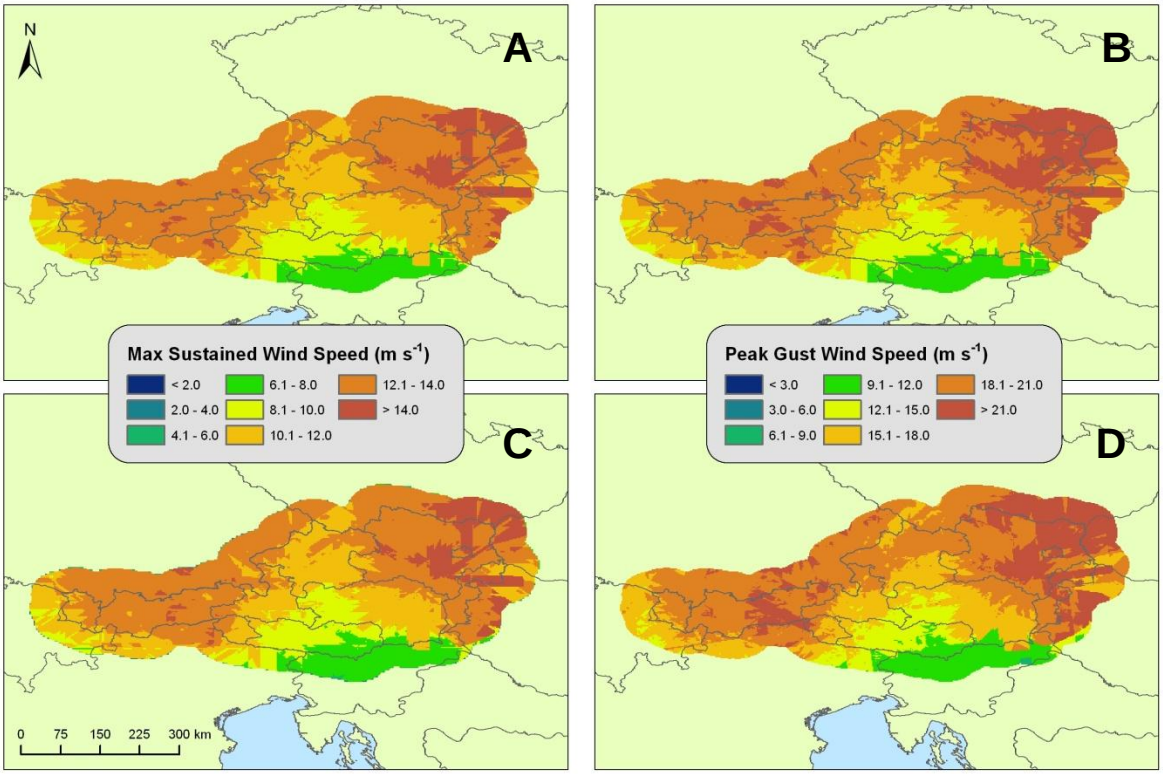

Figure 4-2. Original kriging models for maximum sustained (A) and peak gust (B) wind speeds and cokriging models for maximum sustained (C) and peak gust (D) wind speeds for Jeanette (2002).

Table 4-1. Jeanette (2002) accuracy metrics for local kriging/cokriging models in Austria indicating dominant automatic wind speed direction, inter-model error comparison (RMSPE), intra-model error comparison (ME and RMSE), and number of high error stations.

Wind Type	Method	Anisotropy	RMSPE	ME	RMSE	SE (> +/- 2.0)
Max Sustained	Original Kriging	90.0	7.97	-0.03	0.99	4
	Cokriging w/LC	90.0	7.98	-0.02	0.99	4
Peak Gust	Original Kriging	90.0	12.91	-0.02	0.98	4
	Cokriging w/elev & asp	81.2	12.92	-0.01	0.83	2

4.3.1.2 Wind storm Kyrill

Based on results from Study Two, the original kriging algorithm was used to produce a local maximum sustained (4-3A) and peak gust (4-3B) wind surface estimate for Austria, while the cokriging method with aspect as the covariate was utilized to produce the same surface estimates (4-3C and 4-3D) for comparison. All four surface estimates identified a large area of strong wind in northern and western Austria in an area that coincides with the northern slopes of the Alps. In each of the four models, a small pocket of intense wind also occurred in southern Kärnten, west of the town of Villach. The exact location of the high wind zone centers on the peak of the Dobratsch

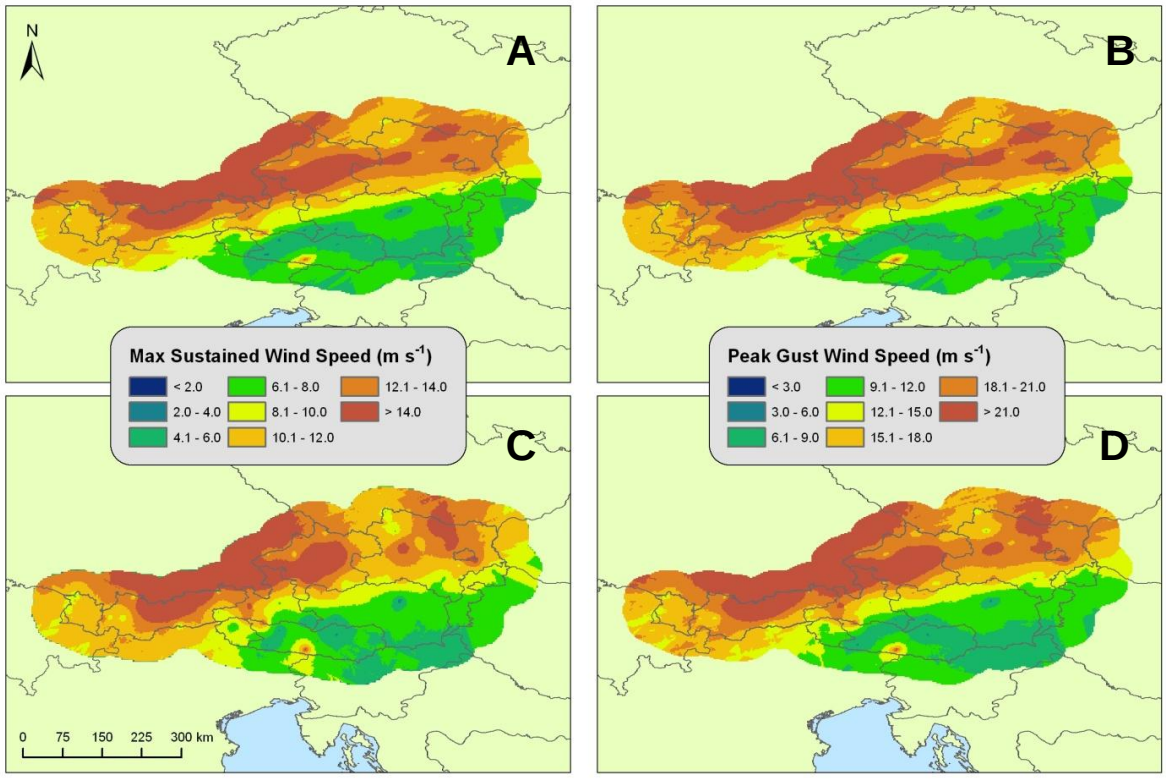

Figure 4-3. Original kriging models for maximum sustained (A) and peak gust (B) wind speeds and cokriging models for maximum sustained (C) and peak gust (D) wind speeds for Kyrill (2007).

Mountain, which at ~2,170 meters is one of the highest mountains in the region. There were other pockets of high and low wind scattered throughout northeastern Austria, with predominantly lighter winds in southern and southeastern Austria. Table 4-2 shows the accuracy metrics for each map. The kriging and cokriging methods produced similar results for both the maximum sustained and peak gust wind speed models, with the cokriging model increasing the number of high-error stations for maximum sustained wind compared to its kriging counterpart.

Table 4-2. Kyrill (2007) accuracy metrics for local kriging/cokriging models in Austria indicating dominant automatic wind speed direction, inter-model error comparison (RMSPE), intra-model error comparison (ME and RMSE), and number of high error stations.

Wind Type	Method	Anisotropy	RMSPE	ME	RMSE	SE (> +/- 2.0)
Max Sustained	Original Kriging	72.4	6.62	0.02	0.97	5
	Cokriging w/asp	72.0	6.81	0.01	1.04	7
Peak Gust	Original Kriging	71.9	10.54	0.02	0.97	5
	Cokriging w/asp	75.0	10.54	0.01	0.99	5

4.3.1.3 Wind storm Paula

Again, based on results from Study Two, the original kriging algorithm was used to produce a local maximum sustained (4-4A) and peak gust (4-4B) wind surface estimate for Austria, while the cokriging method with land cover as a covariate was utilized to produce the same surface estimates (4-4C and 4-4D) for comparison. All four surface estimates identified a large area of intense wind in northeastern Austria in an area that is less mountainous than central and western Austria. In three of the four models, small pockets of strong wind also occurred along the Kärnten, Salzburg, and Tirol borders as well as the Steiermark and Oberösterreich borders. There were even smaller pockets of intense wind scattered throughout other parts of the country. Table

4-3 shows the accuracy metrics for each map. The cokriging method produced the optimal maximum sustained wind speed model, while the original kriging method produced the optimal peak gust wind speed model based on the various metrics. The cokriging model for peak gust wind speed (Figure 4-4D) also appears highly fragmented, indicating a poor fit.

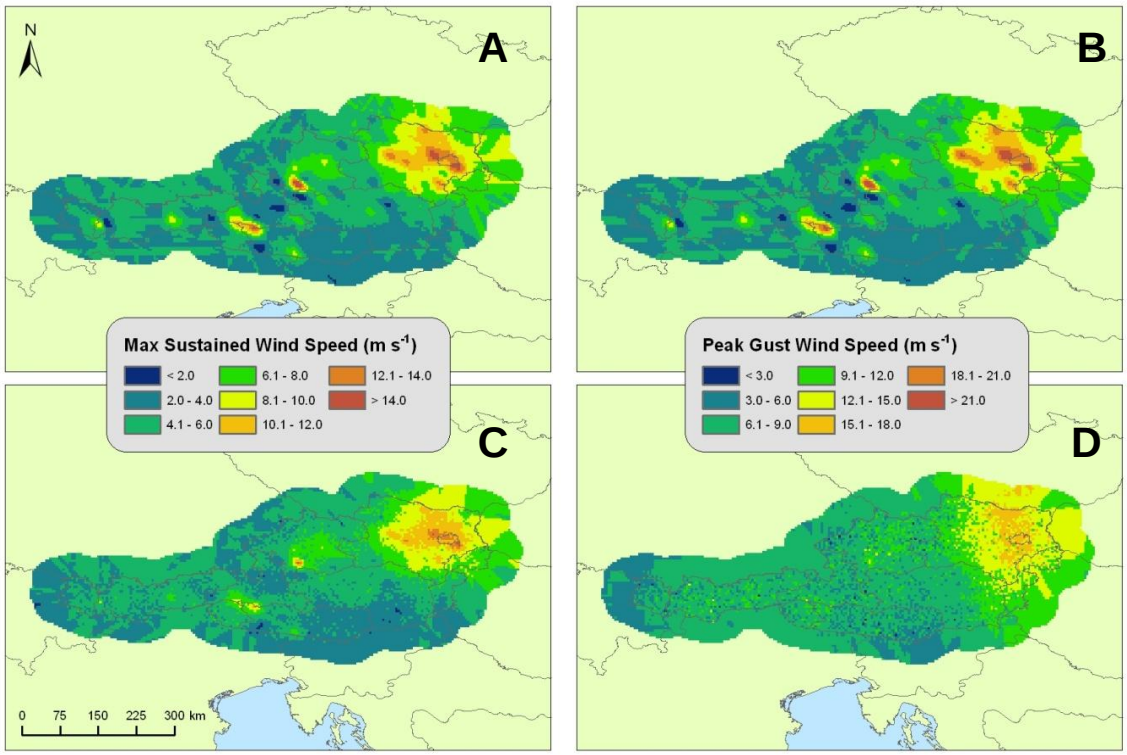

Figure 4-4. Original kriging models for maximum sustained (A) and peak gust (B) wind speeds and cokriging models for maximum sustained (C) and peak gust (D) wind speeds for Paula (2008).

Table 4-3. Paula (2008) accuracy metrics for local kriging/cokriging models in Austria indicating dominant automatic wind speed direction, inter-model error comparison (RMSPE), intra-model error comparison (ME and RMSE), and number of high error stations.

Wind Type	Method	Anisotropy	RMSPE	ME	RMSE	SE (> +/- 2.0)
Max Sustained	Original Kriging	123.2	3.68	-0.02	0.87	2
	Cokriging w/LC	123.0	3.62	-0.02	0.87	2
Peak Gust	Original Kriging	122.0	5.92	-0.01	0.88	2
	Cokriging w/LC	178.1	6.00	0.00	0.99	2

4.3.1.4 Wind storm Emma

Again, based on results from Study Two, the original kriging algorithm was used to produce a local maximum sustained (4-5A) and peak gust (4-5B) wind surface estimate for Austria, while the cokriging method was utilized to produce the same surface estimates (4-5C and 4-5D) for comparison. All four surface estimates identified two large areas of strong wind: one in northeastern Austria north of Wien and one in western Austria around Innsbruck. Areas of weaker wind speed were predominantly in the south-central states of Austria including Kärnten and Steiermark. The cokriging models for each wind speed type showed a slightly more fragmented wind surface, but high and low winds occurred in similar areas. Table 4-4 shows the accuracy metrics for

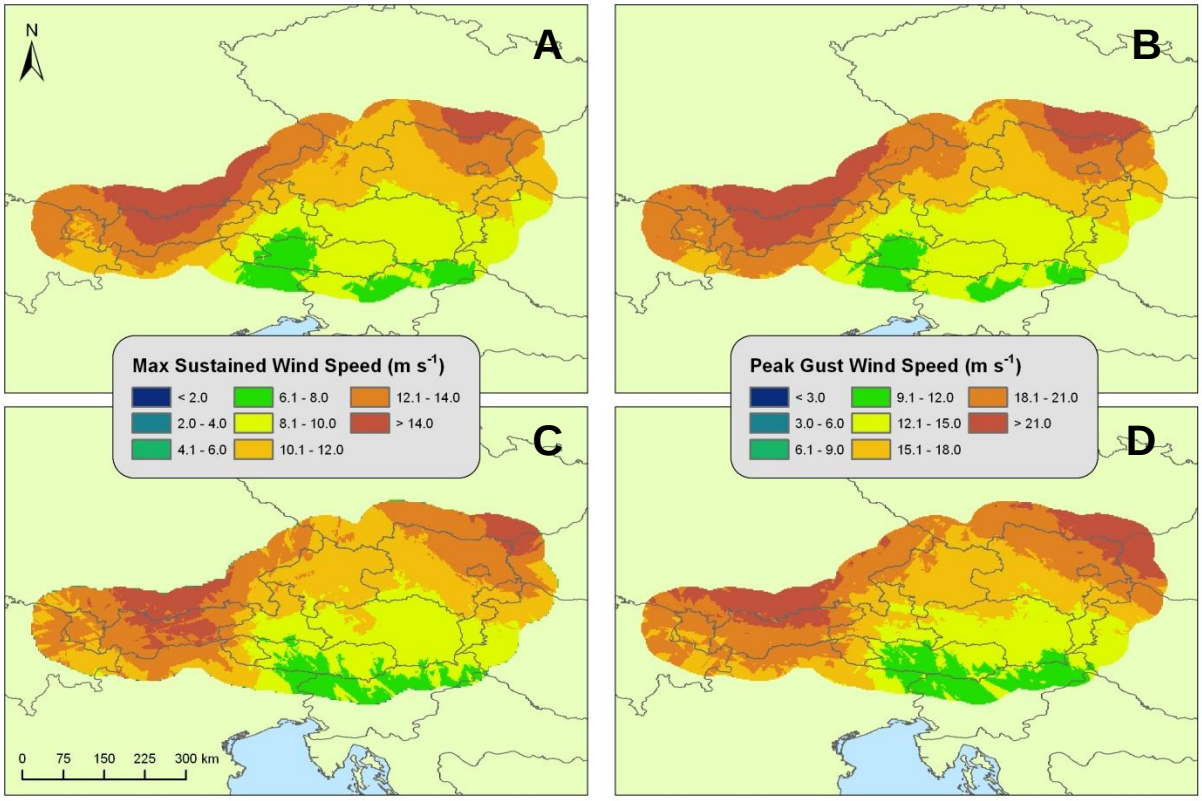

Figure 4-5. Original kriging models for maximum sustained (A) and peak gust (B) wind speeds and cokriging models for maximum sustained (C) and peak gust (D) wind speeds for Emma (2008).

each map. The cokriging method produced the optimal maximum sustained wind speed model, while the optimal peak gust wind speed model was difficult to identify based on conflicting accuracy metrics.

Table 4-4. Emma (2008) accuracy metrics for local kriging/cokriging models in Austria indicating dominant automatic wind speed direction, inter-model error comparison (RMSPE), intra-model error comparison (ME and RMSE), and number of high error stations.

Wind Type	Method	Anisotropy	RMSPE	ME	RMSE	SE (> +/- 2.0)
Max Sustained	Original Kriging	114.6	6.61	0.01	1.08	7
	Cokriging w/LC	72.2	6.59	0.01	1.04	6
Peak Gust	Original Kriging	112.3	10.73	0.01	1.07	6
	Cokriging w/elev & LC	40.2	10.66	-0.01	1.03	7

4.3.2 Wind storm Paula validation in Kärnten and Steiermark, Austria

Forestry damage data in Kärnten and Steiermark were overlaid on two separate wind speed maps: one produced by ZAMG and one produced by the local kriging peak gust model from Figure 4-4B (Figure 4-6). Forestry damage seemed to follow an invisible line from west to east across northern Kärnten and then a southwest-northeast line in Steiermark. Stronger wind speeds were noticeable in the ZAMG wind surface map for most areas of Steiermark where forestry damage occurred, but intense wind speeds from the kriging surface were not present in all areas where forestry damage occurred. Specifically, the southernmost area of the largest block of forestry damage in Steiermark does not align with intense surface wind estimates in the local kriging surface. In Kärnten, forestry damage did not always occur in areas of the highest wind speed as estimated by either wind estimate surface, but instead may have been more dictated by other variables individually. Since damage estimates were provided at point

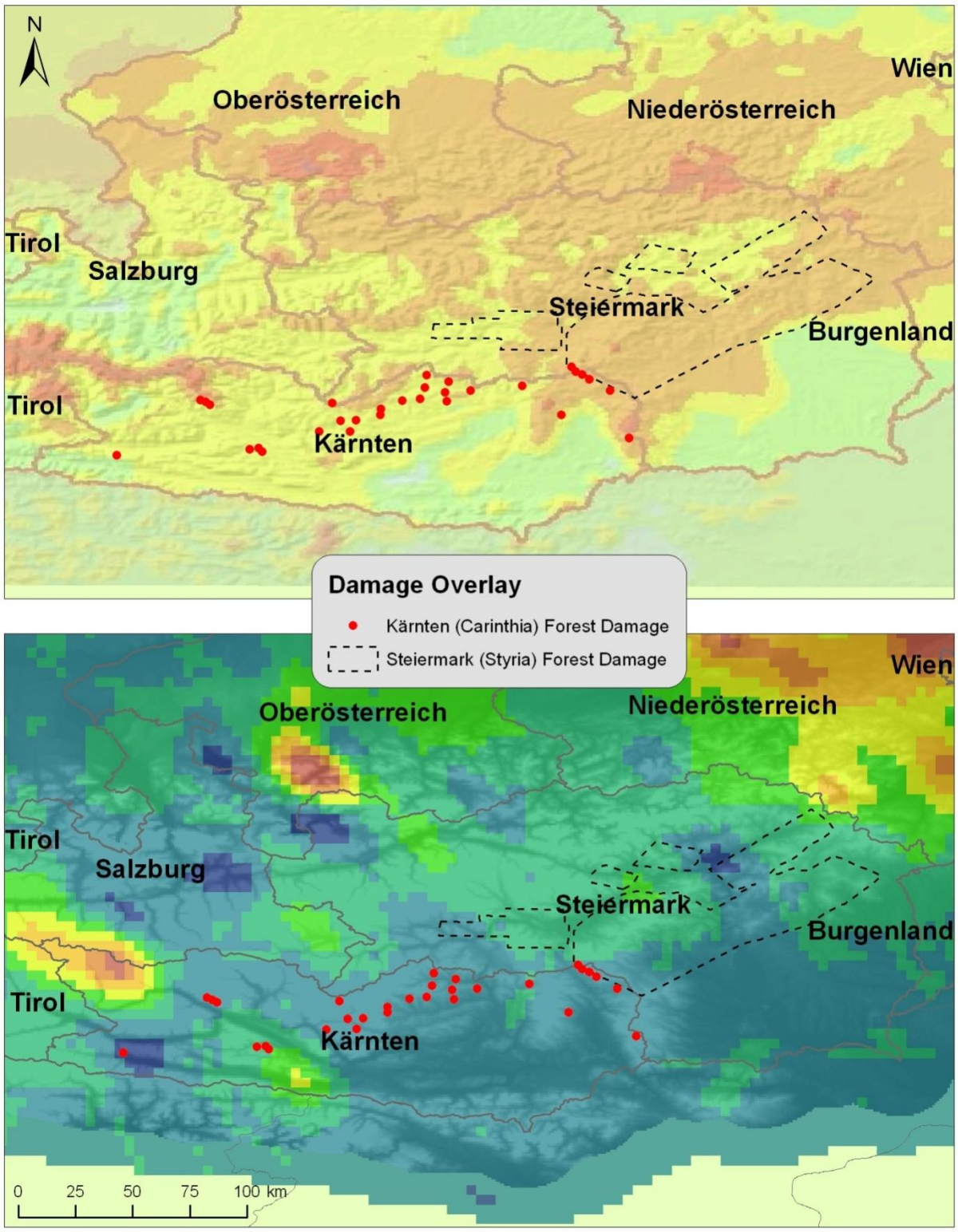

Figure 4-6. Wind surface estimates from ZAMG (A) and local kriging (B) overlaid with forestry damage locations.

(longitude, latitude) locations for Kärnten, values for elevation, land cover, and aspect were extracted for each location and visualized in Figures 4-7, 4-8, and 4-9. For most damage locations, elevation ranged between 750 and 1,750 meters (Figure 4-7). Dense needle-leaved evergreen land cover dominated areas where forestry damage was high (over 60% of damage), indicating that areas with this vegetation type may have been more susceptible to wind damage than other vegetation types (Figure 4-8). Caution should be given for this conclusion because soil saturation may have destabilized certain vegetation types depending on location and slope. Wind storm Paula tracked from west to east and most wind speed directions indicated a northwest-southeast wind during the most intense segment of the storm, but the majority of forestry damage occurred on slopes that were either north/northeast-facing or south/southwest-facing (Figure 4-9). Figure 4-9 also clearly illustrates the increase in

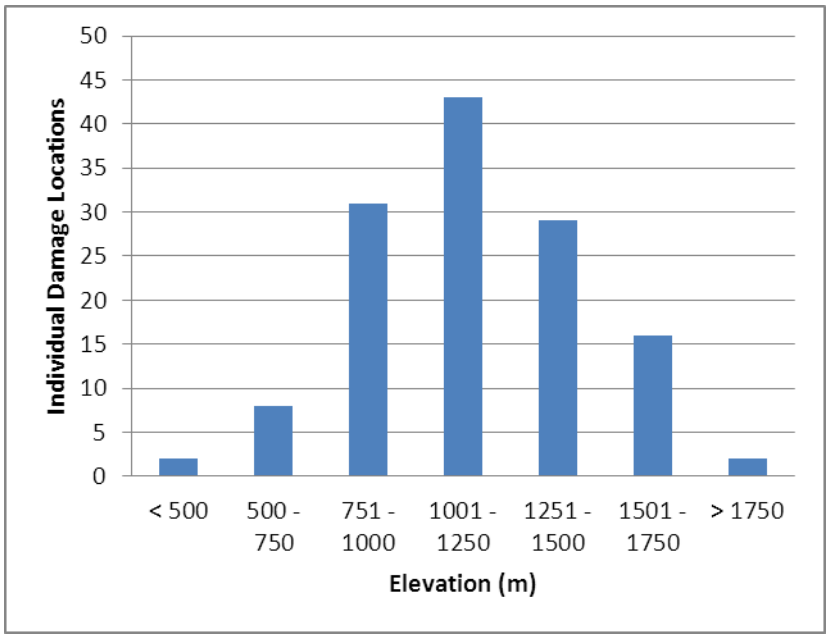

Figure 4-7. Distribution of elevation at each location in Austria where forestry damage was reported.

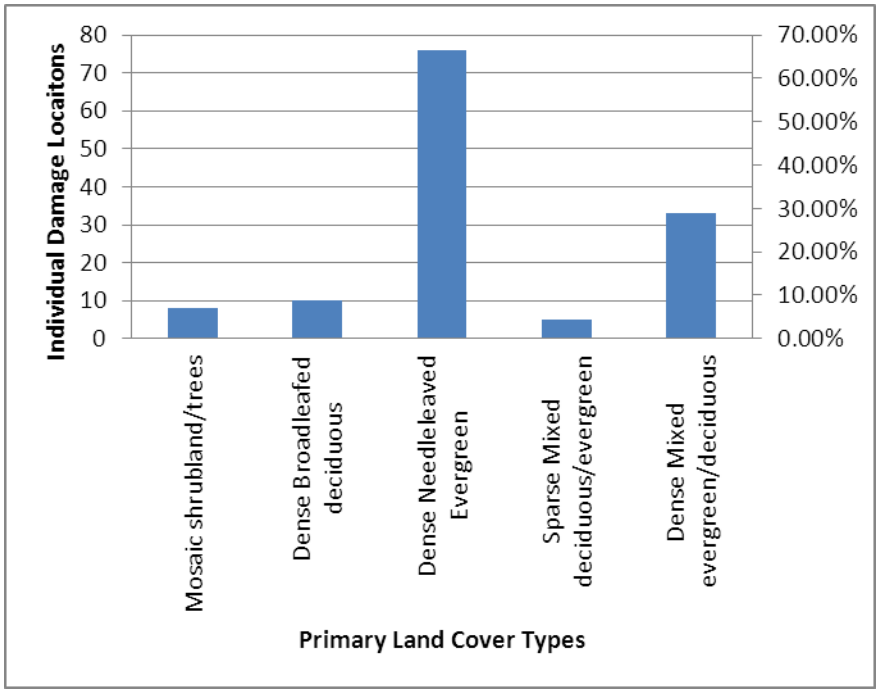

Figure 4-8. Distribution of primary land cover types at each location in Austria where forestry damage was reported.

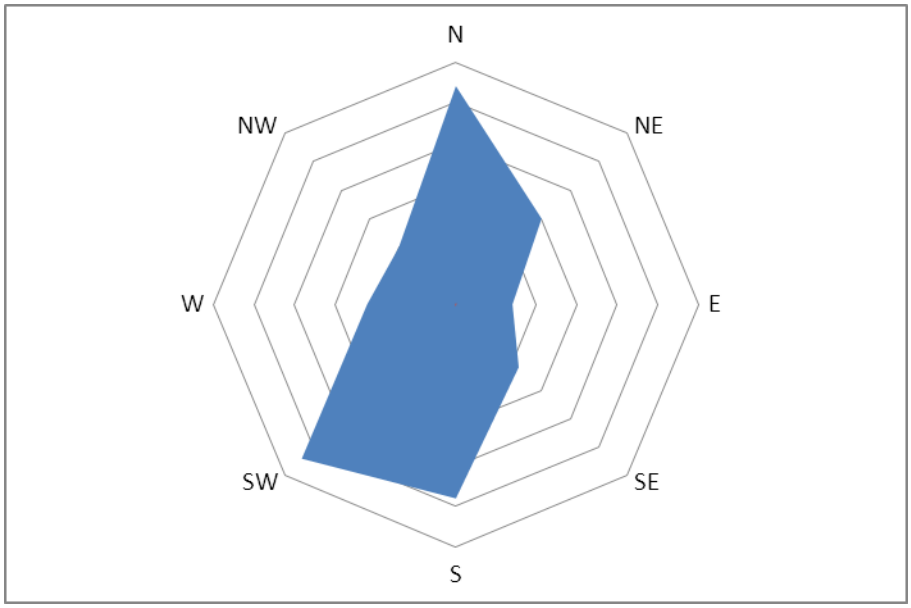

Figure 4-9. Aspect of topography at each location in Austria where forestry damage was reported.

wind speed upslope AND downslope during a wind storm. For this reason, aspect may have added a conflicting element to cokriging models for wind storm Paula since winds often change directions, deflect off mountains, and funnel through valleys, resulting in less favorable accuracy metrics than the best models (original kriging and cokriging with land cover).

Additionally, aerial images were examined for the two stations with high error measurements for all four Paula models (Figures 4-10 and 4-11). Both stations are located on the edge of the north-northeast slope of high mountain ridges in generally open areas – one at a ski resort and another adjacent to a mountain glacier. Aerial photos showing forestry damage inflicted by wind storm Paula are shown in Figure 4-12.

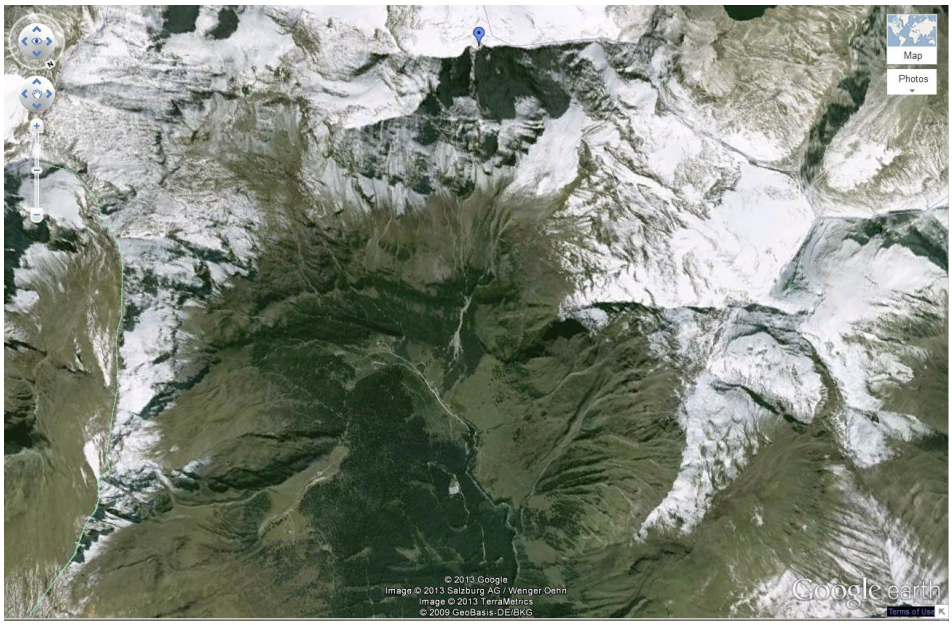

Figure 4-10. Wind observation station (blue marker) located near the border between Salzburg and Kärnten at a height of ~3100 m.

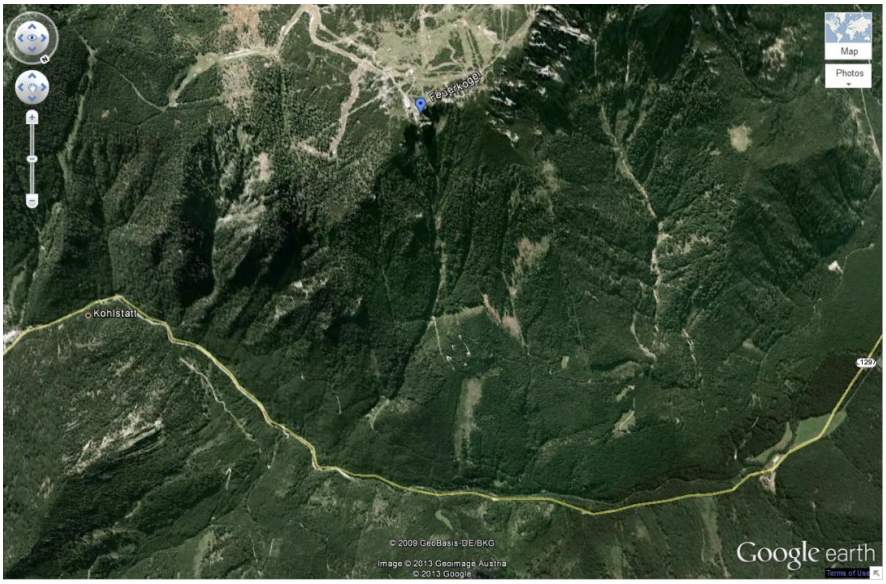

Figure 4-11. Wind observation station (blue marker) located in Oberösterreich near the border with Steirmark at a height of ~1600 m.

Figure 4-12. Aerial images where forestry damage occurred during wind storm Paula.

4.4 Discussion

Through use of local kriging/cokriging, a more detailed wind surface was created for Austria when compared to previous modeling efforts at the continental scale. Specific localized areas (e.g., mountains, ridges) were likely to have experienced stronger wind speeds that were more recognizable when modeled and smoothed at the country-level scale. Wind storms Kyrill and Paula provided excellent examples of

increased surface variability with identifiable high wind spots in locations that previously showed a smooth surface at the continental scale. Additionally, accuracy metrics improved for country-level models, resulting in reduced RMSPE measurements and fewer stations with high SE. Anisotropy was not consistently improved, most likely because the study area was too small to identify the macroscale wind patterns and trends (Luo et al. 2008). Luo et al. (2008) concluded that use of an anisotropic semivariogram had negligible influence on kriging-created wind speed surfaces in the United Kingdom (UK) since the sill of correlation was often not reached within a reasonable range, considering the smaller size of the UK compared to continental Europe. Overall, continental-scale models from Studies One and Two predicted wind speed and trend accurately in most locations since winds were predominantly lower over much of Austria than areas farther north closer to the storm track.

While accuracy metrics for most local-scale models showed an improvement when compared to previous continental-scale models, surfaces for Paula resulted in the same number of high error stations (two). Upon closer examination, the two high-error stations from Study Two were in southern Oberösterreich and the border between Kärnten and Salzburg – areas that now show higher wind speeds more in line with actual observed wind speeds. The high-error stations from local kriging/cokriging were in the same location, indicating either a localized area of intense winds or station error. The station locations were examined through aerial imagery and both were located on ridges above a deep valley. The surface improved because it showed greater wind speeds at these two locations when compared to the surrounding area and more closely matched wind speed surfaces produced by the ZAMG, but the wind surface was still

less than the measured wind at the exact station location, resulting in high SE. The two high-error stations faced in a north-northeast direction and the dominant wind direction during Paula was from the north-northwest. The elevation (highest and 12th highest among all stations in Austria) and aspect at these two locations indicate that high wind speed variability was likely and that anomalously intense wind speeds could have occurred (Wieringa 1973, 1986).

Kriging/cokriging-derived wind surfaces are often modeled at the state- (Akkala et al. 2010) or country- (Luo et al. 2008) scale, but rarely at the continent-scale, primarily because of an increase in station error. However, model results suggest that both scales can be useful for differing reasons. The small-scale (continent) model produced accurate surfaces that predicted wind speeds very well in most locations and showed macroscale wind speed trends and patterns. The large-scale (country) model also produced accurate surfaces that illuminated small areas of greater wind speed that were muted and smoothed on the surface created by the small-scale model, thus identifying microscale variations. General wind speed trends and patterns were more difficult to visualize on the surfaces produced by the large-scale model because the geographic extent of Austria was simply not large enough to detect such patterns. This alludes to results of Luo et al. (2008) concerning use of anisotropic semivariograms at the national scale.

Based on the influence of scale during geostatistical analysis, it is important to address the theoretical issues involved with the "scale problem." Meentemeyer (1989) proposed that there is a hierarchical component to space that should be integrated into hierarchy theory. This hierarchical component can be visualized when examining the

differences between each modeled scale. The two main scale issues that arise during kriging/cokriging center on smoothing and semivariogram creation. Meentemeyer (1989) referenced Clark (1985) by stating that there are no simple rules or parameters available to identify the appropriate scale for different applications, and that continues to be true within geostatistical analysis. Meentemeyer (1989) also warned that if geographic coverage is not available at finer scales, then the examination and inference of patterns should remain at a macro-scale level where there is more statistical certainty in the outcome. Within geostatistical analysis, a minimum number of stations (normally 30) should be used during any modeling process. Both the small- and large-scale models in this study meet this criterion, resulting in a high level of certainty at both scales.

4.5 Future Research

A major area of future research involves the exploration of empirical Bayesian kriging (EBK) (Gribov and Krivoruchko 2011, Castruccio et al. 2012, Zhang 2012) as a possible solution to capturing local-scale changes when modeling at the continental scale. Scale is not only determined when identifying geographic extent, but also when the semivariogram is modeled during the kriging/cokriging process. For kriging and cokriging, only one semivariogram model is produced for the entire surface, but EBK produces multiple smaller semivariograms that fit different parts of the surface – a form of self-partitioning as opposed to forced partitioning (e.g., Zlatev et al. 2010). Theoretically, the smaller semivariograms are combined to produce a single surface, thus eliminating the impact of zonal scale problems inherent to the MAUP and potentially reducing the impact of other scale problems that occur between variably-scaled wind surfaces. An ideal EBK surface would model wind speed surfaces for wind

storms at the continental scale, while also capturing local-scale variation that previously was only captured by country-specific models. Models generated in the exploratory phase of this dissertation using EBK have shown some improvement in the direction of creating an idealized modeled surface, but much more research is needed and an improvement to the EBK tool within ArcGIS may also be necessary. Currently, the EBK model has many predetermined, inalterable settings and is less amenable to user adjustments. Additionally, other variables (e.g., elevation, aspect, land cover) cannot be used to improve the EBK surface because cokriging-based EBK does not yet exist.

Beyond testing other modeling techniques, more effective means of validation are necessary to determine whether predicted surface wind speeds match some equivalent impact on the ground. The available forestry data were limited to two states in Austria that did not experience the highest wind speeds during Paula. Damage data were not available for the two mountains/ridges that experienced the greatest wind speeds. Windward and leeward mountain slopes are influenced by higher wind speeds based on the laws of fluid dynamics. Horizontal winds decelerate as they approach a mountain slop and accelerate downslope of the mountain, both as a result of the increased friction over the mountain – this is especially true of ridges where wind is less likely to deflect around the mountain. The winds going downslope create turbulence on the leeward side of a mountain, often resulting in multiple eddies that can impact wind speeds and wind speed-induced damages. Additional damage data will be needed to proceed with this type of wind speed surface validation. Once an effective means of validation is vetted more thoroughly, then dissemination of results to the appropriate local and

national agencies and organizations will become a priority as well as the expansion of ground-truthing techniques to other countries and regions.

CHAPTER 5. CONCLUSIONS AND FUTURE RESEARCH

This dissertation was written in three distinct, journal-style chapters and each chapter addressed specific objectives. The objectives were as follows:

Chapter 2 (Study One)

1) to quantify the accuracy of numerous types of spatial interpolation methods for predicting extreme European wind storm-induced winds through verification and validation
2) to identify regional patterns and areas of high and low wind speeds associated with eighteen different wind storms

Chapter 3 (Study Two)

1) to reduce error measurements associated with the original ordinary kriging surfaces produced in Study One through a process of cokriging with multiple covariates
2) to identify one or more covariates that produced the most meaningful reduction in individual station error

Chapter 4 (Study Three)

1) to examine how wind speed interpolations vary at differing spatial scales and how local interpolations changed compared to regional interpolated surfaces in the mountainous country of Austria
2) to analyze tree damage in the Austrian state of Carinthia and determine its utility in validating interpolated wind surfaces

5.1 Study One Conclusions

Numerous methods of interpolation have been used for wind surface estimation, but this study confirms that kriging remains one of the better methods because of its ability to account for anisotropy and surface trends. Analysis of 18 major European wind storms over the past 35 years is included in this study. Interpolated surfaces for each storm were created within the same framework so they can be viewed simultaneously for improved visualization of the overall intensity and locations of high winds for each storm. Peak gust and maximum sustained wind speed calculations and adjustments allowed for improved wind surface estimates and accuracy at reporting locations, thus improving final interpolations. The major findings of Study One are as follows:

1) Wind surface maps and an overall climatology for 18 major European wind storms occurring since 1976 have been created and catalogued in one study for the first time.
2) Accurate wind surface estimates can be created for large areas of Europe using an anisotropic semivariogram-derived kriging methodology.
3) Not surprisingly, coastal areas, especially those surrounding the English Channel and North Sea, often experienced the highest wind speeds during a wind storm.
4) Inland areas of Europe, specifically the Black Forest and northern Alps, experienced very high wind speeds relative to the surrounding areas – indicative of a complex topography/wind interaction.
5) Coastal and mountainous weather stations experienced the greatest difference in wind speeds across small distances within the same wind

storm, and therefore reported some of the highest error measurements. Additional research must be undertaken to improve our understanding of local wind variability in these environments.

6) Local wind variability may contribute to weak macroclimatic trends, perhaps at least in part because of changes in storm trajectory and its associated circulation near the station, causing principal trending directionality used in kriging to be poorly estimated.

5.2 Study Two Conclusions

Cokriging was utilized to create maximum sustained and peak gust wind speed surface estimates for five European wind storms over a 10-year period. Results confirmed that cokriging is superior to kriging for most models and that elevation is a useful covariate. The study expanded on the use of covariates by adding aspect and land cover, which also showed improvement in most models from previous kriging models. Maps showing stations with high standard error (SE) were also produced and indicated that some stations were repeatedly found to have high SE measurements. The major findings of Study Two include the following:

1) Aspect and land cover can be effective when used as covariates during the cokriging process.
2) In most model sets, use of land cover as a covariate produced the best surface estimates with the fewest stations receiving high SE measurements.
3) As was found in Study One, stations with high SE measurements occur in coastal and mountainous regions; however, the number of such stations was reduced by using cokriging rather than kriging for the anisotropic semivariogram-derived methodology in most model sets.

4) General wind speed and wind direction patterns were modeled correctly at a hemispheric scale, but more localized patterns were not identified.
5) Use of multiple covariates resulted in differences in semivariogram direction within a storm when identifying the dominant azimuth direction of wind associated with each storm.

5.3 Study Three Conclusions

Local kriging and cokriging procedures were examined to determine whether wind speed surface estimates for wind storms Jeanette, Kyrill, Paula, and Emma vary when modeled at different scales. Based on various accuracy metrics, wind speed surfaces were often improved but surface trends and patterns were less discernible than in continent-scale models from Studies One and Two. In addition to inner-model cross-validation, forestry damage data were utilized to assess a potential relationship between high winds and high damage. While no strong correlations between the two were found, complex relationships between forestry damage and heterogeneous landscape characteristics were identified. The major findings of this study include the following:

1) Modeled local kriging and cokriging wind speed surfaces show greater spatial variability than continental-scale surfaces, resulting in the identification of specific high-wind areas that were smoothed in previous models.
2) Major patterns and trends are more difficult to ascertain for local-scale surfaces when compared to continental-scale surfaces.
3) High station SE can be reduced but not eliminated through local kriging/cokriging, and some instances of surface improvement may continue to under- or over-predict observed wind speeds.

4) Relationships between forestry damage and specific covariate (elevation, aspect, land cover) parameters were identified, but validation of intense winds was difficult to test using forestry damage since damage data are only available for Austrian states that experienced lower wind speeds than other states.

5.4 General Conclusions and Future Research

Collectively, each study provided a major improvement in our basic and applied scientific understanding of multiple European wind storms and wind meteorology in rugged terrain, although it is important to remember that all models oversimplify the reality of rugged terrain. Regardless, improvement of surface wind estimates through a combination of spatial analytic techniques substantially improved meso- and local-scale modeling attempts. Previous wind storm surface estimates were characterized by coarse spatial resolution with little specific local precision. This dissertation also advanced our knowledge of the relative advantages of spatial analytic techniques (i.e., kriging) that are sometimes selected without *a priori* knowledge of appropriateness. In each of the three studies, user-selected criteria played a key role in wind surface estimations. Additionally, cokriging techniques and covariates were previously not applied to surface wind interpolations of wind storms, thus this dissertation was innovative in its testing of a potential relationship between observed wind speeds and elevation, aspect, and land cover.

Models and extreme-event climatologies of wind simulation and hazard/risk assessment that are widely used in the insurance/reinsurance industry can be improved through the incorporation of our research results. Results may also help to inform local cost-benefit studies and subsequently save lives and resources for local government,

private industry, and consumers. Damage estimates may also be refined based on the resulting wind surface estimates, thus improving construction standards and adapting insurance needs. The known impacts of windstorms on vegetation (e.g., trees; Kirk and Franklin 1992) and civil infrastructure (Reed 2008) are severe, and improved spatial interpolations for windstorm-induced wind speeds will be fundamental to evaluating damages as well as potential changes needed for forest management and building codes/regulations. The identification of high wind zones will also help to inform local government vulnerability assessments that may be included in future hazard mitigation plans. The results will also inform understanding of common windstorm features (e.g., directions, wind movements/patterns, surface interactions, etc.) that have long-term, but not necessarily immediate, impacts on sectors such as transportation, agriculture, and recreation.

Multiple avenues for future research exist, including future scale-dependent research in flat or hilly areas of relatively consistent winds (as opposed to highly-variable, storm-generated wind speeds in mountainous areas) and coastal, heterogeneous areas. Subsequent research would be a clear extension of Study Three. Also, additional research should be conducted on the angle of wind that causes the most damage. Anecdotally, it appears that a ~45° angle causes the most damage based on the results from Study Three, but this cannot yet be proven.

A major area of future research involves the potential transferability of methods and models to a different region. It would be ideal to implement the optimal method(s) identified in this dissertation to predict extreme wind speeds associated with mid-latitude cyclones in northwestern North America, or the Pacific Northwest (PNW), using a

different set of extreme wind data. The specific type of mid-latitude cyclones to be studied in this region is called a “winter storm” and is very similar to its European counterpart. Within such a study, there would be two main objectives: 1) to test the transferability of kriging/cokriging methods to the PNW to determine whether the same algorithm for estimating winds in Europe can be applied; and 2) to analyze the spatial patterns of high winds associated with PNW storms.

When considering all 18 studied European wind storms collectively, cluster analysis may aid in identifying commonalities in storm tracks, high error station locations, and other wind storm-induced wind speed characteristics. Based on the initial results of Study Two, additional change detection maps should be created to identify specific areas where wind speed predictions vary the most between the original kriging models and the optimal cokriging models. These areas must be studied more closely to identify reasons for the disparity in wind speed predictions. Additionally, analyzing a potential relationship between station error and covariates may reveal a trend in high error stations and certain landscape characteristics (e.g., are high elevation stations consistently reporting high error measurements? What are the characteristics of consistently “anomalous” stations?). Based on preliminary analysis from Study Three, correlation and regression analysis may be helpful in pinpointing significant relationships between tree damage and elevation, aspect, and/or land cover as well as other variables (e.g., soil type, moisture, etc.), but more tree damage data would be helpful to reach a broader conclusion.

Another major area of future research is the creation of a ruggedness variable that synthesizes the major covariates and reduces autocorrelation among the potential

predictor covariates. Just as principal components analysis (PCA) is used to combine strongly correlated variables into various components, a data reduction technique could be applied to create a “ruggedness” variable. Issues of autocorrelation could potentially be eliminated, or at least minimized, through the development of one variable that incorporates both elevation and land cover to represent terrain ruggedness (R_t). This future project would be the first known study to incorporate such a variable in a cokriging model for wind data.

Improved modeling of the effect of ruggedness in the surface boundary layer (SBL) will rely on the concept of roughness length (z_0) – the theoretical height at which the wind speed approaches zero, ranging from 1 mm for very smooth surfaces to a few meters for forests and urban areas (Arya 2001). According to boundary layer theory, z_0 is related to, the height of the roughness elements and is also a function of the shape and density distribution of the elements, with z_0 maximized for an intermediate density of roughness elements. A rule of thumb that is often employed is that z_0 is about ten percent of the canopy height, but this can vary widely. Davenport (1960) initially developed approximate z_0 values for eight different terrain classes (Table 5-1). An anisotropic cokriging model will likely improve prediction of the contrasting effects on wind speeds caused by rough-to-smooth vs. smooth-to-rough terrain transition areas where z_0 values may change abruptly. A drag coefficient utilizing zero plane displacement (d) – the vertical displacement caused by surface elements – may also be needed in Classes 4 or higher which encompass more complex terrain (Table 5-1). In general, d is approximately two-thirds the height of the tree canopy. For example, z_0 may be 1 m and d may be 7 m for a forest. Because z_0 and d will be utilized across

diverse terrain types in two different regions, these values will be revised to represent the study area appropriately.

Wieringa (1986) developed a mesoscale roughness parameter (z_{0m}) and a two-layer boundary layer model to assess mean regional surface wind speeds in the lower (at 10 m height) and upper SBL (60 m height). To calculate z_{0m}, Wieringa (1986) employed the Davenport roughness classification system (Davenport 1960) and made a few adaptations to model the terrain of the Netherlands (Wieringa 1980, 1986) (Table 5-1). Additionally, Wieringa (1986) utilized a formula developed by Smith and Carson (1977) to evaluate and define 'elevation variability roughness lengths' (z_{oh}):

$$z_{0h} = 0.2(dH)^2/L$$

where dH represents the largest terrain elevation difference per block and L represents horizontal block distance. For example, if the largest terrain difference over a 5 x 5 km block is 20 meters then dH would be 20 and L would be 5000. To create z_{0m}, the average surface roughness for each (perhaps 5 x 5 km) block (z_{0b}) is multiplied by z_{0h}. For example, if the 5 x 5 km block is dominated by bushes and numerous obstacles (class 6 in Table 5-1), then z_{0b} would be 0.5.

The ruggedness variable, R_t, could be calculated through a combination of terrain roughness descriptions following the Davenport roughness classification system (Davenport 1960, Wieringa 1992, Wieringa et al. 2001) and elevation variable roughness lengths (z_{0h}; Wieringa (1986) and Smith and Carson (1977)):

$$\mathrm{R}_t = \ln(z_{0h} * z_{0b})$$

where z_{0b} is the average block area surface roughness. A spatial weights analysis may be necessary to determine the influence of roughness descriptions vs. topography. The Davenport classification of effective terrain roughness identifies roughness coefficients (z_0) for eight different terrain types, thus obviating the need for the land cover covariate while simultaneously assigning a quantification for how wind is impacted over specific land cover types. Classifications can be subdivided for more specific terrains (Wieringa 1986). Although Wieringa (1986) utilized block areas of 5 x 5 km for the Netherlands, multiple block sizes could potentially be tested. Ruggedness produces a drag coefficient that accounts for elevation variability and land cover over the specified block area, which may be storm and site-specific. Mapping of R_t could be done initially for Europe and subsequently for the PNW. Ideally, ruggedness would then be employed as the only covariate in a revised cokriging model for both regions.

Regardless of the particular direction of future research that advances this methodology, the technique has the potential to protect lives and property to a greater extent than previously, because it enhances our ability to generate return periods for risk management applications.

Table 5-1. Davenport roughness classification, adapted from Davenport (1960) and Wieringa (1980, 1986).

Class	Terrain Description	Roughness Length [z_0 in meters)]
1	Open sea (fetch > 5 km)	~0.0002
2	No vegetation/obstacles (*e.g.*, snow)	~0.005
3	Open flat terrain; grass	~0.03
4	Low crops; occasional tree	~0.10
5	High crops; scattered obstacles	~0.25
6	Bushes; numerous obstacles	~0.5
7	Regular large obstacles (*e.g.*, suburb, forest)	~1.0
8	City center with varied building heights	>2.0

REFERENCES

Akkala, A., V. Devabhaktuni, and A. Kumar. 2010. Interpolation techniques and associated software for environmental data. Environmental Progress & Sustainable Energy **29**:134-141.

Aon Benfield. European Winter Storms: Traditional Perils Posing New Challenges.

Arya, S. P. S. 2001. Introduction to Micrometeorology (International Geophysics). Second edition. Academic Press.

Atkinson, P. M. and N. J. Tate. 2000. Spatial scale problems and geostatistical solutions: a review. The Professional Geographer **52**:607-623.

Aznar, J. C., E. Gloaguen, D. Tapsoba, S. Hachem, D. Caya, and Y. Bégin. 2012. Interpolation of monthly mean temperatures using cokriging in spherical coordinates. International Journal of Climatology:n/a-n/a.

Bentamy, A., Y. Quilfen, F. Gohin, N. Grima, M. Lenaour, and J. Servain. 1996. Determination and validation of average wind fields from ERS-1 scatterometer measurements. International Publishers Distributor, Newark, NJ, ETATS-UNIS.

Bowen, A. J. and D. Lindley. 1977. A wind-tunnel investigation of the wind speed and turbulence characteristics close to the ground over various escarpment shapes. Boundary-Layer Meteorology **12**:259-271.

Castruccio, S., L. Bonaventura, and L. Sangalli. 2012. A Bayesian Approach to Spatial Prediction With Flexible Variogram Models. Journal of Agricultural, Biological, and Environmental Statistics **17**:209-227.

Cattle, J. A., A. B. McBratney, and B. Minasny. 2002. Kriging method evaluation for assessing the spatial distribution of urban soil lead contamination. J. Environ. Qual. **31**:1576-1588.

Cellura, M., G. Cirrincione, A. Marvuglia, and A. Miraoui. 2008. Wind speed spatial estimation for energy planning in Sicily: A neural kriging application. Renewable Energy **33**:1251-1266.

CGIAR-CSI. SRTM 90m Digital Elevation Data version 4: http://srtm.csi.cgiar.org/ Last accessed 7 January 2012.

Clark, W. C. 1985. Scales of climate impacts. Climatic Change **7**:5-27.

Cook, N. J. 1986. Designers guide to wind loading of building structures. Part 1.

Cressie, N. 1986. Kriging nonstationary data. American Statistical Association, Alexandria, VA, ETATS-UNIS.

Cressie, N. 1990. The origins of kriging. Mathematical Geology **22**:239-252.

Dark, S. J. and D. Bram. 2007. The modifiable areal unit problem (MAUP) in physical geography. Progress in Physical Geography **31**:471-479.

Davenport, A. G. 1960. Rationale for determining design wind velocities. ASCE Journal of the Structural Division **86**:39-68.

Della-Marta, P. M., H. Mathis, C. Frei, M. A. Liniger, J. Kleinn, and C. Appenzeller. 2009. The return period of wind storms over Europe. International Journal of Climatology **29**:437-459.

Durst, C. 1960. Wind speeds over short periods of time. Meteorological Magazine **89**:181-187.

EQE. 2000. The European Storms Lothar and Martin, December 26-28, 1999. ABS Consulting.

EQE International. The European Storms Lothar and Martin, December 26-28, 1999.

EQECAT. 2002. Report into the Storm "Jeanette," 27th October, 2002.

EQECAT. 2007. Europe Windstorm Kyrill Causes Losses in Western Europe.

ESRI. 2010. Earth Systems Research Lab: ArcGIS 10.0. Redlands, CA.

Fink, A. H., T. Brucher, V. Ermert, A. Kruger, and J. G. Pinto. 2009. The European storm Kyrill in January 2007: synoptic evolution, meteorological impacts and some considerations with respect to climate change. Natural Hazards and Earth System Sciences **9**:405-423.

Fotheringham, A. S. and D. W. S. Wong. 1991. The modifiable areal unit problem in multivariate statistical analysis. Environment and Planning A **23**:1025-1044.

Gatey, D. 2011. The Analysis of Extreme Synoptic Winds. Monography. University of Western Ontario, London, Ontario, Canada.

Georgakakos, A., P. Kitanidis, H. Loaiciga, R. Olea, and S. Yates. 1990. Review of geostatistics in geohydrology: I. basic concepts. Journal of Hydraulic Engineering (ASCE) **116**:612-632.

Gilbert, R. O. and J. C. Simpson. 1985. Kriging for estimating spatial pattern of contaminants: Potential and problems. Environmental Monitoring and Assessment **5**:113-135.

GlobCover. 2008. GlobCover Land Cover v2 2008 database. European Space Agency (ESA) GlobCover Project, led by MEDIAS-France. http://ionia1.esrin.esa.int/index.asp Last accessed 7 January 2012.

Gribov, A. and K. Krivoruchko. 2011. Local polynomials for data detrending and interpolation in the presence of barriers. Stochastic Environmental Research and Risk Assessment **25**:1057-1063.

Gribov, A., K. Krivoruchko, and J. Ver Hoef. 2000. Modified weighted least squares semivariogram and covariance model fitting algorithm. Stochastic Modeling and Geostatistics - AAPG Computer Applications in Geology **2**.

Guy Carpenter. 2008. Windstorm Emma.

Guy Carpenter & Company Ltd. 2005. Windstorm Erwin / Gudrun – January 2005.

Handorf, D. and K. Dethloff. 2009. Atmospheric teleconnections and flow regimes under future climate projections. The European Physical Journal - Special Topics **174**:237-255.

Helterbrand, J. and N. Cressie. 1994. Universal cokriging under intrinsic coregionalization. Mathematical Geology **26**:205-226.

Heneka, P. and T. Hofherr. 2011. Probabilistic winter storm risk assessment for residential buildings in Germany. Natural Hazards **56**:815-831.

Hertenstein, R. F. and J. P. Kuettner. 2005. Rotor types associated with steep lee topography: influence of the wind profile. Tellus A **57**:117-135.

Hewston, R. 2007. Windstorm Kyrill.*in* U. o. E. A.-. Norwich, editor.

Hofherr, T. and M. Kunz. 2010. Extreme wind climatology of winter storms in Germany. Climate Research **41**:105-123.

Huang, D., T. T. Allen, W. I. Notz, and N. Zeng. 2006. Global optimization of stochastic black-box systems via sequential kriging meta-models. Journal of Global Optimization **34**:441-466.

Jelinski, D. and J. Wu. 1996. The modifiable areal unit problem and implications for landscape ecology. Landscape Ecology **11**:129-140.

Journel, A. and C. Huijbregts. 1978. Mining Geostatistics Academic Press, London.

Joyner, T. A., A. M. Treviño, C. J. Friedland, S. Gosh, C. Huyck, and M. Weatherhead. *in review*. Peak gust and maximum sustained wind speed estimates for European mid-latitude cyclones. (Submitted to International Journal of Climatology).

Keim, B. D., R. A. Muller, and G. W. Stone. 2007. Spatiotemporal patterns and return periods of tropical storm and hurricane strikes from Texas to Maine. Journal of Climate **20**:3498-3509.

Kirk, R. and J. Franklin. 1992. The Olympic rain forest: an ecological web. University of Washington Press, Seattle, Washington, USA.

Klawa, M. and U. Ulbrich. 2003. A model for the estimation of storm losses and the identification of severe winter storms in Germany. Natural Hazards and Earth System Sciences **3**:725–732.

Krayer, W. R. and R. D. Marshall. 1992. Gust factors applied to hurricane winds. Bulletin of the American Meteorological Society **73**:613-617.

Krige, D. 1951. A statistical approach to some basic mine valuation problems on the Witwatersrand. Journal of the Chemical, Metallurgical and Mining Society of South Africa **52**:119-138.

Lam, N. S.-N. and D. A. Quattrochi. 1992. On the issues of scale, resolution, and fractal analysis in the mapping sciences. The Professional Geographer **44**:88-98.

Lanza, L., J. Ramirez, and E. Todini. 2001. Stochastic rainfall interpolation and downscaling. Hydrology and Earth System Sciences **5**:139-143.

Larsén, X. G. and J. Mann. 2009. Extreme winds from the NCEP/NCAR reanalysis data. Wind Energy **12**:556-573.

Leckebusch, G. C., U. Ulbrich, L. Frohlich, and J. G. Pinto. 2007. Property loss potentials for European midlatitude storms in a changing climate. Geophysical Research Letters **34**.

Li, L., J. Wu, M. Wilhelm, and B. Ritz. 2012. Use of generalized additive models and cokriging of spatial residuals to improve land-use regression estimates of nitrogen oxides in Southern California. Atmospheric Environment **55**:220-228.

Lloyds. 2008. Exploring Europe's Double Whammy Windstorms. News & Features. Society of Lloyd's.

Luo, W., M. C. Taylor, and S. R. Parker. 2008. A comparison of spatial interpolation methods to estimate continuous wind speed surfaces using irregularly distributed data from England and Wales. International Journal of Climatology **28**:947-959.

Luo, X., Y. Xu, and Y. Shi. 2011. Comparison of interpolation methods for spatial precipitation under diverse orographic effects. Pages 1-5 *in* Geoinformatics, 2011 19th International Conference on.

MacEachren, A. and J. Davidson. 1987. Sampling and isometric mapping of continuous geographic surfaces. The American Cartographer **14**:299-320.

Mahdian, M. H., S. R. Bandarabady, R. Sokouti, and Y. N. Banis. 2009. Appraisal of the Geostatistical Methods to Estimate Monthly and Annual Temperature. Asian Network for Scientific Information, Pakistan.

Mass, C. and B. Dotson. 2010. Major extratropical cyclones of the northwest United States: historical review, climatology, and synoptic environment. Monthly Weather Review **138**:2499-2527.

Matheron, G. 1979. Research on the Simplification of the Cokriging Problem. Research Rept. N-628, Centre de Géostatistique, Fountainbleau.

Meentemeyer, V. 1989. Geographical perspectives of space, time, and scale. Landscape Ecology **3**:163-173.

Newtonu, C. W. and E. Palmén. 1963. Kinematic and thermal properties of a large-amplitude wave in the westerlies. Tellus **15**:99-119.

Odeh, I. O. A., A. B. McBratney, and D. J. Chittleborough. 1995. Further results on prediction of soil properties from terrain attributes: heterotopic cokriging and regression-kriging. Geoderma **67**:215-226.

Ogniewicz, R. and M. Ilg. 1992. Voronoi skeletons: theory and applications. Pages 63-69 *in* Computer Vision and Pattern Recognition, 1992. Proceedings CVPR '92., 1992 IEEE Computer Society Conference on.

Oke, T. 1987. Boundary Layer Climates. 2nd edition. Methuen, London.

Openshaw, S. 1984. Ecological fallacies and the analysis of areal census data. Environment and Planning A **16**:17-31.

Openshaw, S. and P. Taylor. 1979. A million or so correlation coefficients: three experiments on the modifiable aral unit problem. Pion, London.

Öztopal, A. 2006. Artificial neural network approach to spatial estimation of wind velocity data. Energy Conversion and Management **47**:395-406.

Phillips, D. L., E. H. Lee, A. A. Herstrom, W. E. Hogsett, and D. T. Tingey. 1997. Use of auxillary data for spatial interpolation of ozone exposure in southeastern forests. Environmetrics **8**:43-61.

Pinto, J. G., C. P. Neuhaus, G. C. Leckebusch, M. Reyers, and M. Kerschgens. 2010. Estimation of wind storm impacts over Western Germany under future climate conditions using a statistical–dynamical downscaling approach. Tellus A **62**:188-201.

Powell, M. D., S. H. Houston, L. R. Amat, and N. Morisseau-Leroy. 1998. The HRD real-time hurricane wind analysis system. Journal of Wind Engineering and Industrial Aerodynamics **77–78**:53-64.

Powell, M. D., S. H. Houston, and T. A. Reinhold. 1996. Hurricane Andrew's landfall in south Florida. Part I: standardizing measurements for documentation of surface wind fields. Weather and Forecasting **11**:304-328.

Raible, C. C. 2007. On the relation between extremes of midlatitude cyclones and the atmospheric circulation using ERA40. Geophysical Research Letters **34**:L07703.

Reed, D. 2008. Electric utility distribution analysis for extreme winds. Journal of Wind Engineering and Industrial Aerodynamics **96**:123-140.

Risk Management Solutions, I. 2006. Europe Windstorm.

RMS. 2002. RMS Updates Loss Estimates for Windstorm Jeanette; Insured Losses Likely to Exceed Euro 800 Million.

Robinson, W. 1950. Ecological correlations and the behavior of individuals. American Sociological Review **15**:351-357.

Sayre, N. F. 2005. Ecological and geographical scale: parallels and potential for integration. Progress in Human Geography **29**:276-290.

Schiermeier, Q. 2006. Insurers' disaster files suggest climate is culprit. Nature **441**:674-675.

Shapiro, S. S. and M. B. Wilk. 1965. An analysis of variance test for normality (complete samples). Biometrika **52**:591-611.

Simiu, E. and N. A. Heckert. 1996. Extreme Wind Distribution Tails: A "Peaks over Threshold" Approach. ASCE.

Singh, V., C. Carnevale, G. Finzi, E. Pisoni, and M. Volta. 2011. A cokriging based approach to reconstruct air pollution maps, processing measurement station concentrations and deterministic model simulations. Environmental Modelling & Software **26**:778-786.

Sliz-Szkliniarz, B. and J. Vogt. 2011. GIS-based approach for the evaluation of wind energy potential: A case study for the Kujawsko–Pomorskie Voivodeship. Renewable and Sustainable Energy Reviews **15**:1696-1707.

Smith, F. B. and D. J. Carson. 1977. Some thoughts on the specification of the boundary-layer relevant to numerical modelling. Boundary-Layer Meteorology **12**:307-330.

Solari, G. 1993. Gust buffetting 1. Peak wind velocity and equivalent pressure. Journal of Structural Engineering-Asce **119**:365-382.

Steenburgh, W. and C. Mass. 1996. Interaction of an intense extratropical cyclone with complex coastal orography. Monthly Weather Review **124**:1329-1352.

Stein, A. and L. C. A. Corsten. 1991. Universal kriging and cokriging as a regression procedure. Biometrics **47**:575-587.

Sterk, G. and A. Stein. 1997. Mapping wind-blown mass transport by modeling variability in space and time. Soil Sci. Soc. Am. J. **61**:232-239.

Tieleman, H. W. 1992. Wind characteristics in the surface layer over heterogeneous terrain. Journal of Wind Engineering and Industrial Aerodynamics **41**:329-340.

Tobler, W. R. 1970. A Computer Movie Simulating Urban Growth in the Detroit Region. Economic Geography **46**:234-240.

Tolosana-Delgado, R. and V. Pawlowsky-Glahn. 2007. Kriging regionalized positive variables revisited: sample space and scale considerations. Mathematical Geology **39**:529-558.

Venäläinen, A. and M. Heikinheimo. 2002. Meteorological data for agricultural applications. Physics and Chemistry of the Earth, Parts A/B/C **27**:1045-1050.

VRS. 2008. Windstorm "Paula": damage of millions of euros.

Wahba, G. 1981. Spline interpolation and smoothing on the sphere. SIAM Journal of Scientific and Statistical Computing **2**:5-16.

Walter, C., A. B. McBratney, A. Douaoui, and B. Minasny. 2001. Spatial prediction of topsoil salinity in the Chelif Valley, Algeria, using local ordinary kriging with local variograms versus whole-area variogram. Soil Research **39**:259-272.

Wang, X., J. Lv, C. Wei, and D. Xie. 2011. Modeling Spatial Pattern of Precipitation with GIS and Multivariate Geostatistical Methods in Chongqing Tobacco Planting Region, China

Computer and Computing Technologies in Agriculture IV. Pages 512-524 *in* D. Li, Y. Liu, and Y. Chen, editors. Springer Boston.

Wenxia, G., C. Xiaoling, C. Xiaobin, Z. Jian, F. Lian, and X. Xiao. 2010. Spatial interpolation of precipitation considering geographic and topographic influences - A case study in the Poyang Lake Watershed, china. Pages 3972-3975 *in* Geoscience and Remote Sensing Symposium (IGARSS), 2010 IEEE International.

Wernli, H., S. Dirren, M. A. Liniger, and M. Zillig. 2002. Dynamical aspects of the life cycle of the winter storm 'Lothar' (24-26 December 1999). Quarterly Journal of the Royal Meteorological Society **128**:405-429.

Wieringa, J. 1973. Gust factors over open water and built-up country. Boundary-Layer Meteorology **3**:424-441.

Wieringa, J. 1980. Representativeness of Wind Observations at Airports. Bulletin of the American Meteorological Society **61**:962-971.

Wieringa, J. 1986. Roughness-dependent geographical interpolation of surface wind speed averages. Quarterly Journal of the Royal Meteorological Society **112**:867-889.

Wieringa, J. 1992. Updating the Davenport roughness classification. Journal of Wind Engineering and Industrial Aerodynamics **41**:357-368.

Wieringa, J. 1997. Representativity problems of wind stations.*in* EU-COST: Data Spatial Distribution in Meteorology and Climatology, Voltera, Italy.

Wieringa, J., A. Davenport, C. Grimmond, and T. Oke. 2001. New revision of Daveport roughness classification.*in* Proceedings of the 3rd European & African conference on wind engineering, Eindhoven, The Netherlands.

Wilk, M. and R. Gnanadesikan. 1968. Probability plotting methods for the analysis for the analysis of data. Biometrika **55**:1-17.

World Meterological Organization. 2008. WMO guide to meteorololgical instruments and methods of observation. Chapter 5: Measurement of surface wind. Chairperson, Publications Board: World Meteorological Organization (WMO), Geneva.

Wu, J. 2004. Effects of changing scale on landscape pattern analysis: scaling relations. Landscape Ecology **19**:125-138.

Zhang, Z. 2012. Iterative posterior inference for Bayesian Kriging. Stochastic Environmental Research and Risk Assessment **26**:913-923.

Zlatev, Z., S. E. Middleton, and G. Veres. 2009. Ordinary kriging for on-demand average wind interpolation of in-situ wind sensor data.*in* EWEC 2009, Marseilles.

Zlatev, Z., S. E. Middleton, and G. Veres. 2010. Benchmarking knowledge-assisted kriging for automated spatial interpolation of wind measurements. Pages 1-8 *in* 2010 13th Conference on Information Fusion (FUSION).

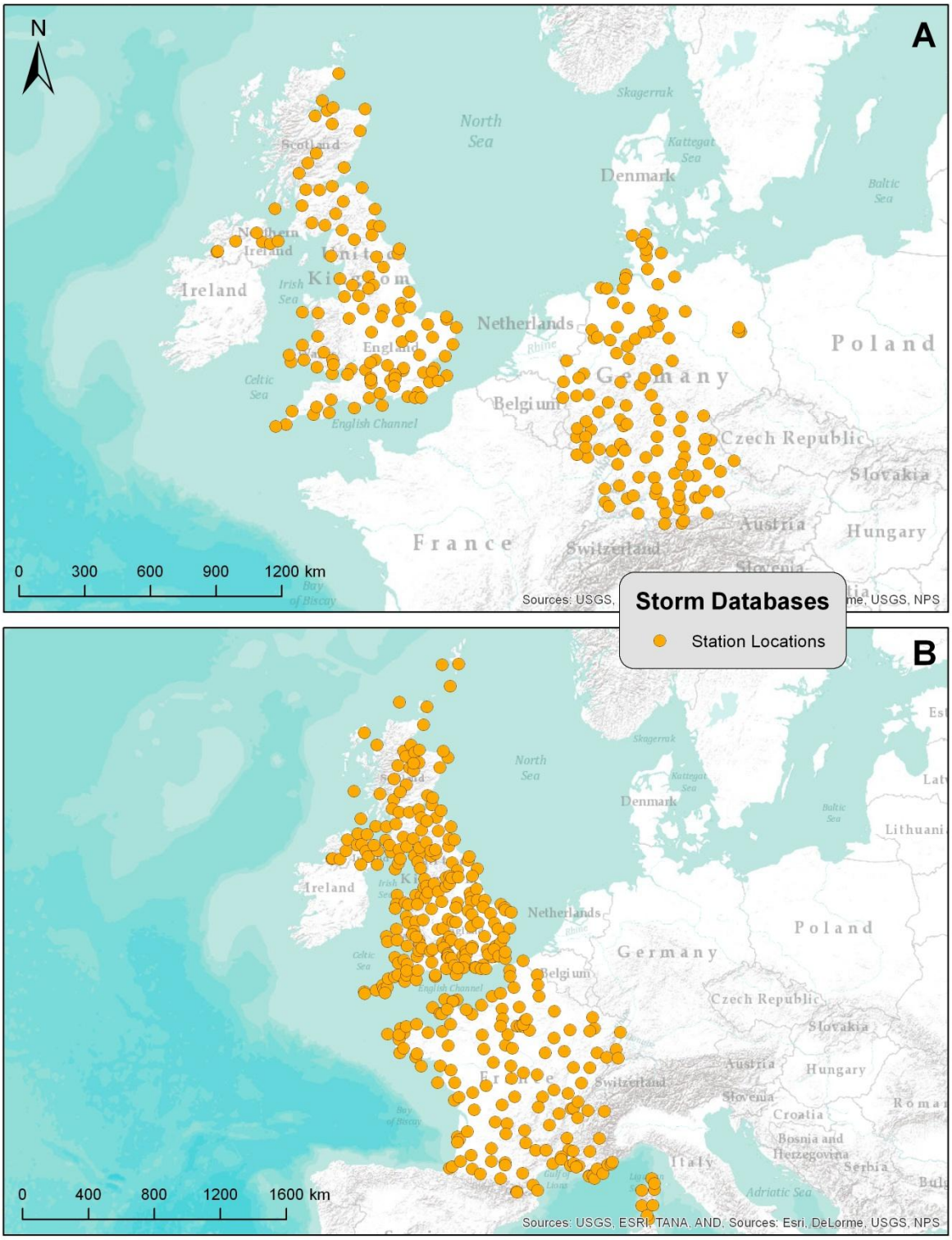

Figure A.1. Station locations for Capella (1976) (A) and Storm 87J (1987) (B).

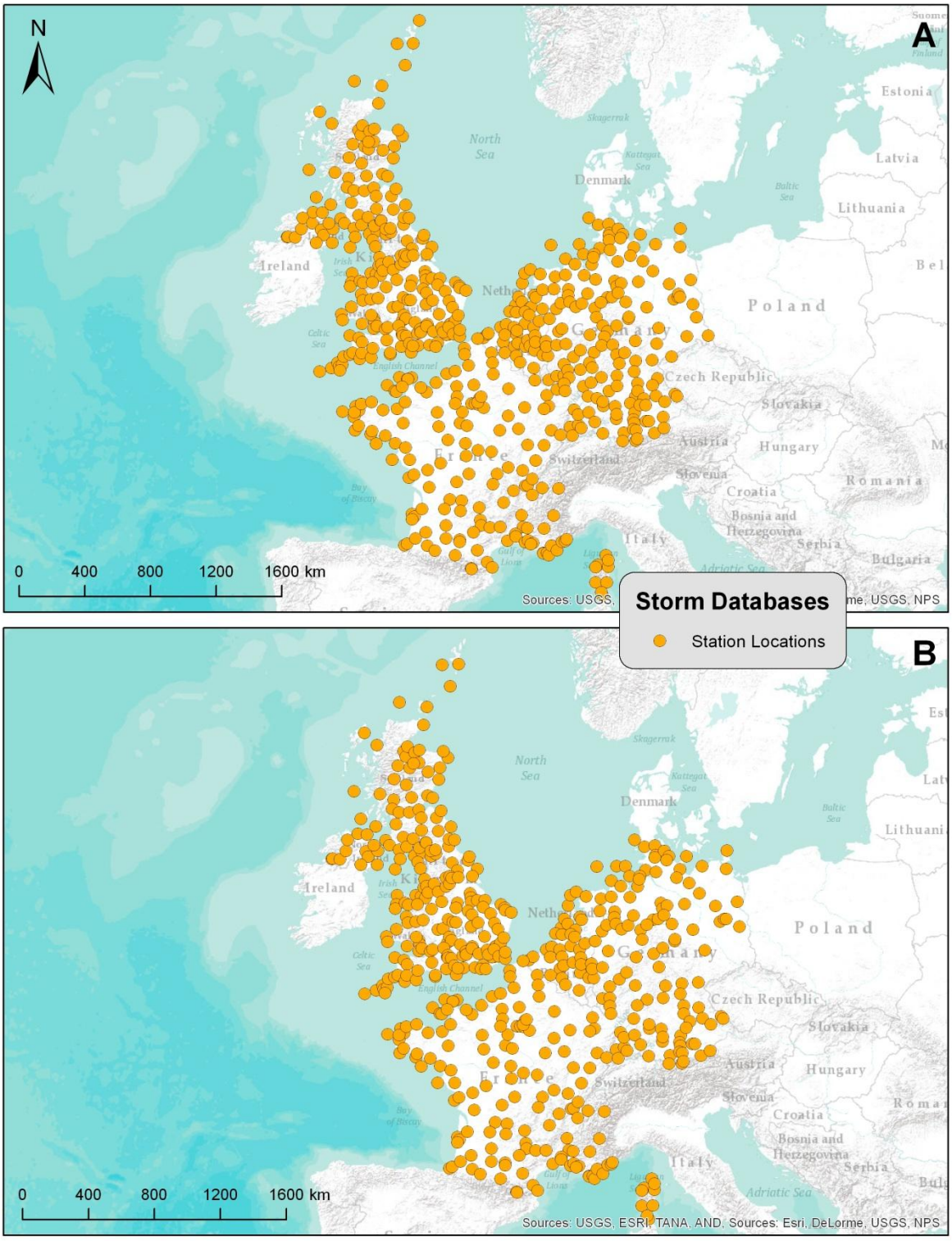

Figure A.2. Station locations for Daria (A) and Herta (B); both storms occurred in 1990.

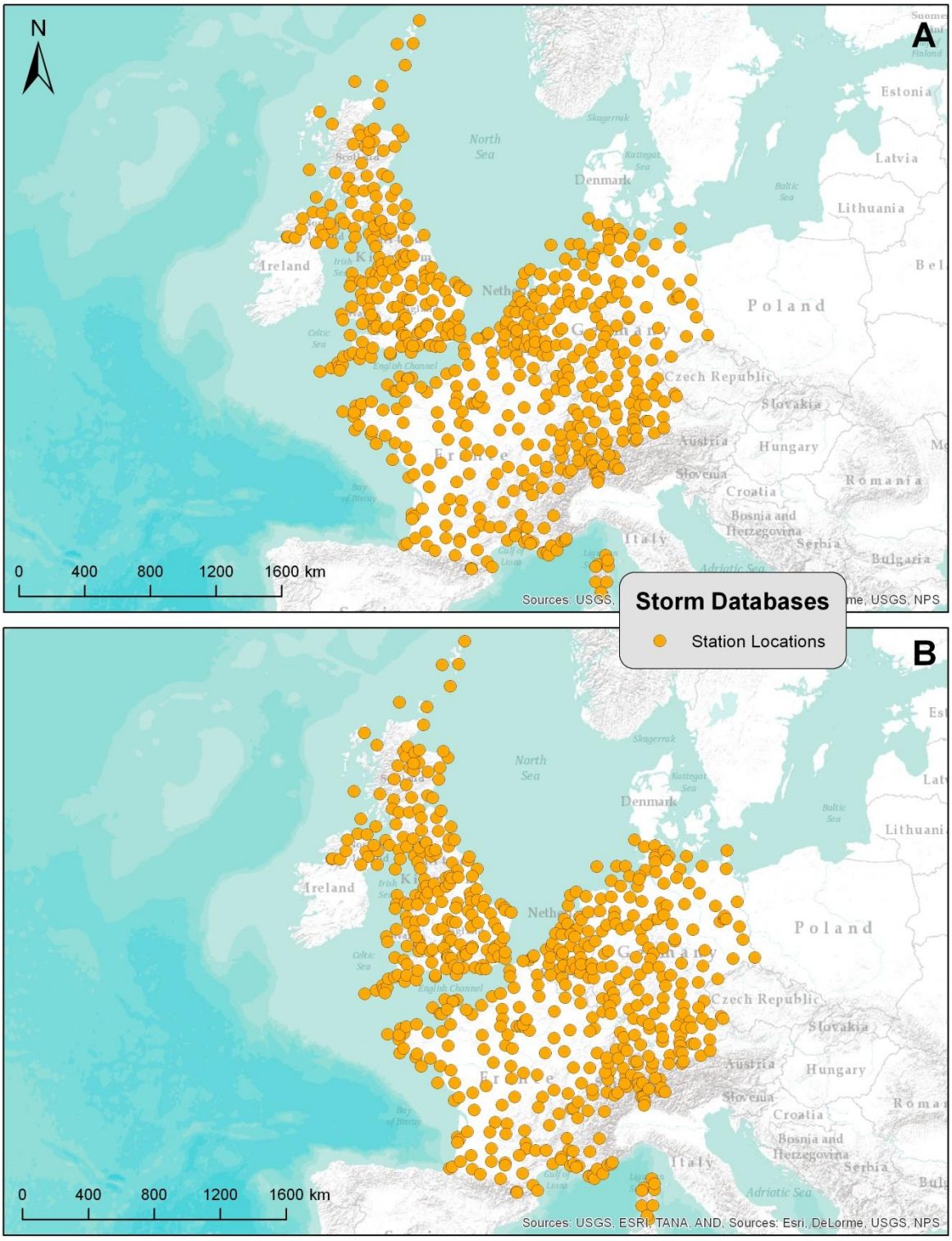

Figure A.3. Station locations for Vivian (A) and Wiebke (B); both storms occurred in 1990.

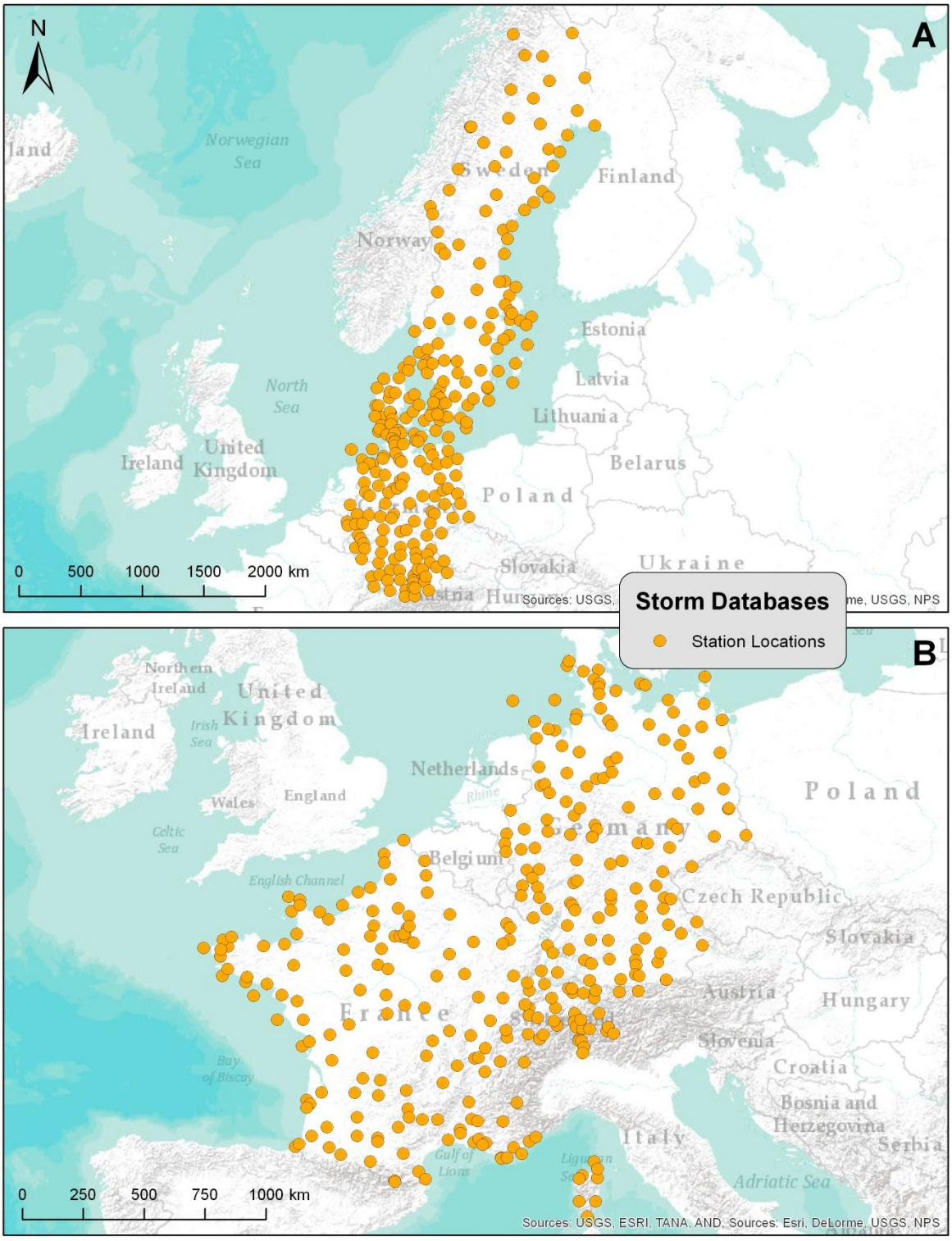

Figure A.4. Station locations for Anatol (A) and Lothar (B); both storms occurred in 1999.

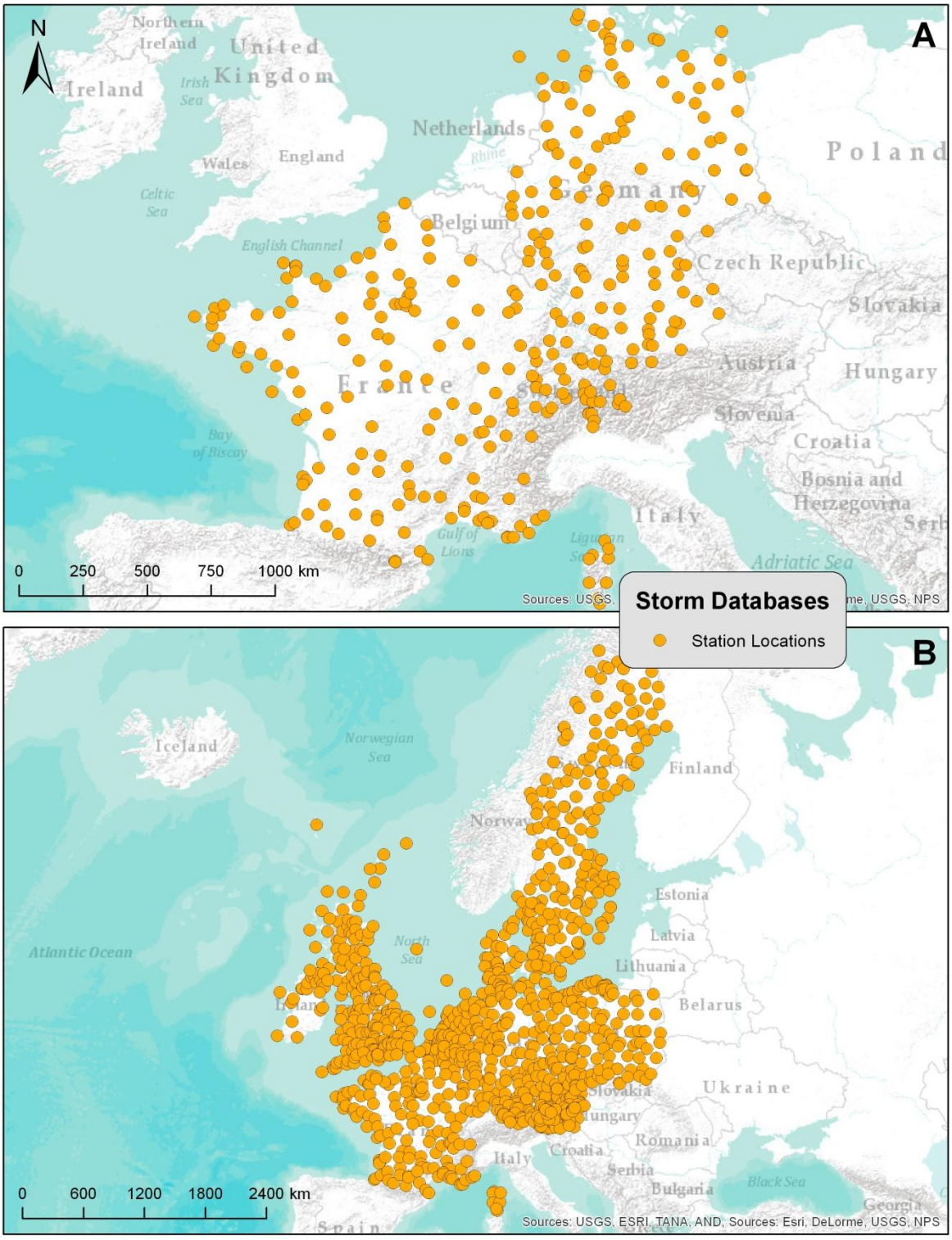

Figure A.5. Station locations for Martin (1999) (A) and Jeanette (2004) (B).

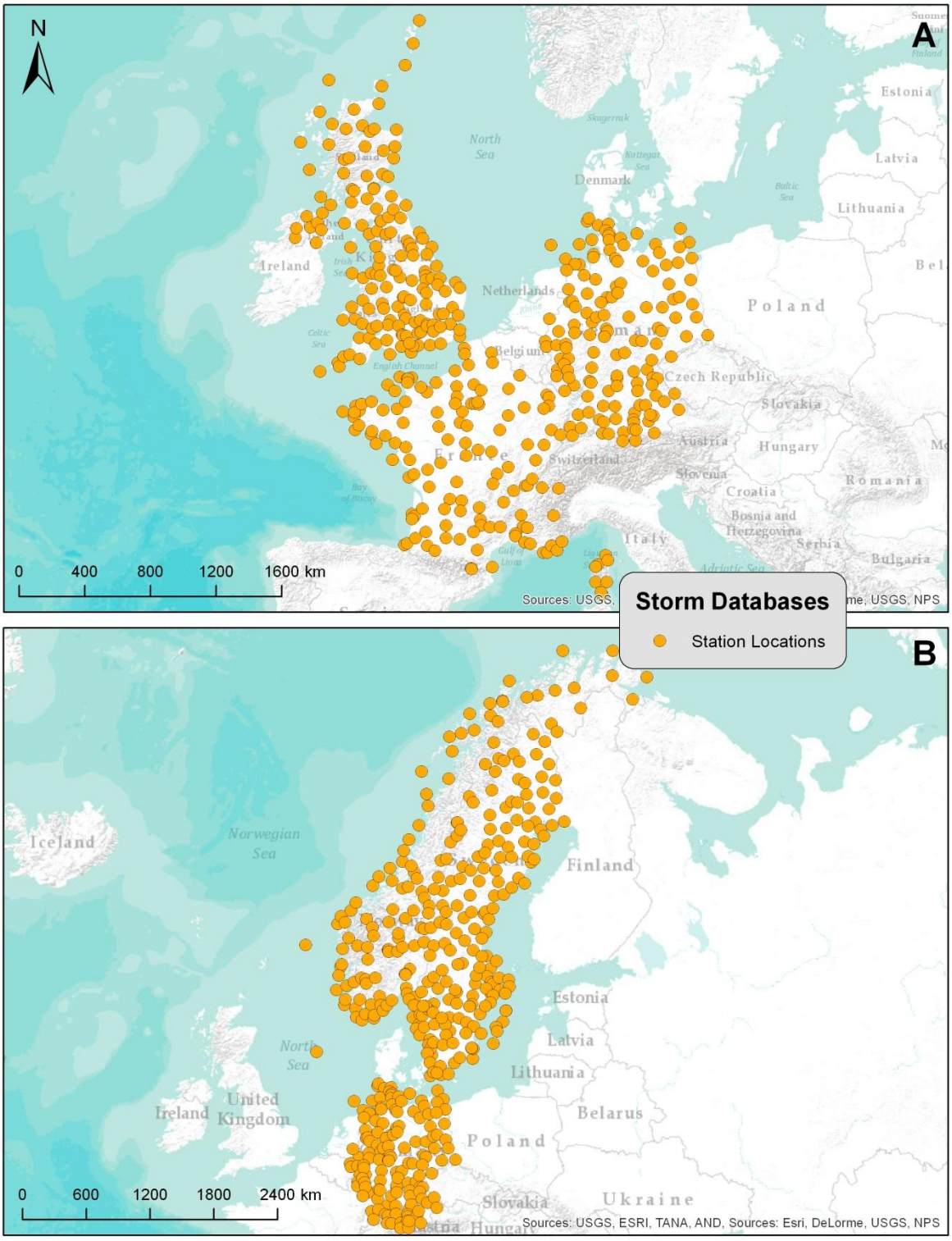

Figure A.6. Station locations for Dagmar (2004) (A) and Erwin (2005) (B).

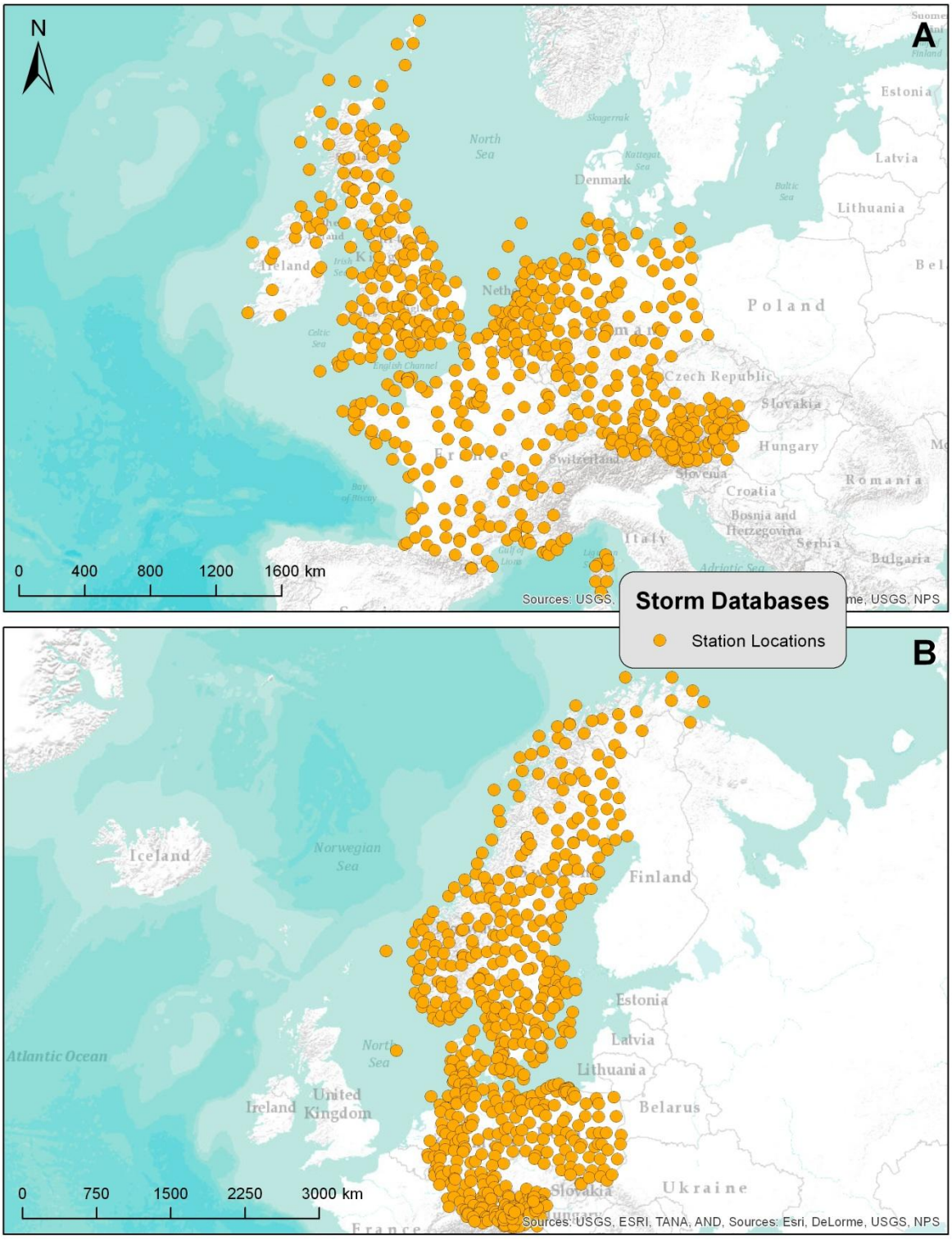

Figure A.7. Station locations for Kyrill (2007) (A) and Paula (2008) (B).

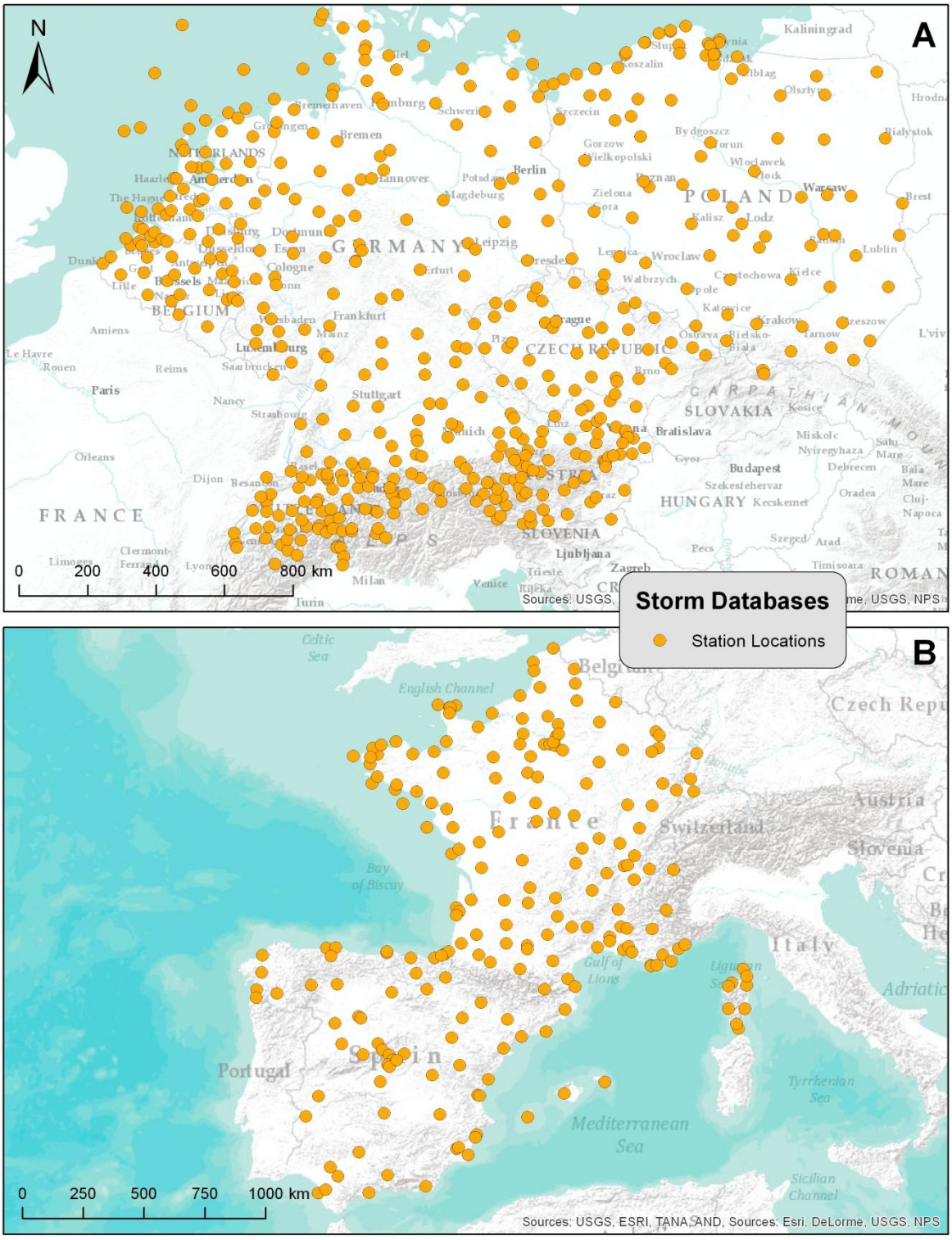

Figure A.8. Station locations for Emma (2008) (A) and Klaus (2009) (B).

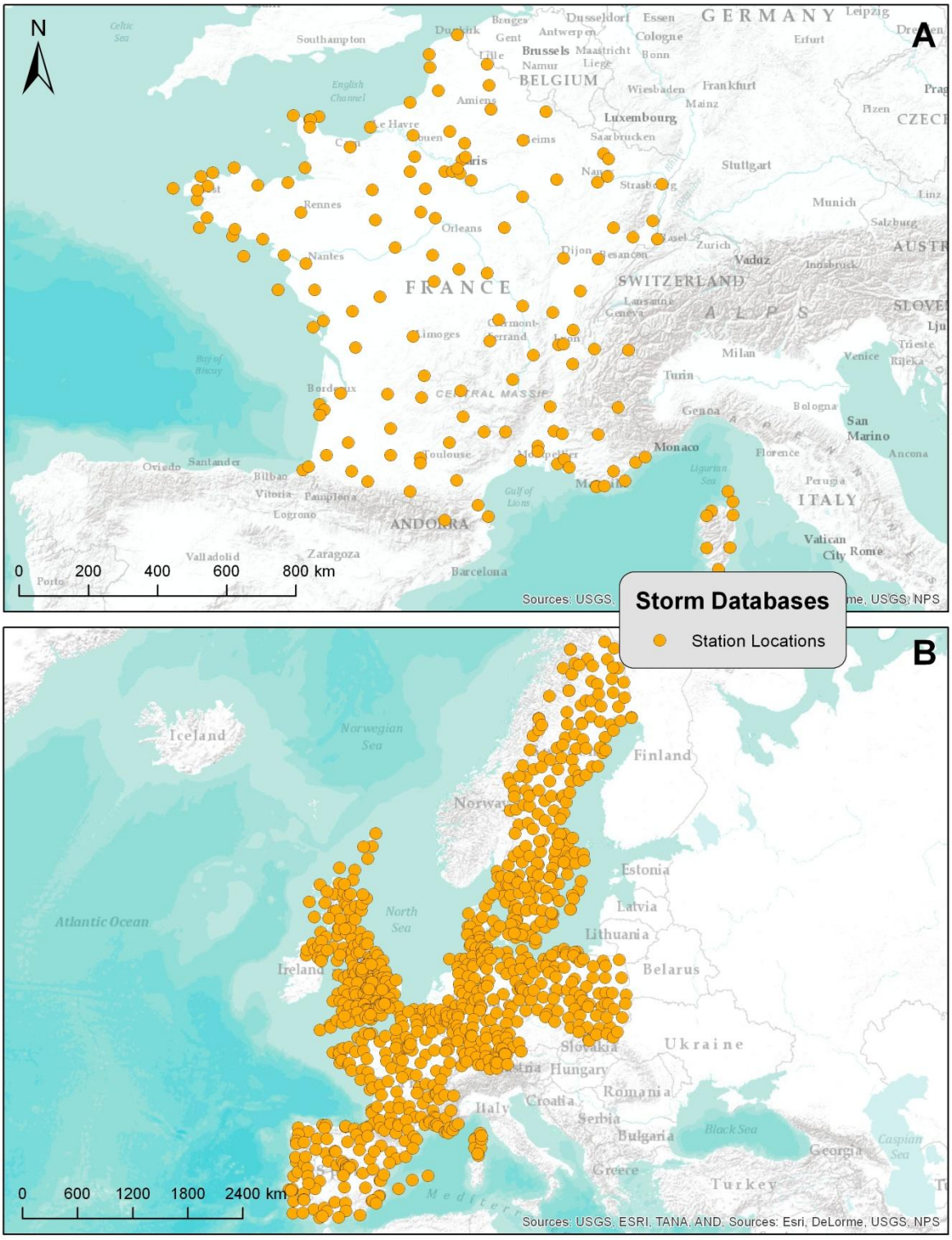

Figure A.9. Station locations for Quinten (2009) (A) and Xynthia (2010) (B).

VITA

Born in 1985 and raised in North Carolina, Timothy “Andrew” Joyner, graduated from Parkwood High School in May of 2004. He subsequently enrolled at Louisiana State University in August of 2004 where he pursued a Bachelor of Science degree in the Department of Geography and Anthropology. During his studies at LSU, Andrew worked at the World Health Organization Collaborating Center (WHOCC) for GIS and Remote Sensing and the Southern Regional Climate Center (SRCC) as a student research assistant. Both the WHOCC and SRCC offered multiple research opportunities for Andrew on various topics including spatial ecology, climatology, medical geography, and mapping sciences. Through his research, Andrew completed an undergraduate Honors Thesis that explored Atlantic basin hurricane densities and centrography over time. Andrew graduated *cum laude* with honors in May of 2008.

Shortly after completing his BS degree from LSU, Andrew moved to Fullerton, California, where he pursued his Master’s degree in the Department of Geography and began working in the Spatial Epidemiology and Ecology Research (SEER) lab at California State University-Fullerton (CSU-F). While at CSU-F, Andrew collaborated on multiple disease mapping and modeling projects in the United States and Former Soviet Union. In August of 2009, the SEER lab moved to the University of Florida and Andrew moved along with the lab to continue his thesis research that focused on modeling the impact of climate change on the ecological niche of *Bacillus anthracis* in Kazakhstan. Andrew completed his thesis in May of 2010 and graduated from the University of Florida with a Master of Science in Geography.

In August of 2010, Andrew returned to LSU to pursue a Doctor of Philosophy degree in Geography with a minor in Disaster Science and Management (DSM). Andrew began working in the DSM lab on the LSU System Hazard Mitigation Plan – a FEMA-sponsored project that profiled all hazards and proposed detailed mitigation actions for each of the LSU system campuses. Andrew maintained the GIS database for the project and created all final mapping products and hazard profiles. As part of a separate project initiated by a risk management company in the summer of 2011, Andrew collaborated with other faculty and students to model the spatial patterns of wind speeds produced by multiple wind storms in Europe. Many questions were left unanswered and the project quickly became the foundation for Andrew's dissertation research. Andrew received an Austrian Marshall Plan Scholarship for the summer of 2012 where he continued his research on European wind storms and collaborated with other researchers in Villach, Austria, at the Carinthian University of Applied Sciences. Andrew will graduate in May of 2013 and will continue exploring his diverse array of research interests as a tenure-track assistant professor within the Department of Geosciences at East Tennessee State University in Johnson City, Tennessee.